Validation of NEXRAD data and models of bird migration stopover sites in the Northeast U.S.

Final Report

August 2017

Prepared by Jeffrey J. Buler[1], James McLaren[1], Timothy Schreckengost[1], Jaclyn A. Smolinsky[1], Eric Walters[2], J. Andrew Arnold[2], Deanna K. Dawson[3]

[1] Department of Entomology and Wildlife Ecology, University of Delaware, Newark, DE 19716
[2] Department of Biological Sciences, Old Dominion University, Norfolk, VA 23529
[3] U.S. Geological Survey, Patuxent Wildlife Research Center, Laurel, MD 20708

Submitted to U.S. Fish and Wildlife Service
Northeast Region
Hadley, MA

The work on which this report is based was performed in accordance with a cooperative agreement (#F13AC00402) between the U.S. Fish and Wildlife Service and the University of Delaware.

Table of Contents

Executive Summary 1
Introduction 2
Objectives 5
Methods 6
Objective 1: Mapping stopover incidence with radar 6
Weather Radar Data Processing 6
Determining a suitable sampling time of migration exodus 7
Mapping and characterizing bird stopover use 9
Objective 2: Modeling stopover incidence with radar 9
Modeling stopover distributions of migrating birds 9
Objective 3: Explaining migratory landbird use of forests via field surveys 12
Bird Surveys 12
Food Availability 15
Vegetation Sampling 16
Regional and Landscape Data 17
Data Analysis 17
Objective 4: Classifying stopover site function 19
Results 20
Objective 1: Mapping stopover incidence with radar 20
Determining a suitable sampling time of migration exodus 21
Mapping observed stopover distributions 21
Objective 2: Modeling stopover incidence with radar 22
Predictor selection and influences 22
Predicted stopover distributions 23
Classification maps 23
Validation with independent radar 24
Objective 3: Explaining migratory landbird use of forests via field surveys 25
Nocturnal Migratory Species Groups 26
Objective 4: Classifying stopover site function 28

Discussion 29
Objective 1: Mapping stopover incidence with radar 29
Objective 2: Modeling stopover incidence with radar 30
Objective 3: Explaining migratory landbird use of forests via field surveys 32
Objective 4: Classifying stopover site function 37
Conservation Implications 38
Acknowledgments 39
Outcomes 40
Literature Cited 43

List of Tables

Table 1. Predictor variables included in the final boosted generalized additive model (BGAM) of seasonal mean landbird density at migration stopover sites (as measured by vertically integrated reflectivity) across the northeastern U.S. 'Category' groups variables according to the scale at which they apply; 'corrective predictors' dRdr and relelev were used to fit models but not for estimating regional densities. 51
Table 2. Independent variables available for use in boosted regression tree (BRT) analyses of ground survey data to identify site or survey characteristics that influence density of landbirds on migratory stopovers. For each variable, the spatial scale (P = Patch, L = Landscape, R = Regional) is given as well as a brief description, mean untransformed value of continuous variables, range of values, whether it was log transformed (Y= yes, N= no), and if it was included in the ensemble models used for the BRT analysis (Y= yes, N= no).. 52
Table 3. List of transect sites, nearby radar (KAKQ = Wakefield, VA; KDOX= Dover, DE; Outside = Outside radar range), state (ES = Eastern Shore of Virginia, VA = Inland SE Virginia), number of visits, detection probabilities, and detection-corrected migrant bird densities within 50 m of the transect centerline during fall 2013 and 2014. 57
Table 4. Cross-correlation strength of potential explanatory variables. Values are Pearson correlation coefficients, and only those with moderate to strong correlations (strength < -0.7 or >0.7) are presented. 54
Table 5. Parameters and predictive performance metrics for all BRT models used in analysis of ground survey data, obtained from 10-fold cross-validation and using the 31 predictor variables detailed in Table 2. Table values indicate: the response variable for each model, each model's optimal learning rate, number of trees fitted for the final ensemble model, proportion of total deviance explained of the training data; and cross validation correlation. For all models, bag fraction was left at 0.5 and tree complexity at 2. Note: See Table 10 for species codes. 62
Table 6. Number of suitable sampling nights for each radar and year for the autumn migration season. The percent of suitable nights out of all screened nights by radar across years is also presented. 55
Table 7. Interactions between predictors selected by Boosted Regression Trees for mean and variability in reflectivity (see text and Table 1 for names and descriptions of predictors) 56
Table 8. Complete list of bird species and species groups detected during fall 2013 and fall 2014 among 48 transect locations. Migration status classifications (mi – transient, su – summer breeder, wi – winter resident, yr – year-round) and total detections are also presented. Species are ordered by the total number of detections. 57
Table 9. Summary table for the relative contributions (%) of each predictor variable included in boosted regression tree models developed to identify which factors were most influential in determining migrant density for 14 bird species. Species codes defined in Table 8. 63

Table 10. Summary table for the relative contributions (%) of each predictor variable included in boosted regression tree models developed to identify which factors were most influential in determining migrant density for several species groups (defined in text). 65
Table 11. Ranked interaction sizes for the ten most influential predictor variable interactions for the BRT analysis of winter migrant density. 67
Table 12. Ranked interaction sizes for the ten most influential predictor variable interactions for the BRT analysis of transient migrant density. 67
Table 13. Ranked interaction sizes for the ten most influential predictor variable interactions for the BRT analysis of breeding migrant density. 68
Table 14. Ranked interaction sizes for the ten most influential predictor variable interactions for the BRT analysis of frugivorous migrant density. 68
Table 15. Ranked interaction sizes for the ten most influential predictor variable interactions for the BRT analysis of all nocturnal migrant density 69
Table 16. Values of predictor variables to determine stopover functional type classification of 45 transects sites in the mid-Atlantic and Gulf Coast regions. All sites with 4-letter acronyms are from mid-Atlantic region. 70

List of Figures

Figure 1. Location, short name, and radar coverage area (80-km radius) of 16 NEXRAD stations used in the study within USFWS Region 5. Coverage area (60-km radius) of NASA's NPOL radar (red) and the four TDWR stations (blue) used in the study are also denoted and labeled by radar name. 71
Figure 2. Example scatterplot of the increase in mean total reflectivity through time at the onset of a nocturnal bird-dominated flight. Vertical dashed line at the sun angle (100° [i.e., 10° below the horizon]) indicates where the point of the maximum rate of increase in reflectivity occurs. This would be the sun angle at which radar data were sampled for quantifying bird distributions aloft at this radar on this night. 72
Figure 3. Normalized spatial axes towards (top) and along (bottom) the Atlantic Seaboard, rotated 42° clockwise compared to Easting and Northing variables, respectively. 73
Figure 4. Correlation coefficients (left) between mean VIR and 8 landscape-scale predictors at 1-100-km scales (X axis), and (right) between the same predictor at each scale with that at the nominal 5-km scale. 74
Figure 5. Locations of 48 hardwood forest transect survey sites within (red) and outside (blue) of NEXRAD coverage areas (gray shaded areas) where bird surveys were conducted. 75
Figure 6. Visualization of steps for land cover data extraction in ArcGIS. The first image (left of the arrow) shows buffers around all 48 sites, while the second (right) shows the 5-km buffers around eight Eastern Shore of Virginia sites after using 'extract by mask' tool. 76

Figure 7. Locations of 45 hardwood forest transect sites where bird surveys were conducted for determination of stopover duration and the coverage areas (shaded in gray) and names of four associated NEXRAD stations. 76
Figure 8. Radar measures of bird density at static sun elevation angles from 0 - 10° below the horizon. The change in mean reflectivity pooled across radars (KAKQ and KDOX) in autumns 2013 and 2014. Error bars denote ±1 standard error of the mean. 77
Figure 9. Bars indicate the sun elevation angle at the inflection point of flight exodus for individual sampling nights during autumn 2013 and 2014 at KDOX and KAKQ. Sampling days are sorted by increasing day of year. 77
Figure 10. Pearson correlations between seasonal average migrant density at the ground and aloft sampled at a series of fixed sun angles and at the daily inflection point of exodus among days. Error bars are bootstrapped 95% CI. 78
Figure 11. Mapped bird stopover density (mean reflectivity) on three nights sampled at either the daily inflection point of exodus (top) or a fixed sun angle of -5.5° (bottom) at the KDOX NEXRAD radar station. 78
Figure 12. Boxplots of the distribution of the nightly sun angles at the inflection point of flight exodus curves for sampling nights at 18 radar stations in the eastern U.S. Radars decrease in latitude from top to bottom. Vertical line denotes the sampling sun angle of -5.5° of Buler and Dawson (2014). 79
Figure 13. Map of regionally-classified (i.e., data pooled across radars) radar-observed bird stopover use during autumn 2008 - 2014 among 16 NEXRAD coverage areas within USFWS Region 5. 80
Figure 14. Map of coefficient of annual linear trend in mean autumn radar-observed bird stopover density (cm^2/ha per year) during autumn from 2008 - 2014 for 16 individual NEXRAD coverage areas within USFWS Region 5. 81
Figure 15. Predicted influence of each predictor on (top) mean fall stopover density and (bottom) daily variability in fall stopover density, based on the BGAM model and log-transformed seasonal mean VIR. See Table 1 for predictor names and descriptions. 82
Figure 16. Predicted response to each (normalized) predictor on log-transformed mean VIR, as proxy for stopover density. Rug plots (red lines) indicate coverage of normalized values of each predictor (or interaction term) among the measured data..... 83
Figure 17. Predicted response to each (normalized) predictor on coefficient of variation in VIR, as proxy for variability in stopover density. Rug plots (red lines) indicate coverage of normalized values of each predictor (or interaction term) among the measured data. 84
Figure 18. Predicted response (solid blue lines) in mean stopover to, and frequency distribution (dotted red lines) of, fractional hardwood cover at 50-km scales (upper left), 5 km (upper right), to mean NDVI (Normalized Difference Vegetation Index; lower left) and to hardwood at 1 km scales (lower right). The vertical axis represents additive factors in log-transformed stopover density, i.e. multiplicative factors in stopover density. Dotted red lines indicate frequency of normalized values of each predictor (or interaction term) among grid cells..... 85

Figure 19. Predicted response (solid blue lines) in mean stopover to, and frequency distribution (dotted red lines) of, fraction of emergent marsh (left), coniferous forest and (middle) and agricultural landcover (right), all at 5-km scales. Panels are presented in descending order of model influence. 86
Figure 20. Predicted response (solid blue lines) in mean stopover to, and frequency distribution (dotted red lines) of, distance to the Atlantic coast (within 150 km) and to the brightest (4%) light sources, and their interactions with fractional hardwood cover at 50 km. Panels are presented in order of descending model influence (upper left, upper right, lower left, lower right. 87
Figure 21. Predicted response (solid blue lines) in mean stopover to, and frequency distribution (dotted red lines) of, distance from bright lights (left) and fractional developed (urban) cover within 5 km (right). Panels are presented in descending order of model influence. 88
Figure 22. Predicted response (solid blue lines) in mean stopover to, and frequency distribution (dotted red lines) of, distance to the radar (left) and elevation relative to the radar (right). Panels are presented in descending order of model influence. 88
Figure 23. Predicted response to each (normalized) predictor on mean VIR in weeks 1-2, as proxy for stopover density. Rug plots (red lines) indicate coverage of normalized values of each predictor (or interaction term) among the measured data. 89
Figure 24. Predicted response to each (normalized) predictor on mean VIR in weeks 3-4, as proxy for stopover density. Rug plots (red lines) indicate coverage of normalized values of each predictor (or interaction term) among the measured data. 90
Figure 25. Predicted response to each (normalized) predictor on mean VIR in weeks 5-6, as proxy for stopover density. Rug plots (red lines) indicate coverage of normalized values of each predictor (or interaction term) among the measured data. 91
Figure 26. Predicted response to each (normalized) predictor on mean VIR in weeks 7-8, as proxy for stopover density. Rug plots (red lines) indicate coverage of normalized values of each predictor (or interaction term) among the measured data. 92
Figure 27. Predicted mean VIR during autumn 2008 – 2014 within USFWS Region 5 as proxy for mean stopover density, based on the BGAM model. 93
Figure 28. Predicted coefficient of variation in VIR during autumn 2008 – 2014 within USFWS Region 5 as proxy for daily variability in stopover density, based on the BGAM model. 94
Figure 29. Map of regionally-classified predicted bird stopover use during autumn 2008 - 2014 within USFWS Region 5. 95
Figure 30. Maps depicting predicted stopover use classified at various window sizes (e.g. 10-km radius, 50-km radius, and region-wide) during autumn 2008 – 2014 within USFWS Region 5. Inset region of the Delmarva Peninsula is also shown with the locations of transect survey sites (black dots). Land cover of the Delmarva Peninsula is shown for reference. 96
Figure 31. Map of regionally-classified predicted bird stopover use during four bimonthly periods averaged across autumn 2008 - 2014 within USFWS Region 5. 97

Figure 32. Map of predicted mean VIR during four bimonthly periods averaged across autumn 2008 - 2014 within USFWS Region 5. 98
Figure 33. Map of the Cumulative Stopover Importance Index for autumns 2008 – 2014 within USFWS Region 5. 99
Figure 34. Mean VIR of observed NPOL data versus co-located NEXRAD data as a function of distance to the NEXRAD (dist NEX) radar (see color bar). 100
Figure 35. Mean VIR of observed TDWR (TD) data versus NEXRAD data as a function of distance to the NEXRAD (dist NEX) radar (see color bar). 100
Figure 36. Mean VIR of observed NPOL data versus GAM-predicted data as a function of distance to the NPOL radar (see color bar). 101
Figure 37. Mean VIR of observed TDWR data versus GAM-predicted data as a function of distance to the TDWR radar (see color bar). 101
Figure 38. Total number of migrants (Neotropical versus temperate) detected throughout the fall field season for all 48 transects by year. Sampling periods start on August 15 and end on November 7. 102
Figure 39. Partial dependence plots for the nine most influential variables that predict migrant density for wintering landbird migrant species included in the analysis. Rug plots show the distribution of data, in deciles, for the X-axis variable. Relative influence in parentheses.. 103
Figure 40. Partial dependence plots for the nine most influential variables that predict migrant density for transient landbird migrant species included in the analysis. Rug plots show the distribution of data, in deciles, for the X-axis variable. Relative influence in parentheses.. 104
Figure 41. Partial dependence plots for the nine most influential variables that predict migrant density for breeding landbird migrant species included in the analysis. Rug plots show the distribution of data, in deciles, for the X-axis variable. Relative influence in parentheses.. 105
Figure 42. Partial dependence plots for the nine most influential variables that predict migrant density for frugivorous landbird species included in the analysis. Rug plots show the distribution of data, in deciles, for the X-axis variable. Relative influence in parentheses.. 106
Figure 43. Partial dependence plots for the nine most influential variables that predict migrant density for all nocturnal landbird species included in the analysis. Rug plots show the distribution of data, in deciles, for the X-axis variable. Relative influence in parentheses.. 107
Figure 44. Partial dependence plots for the response of migrant density to distance from bright areas (top row) and distance from the Atlantic coast (bottom row) for breeding, transient, and wintering landbird migrant species included in the analysis. Rug plots show the distribution of data, in deciles, for the X-axis variable. Relative influence in parentheses. 108
Figure 45. Partial dependence plots for the response of breeding migrant density to 4 select predictors when modeled using data separated by sampling period (Period 1 on the left and Period 3 on the right). Rug plots show the distribution of data, in deciles, for the X-axis variable. Relative influence in parentheses. 109

Figure 46. Cluster plots of 45 transect sites along two component axes and designated as members of four labeled stopover functional types by colored ellipses. The number of sites within each cluster group is presented in parentheses after cluster label name..... 110
Figure 47. Boxplots of values of residual migrant stopover duration, insect density, distance to coast, and forest cover within 5 km among four stopover site functional type clusters (coastal fire escape, inland rest stop, convenience store, and hotel) comprised of 45 transect sites in the mid-Atlantic and Gulf of Mexico coastal regions during fall migration. Clusters with the same letters above boxes are similar with respect to mean values of each variable..... 111
Figure 48. Maps of classified fall migration stopover functional types for 45 transect sites near the Mid-Atlantic (top panel) and Gulf of Mexico (bottom panel) coasts. 112

List of Appendices

Appendix A. Radar analysis of bird migration stopover sites on the lower Delmarva Peninsula. Final report by Jeffrey Buler and Jaclyn Smolinsky. Submitted to Virginia Department of Game and Inland Fisheries August 2015. 38 pages.
Appendix B. Bird density in forested migration stopover sites on the lower Delmarva Peninsula and a comparison with radar-based predictive models. Final report by J. Andrew Arnold and Eric Walters. Submitted to Virginia Coastal Zone Management Program October 2014. 64 pages.
Appendix C. Radar analysis of bird migration stopover sites on the Delmarva Peninsula and validation of NEXRAD-based predictive models (Year 1 – 2013). Interim report by J. Andrew Arnold and Eric Walters. Submitted to Maryland Department of Natural Resources December 2014. 61 pages.
Appendix D. Maps of classified bird stopover density during fall 2008 through 2014 at 20 radars throughout the Northeastern United States. 20 pages.
Appendix E. Maps of coefficient of annual linear trend in mean autumn radar-observed bird density from 2008 – 2014 at 16 radars throughout the Northeastern United States. 16 pages.
Appendix F. Results of analyses of models explaining individual bird species densities from ground surveys. 23 pages.
Appendix G. Methods for studying stopover ecology of migrating landbirds with weather surveillance radar. Master's Thesis by Timothy Schreckengost. Submitted to University of Delaware Winter 2017. 76 pages.

Executive Summary

The national network of weather surveillance radars (NEXRAD) detects birds in flight, and has proven to be a useful remote-sensing tool for ornithological study. We used data collected during Fall 2008 to 2014 by 16 NEXRAD and four terminal Doppler weather radars (TDWR) in the northeastern U.S. to map and study the spatial distribution of landbirds shortly after they leave daytime stopover sites to embark on nocturnal migratory flights. Given observed variability in the precise timing of migratory exodus, we developed a new method to sample the onset of migration at the point of maximum rate of increase in bird densities aloft to consistently sample exodus across radars and days.

The mean linear trend in aggregate stopover densities of migrants indicated a 4% decline per year from the 2008 baseline density (29% decline over the seven years). Regionally, coastal Virginia and Maine had the steepest declines. The steepest increases in migrant densities across years occurred within the Delmarva Peninsula and in coastal Connecticut.

We used NEXRAD observations to develop models to predict potentially important stopover sites throughout USFWS Region 5. Observed NEXRAD data were positively correlated to observations from TDWR and NASA's S-Band Dual-Polarimetric Radar (NPOL), though not strongly. Predicted densities increased with increasing hardwood cover across multiple scales and with vegetation productivity. Contrastingly, predicted densities decreased with increasing agricultural, emergent marsh and coniferous land cover, but did not change with fraction of urban cover. Stopover density increased closer to bright areas and the Atlantic coast. Moreover, interactive effects indicated that migrants were more concentrated in forested areas that were both brightly lit and near the Atlantic coast. Large areas of predicted regionally important stopover sites were located along the coastlines of Maine, Long Island Sound, New Jersey, the lower Delmarva Peninsula, within the Adirondack Mountains, Catskill Mountains, and eastern Virginia.

We also created maps of classified stopover use during bimonthly periods and at multiple-scales. Migrant densities peaked along the Adirondack Mountains early in September, and along the Atlantic coast in late September with the passage of Neotropical migrants. Stopover densities peaked in the most northern extent of Maine and New England States in late October with the departure of temperate migrants.

Ground surveys conducted at 48 forested sites within the Delmarva Peninsula and Tidewater Virginia during Fall 2013 and 2014 revealed that nocturnal migrant densities pooled across species and for 14 individual species, after accounting for temporal phenology in their passage timing, were related to factors operating at multiple scales including food resources (primarily arthropod abundance in understory) and understory shrub density at a patch scale, and latitude and proximity to the Atlantic coast at a regional scale.

We integrated field survey and radar data to estimate relative stopover duration and to identify stopover functional types among 45 sites that included data from a past study near the Gulf of Mexico. We identified four functional types spanning the gradient of short rest stops to refueling stops with variable duration of stopover in relation to food abundance. The Mid-Atlantic sites were dominated by rest stops near coastal areas and lacked quick refueling stops due to low overall food abundance. The maps and ecological understanding produced can help inform conservation planning to protect and enhance stopover sites for migratory landbirds in the future.

Introduction

Avian migration is a complex and poorly understood phenomenon that occurs biannually in a variety of taxa. Over two-thirds of all the landbirds that breed in temperate North America migrate to and from nonbreeding areas in Mexico, Central and South America and the islands of the Caribbean (Keast and Morton 1980, Rappole 1995). Landbirds stop frequently during their migratory journey and spend upwards of 95% of their time resting and refueling at stopover sites rather than in actual migratory flight (Hedenström and Alerstam 1997, Alerstam 2003). The migratory phase could be a limiting period of the annual cycle in many of these species (Sillett and Holmes 2002, Newton 2006, Faaborg et al. 2010a, 2010b). For example, Black-throated Blue Warblers (*Setophaga caerulescens*), a Nearctic-Neotropical migratory species, sustain up to 85% of their total adult mortality during the migration periods. This loss is disproportionately high given that migration generally accounts for only 13 to 17 weeks (25–33%) of a bird's annual cycle (Sillett and Holmes 2002). Thus, identifying important stopover sites is a critical step in development of comprehensive conservation plans for migratory landbirds (Hutto 2000, Rich et al. 2004, Mehlman et al. 2005, Sheehy et al. 2011).

Interest and technology to improve our understanding of migration and where birds stopover has increased (Bowlin et al. 2010, Bridge et al. 2011, Buler and Dawson 2014). The national network of weather surveillance radars (NEXRAD) is one such research tool, detecting landbirds as they emerge from terrestrial habitats to initiate nocturnal migratory flights and providing comprehensive observations over large spatial extents to allow mapping their stopover distributions (e.g., Bonter et al. 2009, Buler and Diehl 2009, O'Neal et al. 2010, Buler and Moore 2011, Ruth et al. 2012, Buler and Dawson 2014, LaFleur et al. 2016). We recently mapped important migratory landbird stopover areas for the northeastern U.S. (USFWS Region 5) and assessed stopover use at national wildlife refuges using NEXRAD data (Buler and Dawson 2012, 2014). To do this, we developed simple and geographically-weighted linear models to predict stopover site use in portions of the region not sampled by the radars, based on landscape habitat composition, elevation, and geographic location. These initial maps were the first to offer site-specific information on stopover use to inform conservation planning. However, continuing to improve radar data processing methods, expanding the amount and robustness of processed radar data, and refining models to predict stopover distributions of migrating birds is essential for providing more-accurate information for bird conservation purposes.

One way to externally validate predictive stopover distribution models is to compare ancillary radar datasets of observed bird stopover densities with model predictions. The Delmarva Peninsula is a particularly important area for migratory birds in North America (Watts and Mabey 1994, Buler and Dawson 2014). Most of the lower Delmarva Peninsula is not covered by NEXRAD but is sampled by the NPOL radar operated by NASA through their Wallops Flight Facility with some overlap of the area sampled by the KDOX NEXRAD station. NPOL has finer spatial resolution and greater flexibility in its sampling strategy than NEXRAD radars, providing a more precise and accurate discrimination than was previously possible of the

sites and habitats from which migrants emerge. Through an agreement between The Nature Conservancy and NASA, NASA collected radar data at no cost in a unique opportunity to study bird distributions during migration within Lower Delmarva; we had a major role in coordinating data collection of NPOL. There are also four Terminal Doppler Weather Radars (TDWR) located within Region 5 that provide radar coverage outside that of the NEXRAD network. TDWR data are available to use for validating NEXRAD-based predictive models.

A broad-scale ground survey effort within the Delmarva region also provides data to compare the influence of factors operating at different spatial scales in explaining habitat use patterns of *en route* landbirds. Assessing factors at the habitat-patch (e.g., habitat composition and structure, food abundance), landscape (e.g., proportion of forest cover), and regional (e.g., proximity to ecological barrier) scales complement similar efforts done previously to examine multi-scale factors in explaining bird stopover distributions on the Delmarva Peninsula (Watts and Mabey 1994) and in other regions: Gulf Coast (Buler et al. 2007, Cohen et al. 2014, LaFleur et al. 2016), Great Lakes (Johnson 2013, R. Smith, unpubl. data), and Maine coast (Woodworth et al. 2014, McCabe and Olsen 2015).

Factors operating at multiple spatio-temporal scales can influence where birds stop over and how long they stay at individual sites along their journeys. Broad-scale factors, such as weather, preferred migratory route, proximity to a large water body, and energetic condition of a migrant, are generally extrinsic to habitat characteristics and can constrain access to high quality stopover habitats (Moore and Kerlinger 1989, Moore et al. 1990, Gauthreaux and Belser 1999, Schaub et al. 2004, Gauthreaux et al. 2005, Schmaljohann and Naef-Daenzer 2011, LaFleur et al. 2016). Fine-scale factors like habitat physiognomy and floristics, food resource availability, risk of predation, and competition will also influence habitat use by migrants (e.g. Moore and Wang 1991, Cimprich and Moore 1999, Moore and Aborn 2000, Rodewald and Brittingham 2004, Rodewald and Matthews 2005, Buler et al. 2007, Woodworth et al. 2014). All of these factors interact, resulting in scale-dependent habitat use patterns (Hutto 1985, Moore et al. 2005, Buler et al. 2007, Buler and Moore 2011, LaFleur et al. 2016).

Most research on stopover habitat use by migratory landbirds has focused only on localized, patch-scale approaches (Moore and Aborn 2000). At this scale, migrants generally partition themselves relative to food availability, suggesting this intrinsic factor is chiefly responsible for influencing observed trends in localized use of stopover habitat (Hutto 1985). But, even when considering broad, extrinsic factors in addition to patch-scale factors, food availability remains the definitive factor in determining migrant distributions at stopover sites (Buler et al. 2007).

Habitat structure is another patch-scale factor shown to influence stopover site selection, with migrants preferring structurally diverse habitats such as forest edges, where there is not only ample cover to hide, but greater food availability (Moore et al. 1995, Rodewald and Brittingham 2004). Variation in forest composition and structure can also affect the availability of these food resources. Hardwood forests, for example, generally contain a greater abundance and diversity of fruiting species than pine-dominated forests (Greenberg et al. 2012), and bottomland hardwood

forests in particular support a higher arthropod abundance (Buler et al. 2007). These results suggest that hardwoods tend to be a higher quality stopover habitat type than pinelands, at least in terms of food availability. While providing important information, patch-scale studies may mask broader extrinsic factors that are as influential, if not more, than intrinsic factors in driving site use by migratory landbirds. In fact, this bias may consequentially lead to an inaccurate conclusion on the overall importance of site-specific variables by overemphasizing local habitat variables (Petit 2000, Buler et al. 2007).

Alternatively, stopover habitat use studies conducted at a more extensive spatial scale, and only considering landscape and regional variables, have consistently demonstrated the influence of these particular factors on migrant use of stopover sites. Buler et al. (2007) determined that proximity to the coast and amount of hardwood forest cover were moderately important factors in determining overall migrant densities at the regional and landscape scales, respectively. Yet as with many studies not incorporating both fine and broad spatial scale variables, results must be interpreted with caution. For example, sites near the coast may appear to support more migratory birds, and thus be suggestive of an overall better quality habitat, but these increased densities may be an artifact of the "funneling effect" along the coast caused by misdirected and inexperienced juvenile migrants (Ralph 1978). When considering individual migratory trends across multiple years, inexperience and misdirection may be plausible explanations for use of coastal routes and subsequent stopover sites by passerines during their first year. While a juvenile's initial migratory route and wintering destination may be unpredictable, those surviving to the following year show high rates of overwintering site fidelity (Warkentin and Hernández 1996, Cresswell 2014).

Other extrinsic factors such as weather and body condition of individual migrants may strongly influence their decision to stop and their duration of stay at one stopover site over another. Given the stochastic nature of these types of variables, at times it is even possible that the proximity of a habitat to the nearest coast is a stronger predictor of migrant abundance than any particular patch-level factor (Buler et al. 2007). For example, a migratory bird that crosses an oceanic barrier in adverse weather and ends up in poor physical condition from prolonged flight may elect to land at a suboptimal habitat patch due to exhaustion rather than search for higher quality habitat (Moore and Kerlinger 1987). Alternatively, birds may concentrate in coastal areas via morning flights after being drifted over water at sunrise (Van Doren et al. 2016, Archibald et al. 2017). Gauthreaux and Belser (1999) demonstrated, via radar technology, that migrants landed nearly directly on the coast when faced with adverse weather, regardless of intrinsic habitat characteristics.

Assessing the conservation value of stopover sites from radar-based measures of relative migrant use would be enhanced if sites could also be classified by their ecological function (Mehlman et al. 2005). Ecological function of stopover spans a spectrum from 1) "fire escape" sites that offer a temporary place for migrants to rest with limited food resources during an emergency situation, 2) "convenience store" sites that offer a moderately safe place to rest with moderate food resources to allow some or prolonged refueling, and 3) "full-service hotel" sites

that offer a safe place with plentiful food resources for quick refueling. In addition to collecting data on food availability, measuring the mean stopover duration of individual migrants over the course of a season can help determine a site's general functional type.

Determining stopover duration through traditional mark-recapture or mark-resight methods requires intense sampling effort and thus can only be done at a few sites. O'Neal et al. (2012) proposed an approach to estimate stopover duration for waterfowl (i.e., days per duck) by dividing the total number of ducks counted from frequent aerial surveys (i.e., total days of stopover use by ducks) by radar measures of the nightly density of ducks leaving a site over the course of a migration season (i.e., total number of ducks that used the site). A similar approach combining radar data and ground surveys of migrants can be used to more feasibly determine relative stopover duration of landbirds across multiple sites over a broad geographic extent. This would aid in mapping stopover functional types and their distribution on the landscape, which is important for identifying "geographic areas where stopover habitat is scarce (i.e., holes in the stopover safety net), where fire escapes are inadequate or lacking, and where sites that receive heavy and consistent use may be lost" (Mehlman et al. 2005).

Our aim was to provide improved radar-based estimates of the spatial distribution of important stopover sites for southbound landbird migrants throughout USFWS Region 5 and a better ecological understanding of the relationships of migrants to stopover habitats through field surveys focused in the Mid-Atlantic Coastal Plain. Project results and products will allow the USFWS and partners to implement Strategic Habitat Conservation, protecting areas and habitats where they are likely to be most effective, and can contribute directly to the Bird Conservation Region plans of the Atlantic Coast and Appalachian Mountains Joint Ventures, Comprehensive Conservation Plans for Region 5 refuges, State Wildlife Action Plans, and broader region-wide planning for migratory bird conservation.

Objectives

1. Map observed autumn stopover incidence of migrating birds around 16 NEXRAD stations during seven years (2008 – 2014) and four TDWR stations during six years (2009 – 2014). The following are sub-tasks associated with this objective:
    a. Develop an algorithm to determine optimal sampling time of the onset of nocturnal migratory flight on a daily basis among radars.
    b. Estimate linear trends in seasonal mean stopover density over seven years among individual radar sample volumes with observed NEXRAD data.

2. Improve previously-developed models of migrant stopover incidence within USFWS Region 5 by incorporating more years of radar data (2010 – 2014) and additional explanatory variables within a more sophisticated modeling approach. The following are additional sub-tasks associated with this objective:

a. Validate the predictive statistical models using ancillary radar observations (TDWR and NPOL).
b. Develop locally-classified stopover use of modeled radar data based on moving window analyses at various spatial scales.
c. Run bimonthly predictive models for the entire region.

3. Assess the relative importance of various habitat features, including those at the patch scale (e.g. food abundance, habitat composition and vegetative structure), landscape scale (e.g. proportion of habitat types within surrounding buffers), and regional scale (e.g. proximity to major coastline, latitude); to determine their role in explaining migratory landbird use of forested stopover habitats within the Mid-Atlantic Coastal Plain during fall migration.

4. Model variability in relative stopover duration and classify stopover site function among selected sites by integrating radar observations with ground-based bird surveys.

Methods

Objective 1: Mapping stopover incidence with radar

Weather Radar Data Processing

From the National Climatic Data Center archive, we downloaded Level-II radar data from 16 NEXRAD radars in the northeastern U.S. (Figure 1) for five years (2010-2014) during the fall landbird migration period (15 August-7 November). We also downloaded data collected during autumn 2010 through 2014 by four TDWRs. Radar data were processed following methods of Buler and Dawson (2014) using new and existing software developed by the University of Delaware (UD). Data were pooled with the 2-year (2008 & 2009) dataset from Buler and Dawson (2014), resulting in a final dataset of seven years for mapping and modeling autumn bird stopover. Data from the earlier dataset were reprocessed according to the methods developed during the course of this project.

NEXRAD radars transmit horizontally polarized electromagnetic radiation at a wavelength of approximately 10 cm (S band) and a nominal peak power of 750 kW with a half-power beamwidth (3 dB) of 0.95º (Crum and Alberty 1993). The radars make 360° sweeps of the atmosphere every 10 minutes at five beam tilt angles (0.5°, 1.5°, 2.5°, 3.5° and 4.5° above the horizon) if operating in clear air, and every four to six minutes at 11 tilt angles from 0.5° to 19.5° when there is precipitation within the radar range; each set of sweeps constitutes a 'volume scan'. We used two data products produced by the radar: radar reflectivity factor, a measure of radar echo strength in units of Z (mm^6 m^{-3}) that is determined by the density and size of the targets in the sampled volume, and mean Doppler radial velocity, a measure of the mean target velocity (knots) relative to the radar. Both reflectivity and radial velocity are collected in polar coordinates within sample volumes (dimensions 250 m in range by 0.5° in diameter). Radar data from the 0.5° tilt angle were screened to identify bird-dominated nights, contaminated nights

(e.g., precipitation, sea breeze fronts, and smoke), and anomalous beam propagation (Buler and Diehl 2009).

TDWRs transmit radiation at a wavelength of 5 cm (C band) at a nominal peak power of 250 kW. We used the Level III long range base reflectivity scan product (a.k.a. TZL) for analysis, which has sample volume dimensions of 300 m x 0.5°. TZL sweeps are completed every six minutes at a tilt angle of 0.6°. We screened TDWR data to identify bird-dominated nights similar to NEXRAD data. However, because we only used one tilt angle sweep of data from TDWR, we used vertical profiles of reflectivity and target velocity (discussed below) calculated from the NEXRAD station nearest to each TDWR station. This meant that the sampling days for a TDWR station were constrained by the sampling days of the nearby NEXRAD station.

We distinguished migrating birds from insects and non-biological targets by quantifying the airspeeds of radar targets via vector-subtracting the wind velocity from the target ground velocity. We used radial velocity data from the 2.5° tilt angle during the peak of nocturnal activity (~ 3 h after sunset) to determine animal flight directions and airspeeds in conjunction with data on winds aloft archived by the North American Regional Reanalysis (NARR, Mesinger et al. 2006) following Farnsworth et al. (2014). These high resolution modeled wind data are available in three-hour composites across the U.S. at approximately 0.3° (or as fine as 32-km) resolution. We used these data to determine air speeds (u and v wind components) at nine geopotential heights ranging from 650-1000 mb within 100 km of each radar. Mean air speeds were then computed by weighting speeds by the relative density of animals at each height interval based on vertical profiles of reflectivity (VPR) calculated using methods outlined by Buler and Diehl (2009). The VPR is a function describing the ratio of the mean reflectivity of animals in the airspace at a given altitude relative to the mean reflectivity of animals aloft from 0 to 1750 m above the ground. Radar scans with mean animal air speeds greater than or equal to 5 m per s were considered bird dominated (Larkin 1991, Gauthreaux and Belser 1998). Only bird-dominated nights were used in the analysis.

Determining a suitable sampling time of migration exodus

Landbirds initiate nocturnal migratory flights *en masse* in an abrupt exodus near the end of evening civil twilight (Hebrard 1971, Åkesson et al. 1996, Gauthreaux and Belser 1998). Buler and Dawson (2014) interpolated migration exodus for all radars and nights to when the sun was 5.5° below the horizon using inverse distance weighting of the time differences between the radar volume scans collected immediately before and after the target sun elevation time point. However, they recognized that spatio-temporal variability in the timing of the onset of migration across the region and days could produce temporal sampling bias. So we developed a new approach to dynamically determine a suitable sampling time during the onset of migration to minimize any bias.

For this analysis we used data from the Dover, DE (KDOX) and Norfolk, VA (KAKQ) radars collected between August 15 and November 7 during the autumns of 2013 and 2014.

Concurrently, we conducted bird surveys in 29 forested sites in Delaware, Maryland, and Virginia that were stratified in each of three distance bands (10-20 km, 20-50 km, 50-80 km) from these two NEXRAD radars, and determined the mean daily migrant bird density at the ground along 500-m transects (see methods for Objective 3).

For each suitable sampling night, we interpolated reflectivity measures from volume scans to a series of time points at different sun elevation angles (1.5° to 10° below the horizon at 0.5° intervals) collected around the time of migrant exodus. We fit a logistic growth curve to the change in mean reflectivity through time to determine the sun angle at the inflection point of the curve (i.e., at the maximum growth rate) for each radar-sampled night (Figure 2). We then interpolated radar data to this empirically determined sun angle.

For each interpolated scan within a single evening time series, we estimated the vertically-integrated reflectivity (VIR) within each sample volume following previously-established methods (Buler and Diehl 2009, Buler and Dawson 2014). This approach is necessary since the radar beam systematically samples increasing heights as it propagates away from the radar and the VPR varies among radar scans. Each original reflectivity measure is divided by the mean VPR ratio within the sampled volume of airspace to produce an estimate of the mean reflectivity of birds aloft from 0 to 1750 m above the ground. We converted original reflectivity factor in units of Z to the more biologically-meaningful units of cm^2 km^{-3} (Chilson et al. 2012). We then multiplied reflectivity by the height of 1750 m to "flatten" the volumetric measure of reflectivity into a two-dimensional measure in units of cm^2 ha^{-1}, which represents the VIR as the total amount of reflected cross-sectional area of birds per hectare above the ground.

We correlated the mean interpolated radar data at the different static and "inflection point" sun elevation angles, averaged across sampling days, to the observed seasonal mean bird density on the ground at transect sites. To do this, we first georeferenced center transect lines within a geographic information system (GIS) and built 50-m wide buffers around transects to represent the area where we sampled birds with ground surveys. We intersected the two-dimensional boundaries of georeferenced radar sample volumes from around the KDOX and KAKQ radars with the buffered transects to identify the portions of radar sample volumes that coincided with transects. We extracted area-weighted mean VIR over each transect for comparison to ground bird densities. We used Pearson correlation tests and obtained 95% confidence intervals for correlation coefficients by bootstrapping the correlations using the "boot" package (Canty and Ripley 2014) within R (R Development Core Team 2016).

The correlation analysis indicated that the empirically-determined sun angle (i.e. the sun angle at the point of maximum growth rate in mean reflectivity) was the most-suitable time to sample migration exodus rather than using a static sun angle across all night and radars. However, we found that fitting of logistic growth curves to reflectivity during flight exodus was not easily automated, relied on some amount of subjectivity in winnowing down data points to include in fitting curves, and made strict assumptions about the shapes of curves. Therefore, we improved automation, reduced subjectivity, relaxed some data assumptions, and simplified the

process by fitting piecewise cubic spline functions to the data to determine the point of maximum rate of increase in reflectivity. We also restricted the sampling time to be within 15 minutes of the onset of flight exodus to minimize displacement of birds from their ground sources on nights when exodus is protracted. Note that this restriction rarely needed to be implemented.

Mapping and characterizing bird stopover use

Once an instantaneous volume scan for each night was interpolated, we estimated VIR for every sample volume within the scan. We averaged nightly VIR for each sample volume across all sampling nights and years to derive an overall seasonal mean and coefficient of variation in VIR. We also computed averages for four bimonthly (i.e. half month) periods from 1 September to 31 October across years and across the entire season for each year. We assessed linear trends in bird stopover use across years by fitting simple linear regression models to the mean annual VIR separately for every individual sample volume.

We georeferenced and mapped the nightly density of birds emigrating from stopover locations across years, characterized by the mean VIR (MN) and the mean coefficient of variation of VIR (CV). "Important" stopover sites were ranked from least (1) to most (5) important where (1) = MN < 50^{th} percentile, "low emigrant density", (2) = MN ≥50^{th} percentile and < 85^{th} percentile, "moderate emigrant density", (3) = CV ≥75^{th} percentile and MN ≥85^{th} percentile, "high emigrant density with high variability", (4) = CV > 25^{th} percentile and < 75^{th} percentile and MN ≥85^{th} percentile, "high emigrant density with moderate variability", and (5) = CV ≤25^{th} percentile and MN ≥85^{th} percentile, "consistently high density of emigrants". Observed radar data were classified regionally by pooling data across all radars and locally within each radar separately.

Objective 2: Modeling stopover incidence with radar

Modeling stopover distributions of migrating birds

We modeled bird stopover densities using observed MN and CV across the region. Spatially explicit modeling of ecological processes are often confounded by non-linear responses to and interactions between predictors, spatial autocorrelation effects, and over-fitting of imprecisely measured or non-uniformly sampled data (Valcu and Kempenaers 2010, Li 2016). We addressed these concerns using a machine learning approach, which accommodates both non-linearity in responses and autocorrelative effects among predictors and, through a process called boosting, reduces over-fitting to measured data (Maloney et al. 2012). Boosting is a sequential process where fractions of weak 'learner' models are added iteratively to reduce model variance. We chose generalized additive models (GAMs) as learners, allowing explicit quantification of responses to predictor variables.

We used the MATLAB (The Mathworks 2016) package 'bgam' (Mineault 2011), which bases boosted iterations on simple learner functions using a single predictor, in this case a step

function consisting of a step location (threshold) and response (offset). During each iteration, the fit is updated by adding a fraction (known as the learning rate or greed factor) of the learner which minimizes the remaining deviance. The model moreover partitions the data randomly into an ensemble of several subsets, and the final model is calculated as an ensemble average among subsets. Using subsets and fractional learning rates (stochastic gradient boosting) helps reduce over-fitting within the boosting process. We chose 20000 iterations, 7 subsets and a learning rate of 0.075, which we adjusted slightly if the model failed to converge. The model terminates early if subsequent boosts fail to decrease D^2 values (the current divided by maximal deviance, an equivalent to R^2 in GLM models). To speed computation, the package also utilizes MATLAB's parallel computing toolbox.

We were especially interested in quantifying 'typical' as opposed to 'total' stopover use across the fall season. We therefore quantified mean seasonal stopover use in each sample volume using the geometric mean as opposed to arithmetic mean in VIR, and truncated measurements with reflectivity values smaller than 0.001 and larger than 100 cm^2/ha. We further log-transformed mean VIR since the distribution of VIR among nights is typically left-skewed, i.e. low-intensity migration nights heavily outweigh intense migration nights. Modeling log-scaled mean VIR also meant that the additive BGAM factors became multiplicative factors determining predicted mean VIR. Variability in stopover was quantified by the coefficient of variation, i.e. the arithmetic mean divided by the standard deviation in VIR. Finally, we assessed within-season differences in stopover use by modeling bimonthly mean and variability in VIR. Bimonthly periods were 1-15 September, 15-30 September, 1-15 October, and 16-31 October.

We created a sampling grid based on Buler and Dawson (2014) comprised of 637,603 1-km square cells covering the northeastern U.S. For each cell, we computed mean values of spatially explicit predictors, broadly divided among four categories: geographic/regional, coastal, landscape, and corrective. Descriptions of predictors included in final models are listed in Table 1. To relate broad-scale regional patterns in stopover to the general NE-SW coastline along the Atlantic seaboard, we rotated the geographic axes (UTM coordinates) clockwise by 42° (see Figure 3). This resulted in two variables: X, southeastwards towards the coastline and Y, southwestwards along or down the coast. Since some biological and ecological processes will depend on latitude (e.g. daylight, temperature), we retained latitude as a predictor. Since coastal effects are known to act at sub-regional scales (typically within 50-100 km of the coast, Buler and Dawson 2014), we created a separate coastal-scale variable, distance to the coast with a maximal value of 150 km. Distance to both the Atlantic coast (dAtl) and to the Great Lakes (dGtL) were considered.

Landscape influences on migration and stopover are known to act at multiple scales with availability of hardwood forest playing a key role (Buler et al. 2007, Bonter et al. 2009). We considered the following landscape scale variables as predictors at 1- to 100-km scales: fraction of landscape from hardwood and mixed forest, coniferous forest, agricultural land, emergent marsh, and urban development derived from the National Land Cover Dataset (Homer et al. 2015), and mean and standard deviation of normalized difference vegetative index (NDVI)

collected at 16-day intervals at 250-m resolution obtained from the Global Moderate-resolution Imaging Spectroradiometer (MODIS, https://modis.gsfc.nasa.gov/) for each season. Since migrants are known to be attracted to bright nocturnal light sources, we considered a data set of intensity of artificial light at night (hereafter alan), which ranged on a scale from 0 to 63 and was computed from cloud-free composites of Defense Meteorological Satellite Program-Operational Linescan System (DMSP-OLS, https://ngdc.noaa.gov/eog/sensors/ols.html) 30-arc second grids for 2014. In addition to attraction to alan potentially causing enhanced stopover at bright light sources, migrants could instead be temporarily diverted towards these sources and choose more suitable stopover habitat nearby. We therefore also included a predictor quantifying distance to bright light sources (values of 60-63, encompassing 4.1% of values regionally). To account for possible measurement biases (despite rigorous processing following Buler and Dawson 2014), we included distance to the radar (dRdr) and elevation relative to the radar (relelev) as spatial predictors. These responses were not included when making predictions, but as an estimate to remove any potential biases. Finally, to ensure magnitude effects did not occur, we normalized all of these predictors by their extreme values to produce dimensionless variables ranging from 0 to 1 (less for interactions).

Model results were evaluated according to (1) predictor relative influence, defined as the number of boosts involving each predictor weighted by the 'gain' assigned by the model for each boost, (2) estimated responses of mean (MN) and variability (CV) in VIR to predictors, (3) predicted regional mean and variability in VIR as proxy for stopover use and (4) classification of stopover use following Buler and Dawson (2014). Predicted region-wide stopover density was estimated by smoothed responses to predictors, using an rloess MATLAB routine with a span of 5% of the data for landscape predictors at 1-km and 5-km scales, and 40% of the data for 50-km and regional scale predictors (e.g. proximity to the coast).

Preliminary selection of predictor variables and their appropriate scale followed a four-stage process. First, we computed spatial averages at each of the 1-km grid points within 10 distance windows (1, 2, 5, 10, 20, 30, 40, 50, 75 and 100 km) for the six landscape-related variables, NDVI mean and standard deviation, and artificial nocturnal light levels. To gauge apparent influence of these variables at these scales, we computed Pearson's correlation coefficients between each variable at all scales and the log-transformed geometric mean reflectivity (Figure 4). We also computed correlation coefficients between the predictors and between scales. From this analysis, and because the reflectivity data are presumably somewhat spatio-temporally smoothed around the exodus peak and departure sites, we chose to use predictors at 5-km scales. Since hardwood is proposed to act at multiple spatial scales, we also incorporated hardwood fraction at 1-km and 50-km scales. Subsequent sensitivity analysis bore this out, in that influence of other predictors at 1 km was always found to be less in comparison with 5-km levels. Also since urban cover and alan were highly cross-correlated (0.82 to 0.95 at scales of 2 km to 100 km, respectively), we decided to retain only distance to bright light as the predictor of influence of artificial light (correlation with urban cover: -0.49 to -0.67 between 2- and 100-km scales).

Since additive models do not automatically account for interactions among predictors, we identified potentially important interactions among the 136 possible two-way interactions between these 17 pre-selected predictors using boosted regression trees (BRTs) incorporating gradient boosting with R packages gbm (Ridgeway 2006) and dismo (Hijmans et al. 2015). Interaction terms were then added explicitly as predictors in the BGAM. Regression trees are based on nested bifurcations according to predictor values (Elith et al. 2008). We chose not to use BRTs exclusively since predicted responses would depend on marginal probabilities of predictors, reducing interpretability. We used learning trees of depth 2, i.e. limited to single interactions, and a learning rate of 0.075. Based on occurrence among boosts, we selected the most important interactions for inclusion in the BGAM models. Compared to BRTs, boosted GAMs generally provide a more easily interpretable model, presumably more robust and transportable, but also spatially smoothed.

We classified MN and CV for both the entire fall season and the four bimonthly periods. We also summed importance ranks across bimonthly periods to produce a Cumulative Stopover Importance Index that ranged from 4 (lowest importance) to 20 (greatest importance). This index allowed identification of regional hotspots that were consistently used throughout the season at high density. We further classified seasonal mean VIR at 10-, 50- and 150-km radii by classifying quantiles within spatial windows of these extents. In this way, sub-regional hotspots can be identified.

We validated our models by comparing predicted reflectivity at non NEXRAD-measured locations with measurements of mean VIR at the four TDWR stations and NPOL station. Because NPOL and TDWR operate using a different wavelength (C-band) than NEXRAD (S-band), reflectivity measures from these radars are not directly comparable. Therefore, correlations of relative reflectivity values of ancillary radars and NEXRAD model predictions were used to validate the models. See Appendix A for details about the analysis of NPOL data. We analyzed each of these data sets to identify reasonable cutoffs for mean reflectivity, and compared both the mean measured and model-predicted VIR with the parsed NPOL and TDWR data. In particular, the relation of this fit to distance from each radar source was examined.

Finally, we compared our machine-learning approach to the locally defined approach of Buler and Dawson (2014) using geographically weighted regression (GWR). Preliminary comparison of model fits to spatio-temporal exploratory models (STEM), another machine-learning approach (Fink et al. 2010), were also performed.

Objective 3: Explaining migratory landbird use of forests via field surveys

Bird Surveys

We established transects (500 m long) in 48 hardwood stands in Delaware, Virginia, and Maryland across a multi-sponsor collaborative project (Figure 5). Surveys at 24 of these sites were directly funded by this project and placed within 80 km of the KDOX or KAKQ NEXRAD stations. The other 24 sites were sampled through support from other sponsors (see Appendix B

& C). Where possible, transect locations were chosen based on seasonal mean observed reflectivity (i.e., relative emigrant bird density) during fall 2008 & 2009 as determined by Buler and Dawson (2014). We stratified transects within radar coverage areas into three distance bands based on their proximity to the nearest NEXRAD station (10-20 km, 20-50 km, 50-80 km). We chose 18 sites in areas with high reflectivity and 18 in areas with moderate to low reflectivity. This stratification was designed to allow for assessing any residual bias in radar measures after adjusting them for range bias. An additional 12 sites were chosen along Virginia's Eastern Shore, outside of existing NEXRAD coverage, based on predicted abundance (Buler and Dawson 2014). These 12 sites were partitioned equally among high and low densities, and bay or sea sides, and north to south over the lower Delmarva Peninsula.

All forested sites were at least 4 ha in size and, with the exception of those located at the southern tip of Virginia's Eastern Shore, separated from other sites by a minimum of 10 km. We used hardwood forest sites because this habitat type is the most abundant and consistent natural habitat type in the region. Most passerine migrants are forest-dwelling species, with previous findings showing that forests also are important to en route migrants (e.g., Buler et al. 2007). Sites were generally similar in their habitat characteristics, consisting of mostly-flat topography and with strong representations of hardwoods such as oaks (*Quercus* sp.), Sweetgum (*Liquidambar styraciflua*), Red Maple (*Acer rubrum*), and pines (*Pinus* sp.), most notably Loblolly Pine (*P. taeda*). See Plate 1 for a visual example of site characteristics. We also attempted to select mature forests, as prior research has shown this habitat type supports large numbers of migrants and is likely of great importance to conserving migratory species (Rodewald and Brittingham 2007).

Plate 1. Photograph of a typical hardwood-dominant forest habitat site along the Delmarva Peninsula, USA.
Photo credit: J. A. Arnold.

Birds were sampled between 15 August and 7 November of 2013 and 2014 along transects during a 30-min period (a pace of 1 km per hr) from sunrise to four hours post-sunrise, with time of transect surveys and field observers rotated regularly. This schedule allowed for each site to be sampled approximately twice per week, although surveying only occurred on days with favorable weather conditions (no rain and wind speeds < 24 kph as determined at the site prior to surveys). Species, number of individuals, method of detection (visual or aural), and sex and/or age (when possible) were recorded. Any birds in aggregate were recorded as a flock. Distance measurements were also recorded for all detections, and included: 1) observer location along the transect, 2) distance of detection from the observer, 3) perpendicular distance of detection from transect, and 4) vertical height of detection. Height and distances were recorded in distance classes because there is much measurement error in estimating distances (Alldredge et al. 2007): 0-5 m, 5-10 m, 10-15 m, 15-20 m, 20-25 m, 25-50 m, and >50 m within habitat. Flyovers and flythroughs were also recorded, although not included in detection probability analyses.

Food Availability

To assess the amount of food available at each site across the season, we sampled fruit and insect abundance during each site visit. Six 20 m x 20 m plots were placed alongside each transect at 75-m intervals. Sampling within the plots alternated each visit so that the 75-m, 225-m, and 375-m plots were sampled on one visit and the 150-m, 300-m, and 450-m plots on the following visit.

Fruit sampling consisted of recording all species of plants containing fleshy fruit within the plots, including their abundance, ripeness, and relative height. Number of fruits was binned as follows: 1 (1-10), 2 (11-25), 3 (26-100), 4 (101-250), 5 (251-1000), 6 (1001- 3000), and 7 (3001-10000). The ripeness was recorded as the percentage of unripe, ripe, and overripe fruits for each species and relative height was recorded as the percentage found in the understory, midstory, and canopy for each species following the Smith and McWilliams (2009) protocol for rapid fruit assessment (Plate 2). Fruit is an important food resource for many migratory bird species, and the presence of fruiting species has even been suggested to be more important than habitat structure in determining habitat use (Suthers et al. 2000).

Plate 2. Photograph of visual fruit abundance sampling within 20m x 20m plots.
Photo credit: J. A. Arnold.

Insect sampling was performed in two ways: 1) visual count of terrestrial arthropods, and 2) enumeration of arthropods from branch clippings, following established protocols (Cooper

Plate 3. Photograph of an Arachnid collected via branch clipping and stored in a vial with isopropyl alcohol. Photo credit: J. A. Arnold

and Whitmore 1990, Strong 2000, Buler et al. 2007). On each visit to a 20 m x 20 m plot, a visual count was conducted within one 0.5 m x 0.5 m ground plot within the larger plot. Visual surveys were conducted by standing over the ground plot for 3 minutes and recording the size (mm) and Order of any arthropod species. One branch clipping was taken from within the 20 m x 20 m plot and bagged; each clipping consisted of approximately 40 leaves from either the dominant site species or one of four common focal species: American Holly (*Ilex opaca*), Red Maple, Sweetgum, or Blueberry (*Vaccinium angustifolium*). Arthropods on or in the branch sample were collected and identified to Order and size (mm), and then placed in vials with isopropyl alcohol (Plate 3). Arthropod abundance within the understory is presented as a mean number per gram of branch and a mean number per m^2 for those detected during ground surveys. Clipped branches were weighed without drying.

Vegetation Sampling

Vegetation was sampled at each site once mid-season in 2013 using a modified protocol of James and Shugart (1970) within four 11.3-m radius circular plots along the transect centerline. Using the same six distances as for food sampling (75 m, 150 m, etc.), four locations were randomly selected at each site to place the plots. Tree stems with a diameter at breast height (dbh) less than 2.5 cm and with a dbh between 2.5 cm and 8 cm were counted and binned according to their respective dbh classes. Species and dbh were recorded for all trees with a dbh greater than 8 cm. Canopy height was calculated as the mean of the four tallest trees within each plot, measured using a clinometer. Canopy cover was measured using a crown densiometer by standing in the center of the plot and facing each cardinal direction. Vegetation coverage estimates also were obtained for the ground, shrub (<2 m tall), vine (in canopy), and midstory at 1-, 2-, 3-, 4-, and 5-m locations in each of the four cardinal directions (for a total of 20 measurements in each plot); presence or absence of vegetation was assessed via an ocular tube reading. Leaf litter depth was recorded to the nearest millimeter at locations 4, 8, and 12 m from the plot's center in each of the four cardinal directions, for a total of 12 litter depth measurements. Ground cover was measured within a 5-m radius of the plot center, and included percent cover of forbs, ferns, mosses, greenbrier, vines, marsh, downed logs, and shrubs. Within each 11.3-m plot, a smaller 5-m radius circle was established and used for shrub density measurements: stems less than 0.5 m in height and less than 3 cm diameter were counted and identified to species.

We also considered remotely-sensed patch-scale variables measured within 25 m of transects. We included the seasonal mean NDVI aggregated from measurements taken at 16-day intervals and 250-m resolution that were used in the radar-based stopover distribution models. To quantify attraction to nocturnal light sources, we considered a dataset of zenith artificial sky luminance as a ratio to the natural sky brightness as a measure of artificial light at night with a

spatial resolution of 742 m. The dataset was computed by Falchi et al. (2016) by compiling data from the Visible Infrared Imaging Radiometer Suite Day/Night Band sensor on the Suomi National Polar-orbiting Partnership satellite over 6 months during 2014. We measured the mean sky brightness over each transect. We also measured the distance of each transect to "bright" sky areas. We defined "bright" sky areas as minimally 5 times natural values (~870 μcd/m^2), the level at which the Milky Way is invisible to the human eye (Falchi et al. 2016).

Regional and Landscape Data

Stopover habitat data at the landscape level were obtained by creating buffers around each survey site and generating measurements for land cover types occurring in the surrounding landscapes. This was achieved using 'extract by mask' in ArcGIS, a tool that provides an output of values from a defined spatial area using raster data. Spatially explicit landscape data were obtained from the 2011 National Land Cover Database (NLCD 2011). The NLCD 2011 (Homer et al. 2015) database separates land cover types into 20 unique classifications; our samples included open water, four levels of development, barren land, three forest types, two scrubland types, four herbaceous land cover types, two types of agricultural land, and two wetland cover classifications.

Buffers were placed around each transect survey location, using both 1-km and 5-km radii to account for habitat variation at differing scales, and the cell values for each land classification extracted for analysis (Figure 6). Similar classifications, such as low and medium development or pastures and cultivated crops, had their output values combined while some such as barren land were not considered at all, resulting in eight land cover categories; the proportion of each category within the 1-km and 5-km buffers were used in analyses (Table 2). Note that for terrestrial habitats the proportion is that of the total land area (i.e., with water area excluded from the total area).

Regional metrics were obtained through a variety of methods. Survey sites were placed into one of four categories based on their location (Delaware, Maryland Eastern Shore, Virginia Eastern Shore, Virginia), referred to as 'Region' in the dataset, with each region containing 12 sites. Measurements of both distance to the nearest coast and distance to the Atlantic Ocean were obtained for each transect location in ArcGIS via the 'measure' tool. Latitude, collected manually with a GPS while conducting transect sampling, was also included in the potential analysis dataset.

Data Analysis

We estimated detection probabilities and migrant densities within R (R Development Core Team 2016) and the extension package 'unmarked' (Fiske and Chandler 2011). All covariates except for observer were scaled before analysis. Temperature, wind and sky measurements, and observer were incorporated as covariates. All nocturnal migrant landbirds were lumped to ensure adequate sample size. We used detections of nocturnal migrants from all

distances within the habitat to fit a detection function. We then tested models using no, single, and multiple covariates among half-normal and hazard rate detection functions. We used Akaike's Information Criterion adjusted for small sample sizes (Hurvich and Tsai 1989) to rank models based on their ability to explain the data (Akaike 1973). Using the top-ranked detection function model, we computed a mean visit density (birds per hectare per visit) for each transect. Subsequent analyses were run using these detection-probability adjusted migrant densities.

Patch, landscape, and regional habitat variables for each survey site were assessed to determine which factors were most influential in determining the use of stopover sites by migrants. We hypothesized that food availability, and specifically that of arthropods over ripe fruit, would be the best predictors of migrant density. We also hypothesized that, to a slightly lesser extent, habitat buffers such as hardwood forest or water at the landscape scale and distance to the ocean and latitude at the regional scale would influence densities. Lastly, we predicted that these trends in importance, and subsequently the level of influence each variable exhibits, would differ between species and be a result of migration phenology, measured as a function of sampling period.

For all analyses, surveys without all covariates recorded (e.g. survey efforts missing fruit and invertebrate sampling data) were not considered. Additionally, any predictor variables showing unusual discrepancies in their data, and without proper justification, were excluded. For example, site-specific features such as midstory cover and canopy height, while both likely very valuable habitat metrics to consider, were collected inconsistently, resulting in a measurement bias and unusable data.

A correlation analysis was run on all covariates to identify variables that exhibited high multicollinearity (Table 3). Log-transformations were conducted in R on raw data such as food measurements that exhibited non-linearity or did not meet Gaussian assumptions. Preliminary tests to examine for autocorrelation in the data were run in R using the 'acf' function for temporal data, and the Moran.I function in the 'ape' package for spatial data (Paradis et al. 2004). Variables exhibiting high autocorrelation were removed from future consideration when building models. For example, our summarized variables of density measurements for invertebrates detected on branch clippings (InvPerGrBr) were closely correlated with our measurements for Arachnid densities (InvBrAR) and thus we excluded InvBrAR from the analyses. We included 21-day long sampling periods (Period) to characterize seasonal variation.

Analyses were conducted in R using boosted regression tree (BRT) techniques within the packages 'gbm' and 'dismo', and the gbm.step function (Ridgeway 2006, Hijmans et al. 2015). BRTs allow for the modeling of complex functions, as well as quantifying variable interactions, without the need to worry about common analytical issues such as handling different variable types (i.e. categorical, continuous), including additional uninformative variables in models that lead to a reduction in model power, and considering a priori assumptions regarding variable relationships (Ridgeway 2006, De'Ath 2007, Elith et al. 2008, Buston and Elith 2011). We did not use BGAM models for the survey data analysis since we were not interested in creating smoothed model predictions, only explanatory models.

BRT model development requires the adjustment of specific parameters to determine the best fitting model with the greatest performance. These parameters included 'learning rate' (lr; i.e. shrinkage parameter indicating amount each regression tree is contributing to the overall final model) and 'tree complexity' (tc; interaction depth determining the level of independent variable interactions allowed at each split) to identify the optimal 'number of trees' (nt; number of iterations) required to obtain the greatest model accuracy. Model performance can additionally be improved by introducing stochasticity, which in the case of gbm is accomplished by denoting a portion of data to randomly select each step via 'bag fraction' (Elith et al. 2008, Buston and Elith 2011). For all models and analyses, we used a bag fraction of 0.5 and tree complexity of 2 (i.e. allowing simple two-way interactions among predictor variables). Learning rates were adjusted following general guidelines to produce around 1,000 trees in the final ensemble model (De'Ath 2007, Elith et al. 2008). A 10-fold cross-validation (CV) was implemented within each developing gbm.step model to progressively test for and ensure that the final model's fit is still general enough for use on other data, and thus reducing the chance of overfitting (Elith et al. 2008, Buston and Elith 2011).

Our final ensemble of models developed and used in all analyses included 37 predictor variables. We fit separate models for five species groups including all nocturnal migrant species, Neotropical migrant species (i.e., primarily summer breeders), transient species that only occur as passage migrants, species that overwinter in the region, and migrants that are primarily frugivorous during fall migration. We also fit models for individual migrant species that were detected most frequently. For each analysis conducted, a ranked list of the relative influence of each predictor variable was produced, along with partial dependence plots that visually depicted the effect of a particular predictor variable on the response variable while controlling for the effects of all remaining predictor variables in the models. The sum of these relative influence measurements (when scaled) equals 100% for each model and, while all non-zero contributions are still considered important variables (Elith et al. 2008), in subsequent discussion of results we focus on those variables with 5% or more relative influence. Interactions between predictor variables were also automatically calculated for each model, and the most influential interactions are also presented as tables. The goal of these analyses was to use these BRT models to assess which ecological variables of interest, including temporal trends in localized factors such as food availability as well as spatially-explicit metrics such as shrub density at the local scale and proportional buffers at the landscape scale, showed the greatest influence on determining the density of migratory species at Mid-Atlantic forested stopover sites.

Objective 4: Classifying stopover site function

We used data across two fall seasons from 27 of the transect sites that fell within the KDOX and KAKQ radar ranges (Figure 7) to derive relative stopover duration after O'Neal et al. (2012). To get a greater sample size of sites, we added data from 18 forested transect sites near the Gulf of Mexico that were sampled using identical methods during autumn 2003 and 2004 and were located near the KMOB radar in Mobile, AL, and the KLIX radar in Slidell, LA (data from

Buler et al. 2007); radar data were processed using the same methods as well. According to the O'Neal et al. (2012) approach, observed bird density at the ground is considered a relative measure of bird use days given that individuals can be recounted during repeat visits. The quotient of mean daily migrant density on the ground (an index of the total number of migrant use days) divided by the mean daily VIR (an index of the total number of unique birds) provides a measure of relative stopover duration in units of days per cm^2 of reflectivity. This approach assumes that the mean daily averages of birds on the ground and birds emigrating measured by each technique are unbiased. However, given that not all sample volumes of radar data over survey sites were comprised purely of forested habitat, they may reflect aggregate emigrants from a mixture of habitats that likely do not harbor the same migrant densities as forests, and therefore may introduce measurement bias. We attempted to statistically control for this potential bias of emigrants emanating from non-forested habitats by fitting a linear regression between the amount of forest cover within radar sample volumes over sites and stopover duration and using the residuals of the regression as our measure of relative stopover duration. Relative stopover duration is an important metric to aid in evaluating how migrants are using a site.

We clustered transect sites into three a priori stopover functional groups based on four variables: relative stopover duration, amount of forest cover within 5 km, distance of site to the nearest coastline, and seasonal mean insect density at the site using the Partitioning Around Medoids (PAM) algorithm of Reynolds et al. (2006) and package 'cluster' in R (Maechler et al. 2016). This approach minimizes dissimilarity among members within clusters. Because cluster group sizes differed and may have had unequal variances, we used a Games-Howell post hoc test (Games and Howell 1976) to determine if there were significant differences in clustering variables between functional types. Because initial clustering produced groupings of only two classes within each geographic region (Gulf Coast or Mid-Atlantic), we increased the number of clusters to four post hoc so that each region had at least three clusters represented. Functional types were identified based on the values of clustering variables within each cluster post hoc.

Results

Objective 1: Mapping stopover incidence with radar

On average, 18% of all nights were suitable for sampling migrants at exodus for mapping stopover distributions (Table 4). However, there was an order of magnitude of variability in the number of sampling nights among radar and years. The number of suitable sampling nights for a given season ranged from 2 to 30 among the NEXRAD radars. The most common sources of contamination of radar data included precipitation (48% of all screened nights), insect-dominated flights (14%), and anomalous radar beam propagation (14%).

Determining a suitable sampling time of migration exodus

We analyzed the onset of evening flights from the KDOX radar for 12 days during fall 2013 and 10 days during fall 2014, and from the KAKQ radar for 15 days during fall 2013 and 7 days during fall 2014. Mean reflectivity increased through the night, indicating an increase in abundance of birds in the airspace that generally followed a logistic growth curve (Figure 8). The daily average increase in reflectivity started when the sun was 2.5º below the horizon, indicating the onset of nocturnal migration. When we modeled logistic growth curves for individual days, the inflection points at a given radar and year tended to occur at a later time (lower sun angle) as the season progressed (Figure 9).

We tested correlations between seasonal mean migrant densities at 27 transects during 2013 and 2014 that were within the KDOX and KAKQ radar ranges and seasonal mean radar reflectivity measured at different sun elevation angles. The bootstrapped mean correlations were low to moderately positive and did not vary much across the range of sun angles tested (Figure 10). However, the peak mean correlation occurred at a sun elevation of 6° below the horizon, which is the end of civil twilight.

Inflection points derived from daily exodus curves varied within years and among radars, ranging from sun angles of 3.06° to 8.12° (mean = 5.38±0.47) below the horizon in 2013 and from 3.28° to 10.16° (mean = 6.41±0.65) in 2014 for KDOX. For KAKQ, the sun angle at the inflection point of the curve ranged from 3.01° to 10.03° (mean = 5.45±0.5) in 2013 and from 3.05° to 8.6° (mean = 5.24±0.7) in 2014. When pooled across radars, the mean correlation of mean radar reflectivity at the peak of exodus to ground bird densities was similar to that of radar data sampled at the nearest static sun elevation angle across days (5.5°) (Figure 10). However, sampling radar data at the time of peak exodus for a given night and radar produced more consistent stopover maps of migrant distributions for individual nights compared to maps of radar data sampled at the static sun elevation angle of 5.5° below horizon (Figure 11). Thus, sampling at a fixed time close to the average peak exodus across nights creates subtle but apparent temporal sampling error due to daily variability in nightly flight timing. This was also apparent at the radar scale when we compared the range of inflection points determined for individual sampling nights for 18 radars in the eastern U.S. (Figure 12). For this we used data from 11 radars from this study and 7 radars analyzed in La Puma and Buler (2013). Latitudinal differences in timing of flight exodus indicated that some radars were always sampled too early in the exodus when using the 5.5° sun angle as in Buler and Dawson (2014). We used the time of peak migration exodus when sampling radar data for all subsequent analyses and mapping.

Mapping observed stopover distributions

We produced classified stopover use maps for each radar (Appendix D) and a map of all radars pooled and then classified across the region (Figure 13). Areas of observed consistently-high bird density occurred within portions of Maine, the Adirondack Mountains, southern New Jersey, the Delmarva Peninsula, and the Tidewater region of Virginia.

Annual trends in observed bird stopover densities pooled across radars showed that about 6% of sample volumes exhibited an increasing trend above 0.1 cm^2/ha/year, while 17% of sample volumes exhibited a decreasing trend below -0.1 cm^2/ha/year (Figure 14). The mean trend across all radars was -0.030 ± 0.007 cm^2/ha/year. This is equivalent to an annual decline of 4.2 ± 1.0 % per year in bird density (based on mean 2008 bird density), or 29% over the seven year period. The most extreme declines occurred in Maine and Virginia. Strong annual increases in bird densities occurred along the coast of Connecticut and within New Jersey and the Delmarva Peninsula. Maps of annual trends at individual radars are presented in Appendix E.

Objective 2: Modeling stopover incidence with radar

Predictor selection and influences

Table 5 lists, for both mean and variability in VIR (MN and CV, respectively), the 11 interaction terms between the predictors described in Table 1 that were considered significant based on the BRT analysis. Interactions were dominated (8 of 11) by regional or coastal scale predictors (5 involving X or Y and 5 involving dAtl, dGtL and dBrLt). Among "landscape" predictors, fractional hardwood cover at 50 km (hw50) was involved in 6 of 11 interactions. Because of the non-linear response of the BGAM factors, and to enhance flexibility in the geographic (flyway-scale) pattern, we modeled responses to all four permutations of the spatial variables X*Y, X*(1-Y), (1-X)*Y, and (1-X)*(1-Y).

The BGAM model typically achieved D^2 (deviance explained) values of ~0.7 when fitting MN and ~0.5 when fitting CV. Convergence and fit depended on the chosen predictors and modeling parameters, but improvement in D^2 was marginal using more than 5,000 boosts. We used 20,000 for the main fits and 10,000 for the bimonthly fits.

Model results indicated that regional and coastal predictors were most influential to both MN and CV (i.e., stopover densities) within 1-km grid cells (Figure 15). Among landscape predictors, hw50 was predicted to be most influential to both MN (Figure 16) and CV (Figure 17). Following the spatial predictors and their interactions, hardwood cover was the most influential predictor: the six most influential landscape-based predictors involved fractional hardwood at 50-km and 5-km scales.

For predicted mean stopover density, in addition to geographic-scale effects, there were consistent responses to land cover and coastal predictors. Highlights are presented in Figure 18 - Figure 22 (note that all predictors have been normalized). MN increased with increasing hardwood cover at each scale and also with seasonal mean NDVI. Contrastingly MN decreased with agricultural, emergent marsh and coniferous fraction, but did not change with fractional urban cover. Instead, the response to distance to bright light indicated increased stopover density at moderate and close distances (100 – 0 km). Moreover, the interaction term between hardwood fraction at 50 km and distance to bright light indicated that stopover was concentrated in brightly lit wooded areas. Stopover was also concentrated within 30 km of the Atlantic coastline, but the Great Lakes elicited no clear coastal effect. Notably, the strongest responses involving both

distance to bright lights and distance to the Atlantic coast were interaction terms with fractional hardwood cover at 50 km. Responses to these interaction terms indicated that above and beyond singular effects, stopover was extra concentrated in wooded areas that were both brightly lit and near the Atlantic coast.

Regarding daily variability in VIR, hardwood at 50-km scales was highly influential, being involved in 6 of the top 7 landscape predictors (the other being hardwood at 5 km). Responses in CV to predictors were typically opposite of responses in MN, i.e. variability was predicted to decrease with increasing fractional hardwood, NDVI and proximity to the Atlantic coast, and to increase with increasing fractional agricultural and coniferous cover. However, CV increased closer to bright light sources similarly to when modeling MN. Also, while response in CV to fractional developed (urban) land cover was generally weak, MN spiked sharply near the heaviest development.

Of the two corrective predictors, distance to the radar had a stronger influence and exhibited a clearer pattern on observations than relative elevation. These both suggested that 'sweet spots' remained in the configuration of the radar and observations, allowing estimation of the 'true' vertically integrated (VIR) signal given the observations and location relative to the receiving station.

Influence of and response to predictors in the bimonthly models generally resembled those of the seasonal models, e.g. regarding fractional land cover, and proximity to both artificial light and to coasts (Figure 23 - Figure 26). Some patterns were less clear and less consistent among bimonthly periods, but response to the Atlantic coast became progressively weaker through the season and indiscernible during the last bimonthly period.

Predicted stopover distributions

When mapped onto the entire region, predicted mean VIR (Figure 27) revealed broad patterns of reflectivity, with higher stopover densities in the Adirondack, Catskill and Pocono Mountains, near the Allegheny National Forest, towards the Atlantic coast and St. Lawrence River, and along the northern and southern portions of the Atlantic coast. This contrasts with Buler and Dawson (2014), who predicted lower density in the northeastern portions of the region and higher densities in the upper Delmarva Peninsula. Here, the lowest densities are predicted in interior and coastal New England and to the south of Lake Ontario and eastern Lake Erie. Predicted variability in stopover (Figure 28) was highest near urban centers, along much of the Atlantic coast and along topographic ridges.

Classification maps

Regional classification over the entire fall season (Figure 29) identified the NE and SE Atlantic coasts; the Adirondack, Catskill, and Pocono Mountains; St. Lawrence lowlands; and forested areas of coastal Connecticut as consistent high-use stopover areas. It is interesting to note that the highest density areas were rarely highly variable (the yellow-coded regions in the

maps), perhaps reflecting adaptation among migrants to congregate in reliably good stopover habitat.

Telescoping into smaller scales, we see that while classification within the 150-km scale (Figure 30) generally resembles the regional classification, the 50-km classification identifies important areas throughout the region. From this figure, the Atlantic coast stands out in particular, possibly reflecting the prevalence of juveniles to drift coastwards. At the 10-km scale, classification can reveal local hotspots more evenly stratified within counties (e.g. riparian forests throughout the Delmarva Peninsula).

Bimonthly classifications (Figure 31) were overall similar to the seasonal classifications. While stopover use in southeastern portions of the study region gradually decreased through the season, there was a gradual increase in stopover densities to the northeast, especially along the St. Lawrence River in the last bimonthly period, 16 – 31 October. These changes in bird distributions are more easily seen when looking just at predicted mean VIR during the bimonthly periods (Figure 32). Migrant densities peaked along the coast of Maine and in eastern Virginia during the last half of September. After that there were more migrants arriving in than leaving southern portions of the region, and we only sampled departures. Migrant densities close to the northernmost borders of the U.S. peaked in the last half of October when a last rush of temperate migrants (e.g., White-throated Sparrows, juncos) depart for southerly wintering areas. By summing the ranking of stopover use in terms of importance across the four bimonthly periods, we were able to resolve those areas that were regionally important throughout the entire autumn migration period (Figure 33). Some of these areas included the Adirondack Mountains, the eastern coast of Maine, the lower Delmarva Peninsula, and the western shore of the Chesapeake Bay in Virginia.

Validation with independent radar

Observed NEXRAD data were consistent with but not tightly correlated with the observed TDWR and NPOL data. Regarding observed mean VIR, the fit between the NPOL and the KDOX data was reasonable ($R^2 = 0.51$, Figure 34), but the overlap zone between the NPOL and KDOX coverage areas was rather narrow (45-60 km to the south of KDOX). The relation between distance to the NEXRAD stations is evident when comparing reflectivity between NEXRAD and TDWR data, suggesting a dichotomy between shorter (10-40 km) and longer range NEXRAD measurements (Figure 35, $R^2 = 0.17$). Indeed, higher correlations are found when limiting these data to within 40 km of the NEXRAD radar ($R^2 = 0.69$). However, fits regarding variability in VIR between these radar measurements were rather low (not depicted, $R^2 = 0.25$ for TDWR and $R^2 = -0.05$ for NPOL data). Effects of distance to NEXRAD when correlating NEXRAD data with data from the NPOL and TDWR radars were less apparent (e.g. Figure 34 & Figure 35 for mean VIR). Limiting data according to distances to these radar stations did not consistently nor significantly improve the fits.

Validating the BGAM to the independent radar data sets (Figure 36 & Figure 37) regarding mean VIR yielded correlations similar to those between observed NEXRAD data and

the independent radar data measurements. The correlation coefficient between the BGAM and TDWR data was $R^2 = 0.33$ (0.44 for locations greater than 20 km from the radar) and between the BGAM and NPOL was $R^2 = 0.40$. Restricting the TDWR data to between 20 and 45 km from the radar improved the fit with BGAM predictions to $R^2 = 0.48$ (versus 0.33), but there were overall no consistent effects of distance to the TDWR and NPOL radar. Fits regarding variability in VIR were more reasonable in comparison to BGAM predictions: $R^2 = 0.40$ with the TDWR data and $R^2 = 0.30$ for the NPOL data (versus $R^2 = 0.25$ and $R^2 = -0.05$ with NEXRAD versus TDWR and NEXRAD versus NPOL, respectively).

Objective 3: Explaining migratory landbird use of forests via field surveys

We conducted a total of 1,593 avian transect surveys during the two fall migration seasons, 836 in 2013 and 757 in 2014. On average, we visited each survey site 17 times (range 13-20) in 2013 and 15 times (range 13-18) in 2014 (Table 6). After omitting surveys with missing variable measurements, a dataset containing 1,505 transect surveys and accompanying habitat and environmental metrics remained (772 in 2013, 733 in 2014) and were used in BRT analyses.

We detected and identified 128 bird species on the surveys (Table 7). Nocturnal migrants comprised 74.92% of all migrant birds detected in 2013 and 75.46% in 2014. Seasonal mean migrant densities for transects ranged from 1.09 to 5.23 with an overall mean of 2.75±0.13 birds per hectare per visit in 2013, while detection probabilities ranged from 0.23 to 0.73 with a mean of 0.53±0.02. In 2014, seasonal mean migrant densities for transects ranged from 1.16 to 8.88 with an overall mean of 2.87±0.24 birds per hectare per visit, while detection probabilities ranged from 0.19 to 0.73 with a mean of 0.52±0.02. Neotropical migrant species showed a steady decline in detections throughout the autumn, while temperate migrants showed a steep increase in detections in early October and peaked in late October (Figure 38). Accordingly, August and September were dominated by detections of Neotropical migrants, while October and November were dominated by temperate migrant detections.

Nineteen models of migrant density were developed for five non-exclusive groups of nocturnal migrant species and 14 individual nocturnal migrant species with at least 90 detections across all surveys (Table 8). The individual species included six breeding species, six overwintering species, and two transient (passage) species. Adjustment of model parameters resulted in use of learning rates ranging from 0.025 down to 0.001, and number of trees in each final optimized model ranged from 1,100 to 1,800. Out of the 37 total predictor variables that were included in each BRT model, 25 variables (added across all models) showed a relative contribution of 5% or greater, the chosen limit for signifying predictor variables with high enough influence to warrant interpreting them in our discussion for individual species (Table 9) and grouped species (Table 10). Model fits were generally moderate based on proportion of deviance explained (0.16 to 0.64) and cross-validation correlation (0.30 – 0.64). Sampling period was included as one of the most highly influential predictors for all models, and showed strong interactions with other variables in each model as well. It should be noted, however, that these

observed interactions with “Period” may in many cases simply reflect relationship changes with predictors when the avian species of interest was generally absent.

Nocturnal Migratory Species Groups

Winter migrant density was the greatest during the last half of October and increased sharply with proximity to the coast within 15 km of the coast (Figure 39). Winter migrant density was best explained by period and distance from the coast. Although these two variables accounted for 71% of total relative variable influence of the model, other responses included increasing migrant density with increasing abundance, presence of partridge berry (*Mitchella repens*) fruit, increasing stem density and visual cover of the shrub layer, and increasing latitude. There were no strong interactions besides those between period and several predictors (Table 11).

Transient migrant density peaked during the first half of October, and was best explained by period, agriculture cover, shrub cover, abundance of Lepidoptera larvae in understory, abundance of arthropods on the ground, urban cover, distance from the coast, and total abundance of fruits. It increased with increasing agriculture, shrub cover, Lepidopteran larvae abundance, arthropod abundance, urban development, and proximity to the coast (Figure 40). Interactions were rather weak (below 1) (Table 12).

Breeding migrant density was best explained by period, NDVI, arthropod density in the understory, shrub cover, and black gum (*Nyssa sylvatica*) fruit abundance. Breeding migrant density declined steadily with period, varied with NDVI (declined steadily with NDVI with a spike upwards at NDVI of 9000), declined with increasing arthropod density, increased sharply with shrub cover above 80%, and peaked at moderate amount of black gum fruit abundance (Figure 41). There were strong interactions between hardwood forest cover and arthropod abundance in the understory (Table 13), such that the relationship of migrant density with hardwood forest cover went from being positive at low arthropod density to being negative at high arthropod abundance. Additionally an interaction between litter depth and NDVI indicated that at high NDVI values, migrant density was positively related to litter depth, and at low NDVI values, migrant density was negatively related to litter depth.

Frugivorous migrants were detected primarily during the last half of October. Frugivorous migrant density was best explained by period, total fruit abundance, distance from the coast, partridge berry fruit, and arthropod abundance on the ground. Their density increased with increasing total fruit and partridge berry abundance, proximity to the coast, and declining arthropod abundance on the ground (Figure 42). There were no strong interactions besides those with period and several predictors (Table 14).

Total nocturnal migrant density was best explained by period, fruit abundance of partridge berry and black gum, distance from the coast, water cover, fruit abundance of holly and all fruits, latitude, and shrub cover. Nocturnal migrant density was by far the greatest during the last half of October, (Figure 43). Migrant density generally increased with more fruit of partridge berry, black gum, all fruit, and variably with holly. It also peaked at the coast, declining sharply

until 40 km away from the coast, and then rising again beyond 60 km. Migrant density was also greatest with presence of water in the landscape, increasing latitude, and increasing shrub cover. Interactions of note include an interaction between water cover and black gum fruit abundance (Table 15) such that water cover was stronger where black gum fruit abundance was low. Species groups had different responses to two predictors, distance from bright lights and distance from the coast, which were of great importance for radar-based stopover density models (Figure 44). Transient migrant density was greater with proximity to bright lights, peaking at 30 km from bright lights. Breeding migrants displayed a mixed reaction with density generally increasing with distance, but also showing a small peak in density around 30 km from bright areas. Wintering migrant density was greatest at distances farthest from bright lights. Wintering migrant density also decreased monotonically with distance from the coast. Breeding and transient migrant density within 40 km of the coast also decreased with distance from the coast. However, they both increased with distance from the coast beyond 50 km, with breeding migrants having the relatively highest densities beyond 60 km.

Given the overall mixed reaction of breeding migrants, which matched elements of the responses of both transients and residents, we conducted a post-hoc analysis for which we modeled breeding migrant species densities with data from two sampling periods separately: early in the season when breeding migrants were likely dominated by resident individuals (Period 1 [Aug. 15 – Sep. 4]) and later in the season when they were likely dominated by transient individuals (Period 3 [Sep. 26 – Oct. 16]). The two models produced markedly different response functions of note (Figure 45). During period 1, breeding migrant density was positively related to hardwood forest cover in the landscape, distance from the Atlantic coast, and distance from bright areas, and negatively related to arthropod abundance in the understory. Conversely, during period 3, breeding migrant density was negatively related to hardwood forest cover in the landscape, distance from the Atlantic coast, and distance from bright areas, and positively related to arthropod abundance in the understory.

Individual species varied in both the direction and magnitude of relationships among predictors. Responses to important predictors for each species can be found in Appendix F (Figure F.1 - F.14). Additionally, interactions among predictors for individual species models were generally weak and dominated by interactions with sampling period (Appendix F; Table F.1 – F.14). We do not report on specific results for individual species models here for sake of brevity. However, a few consistencies emerged among species with similar migration status that bear highlighting.

The two transient migrant species, American Redstart and Black-throated Blue Warbler, were the only individual species to both show strong responses to agriculture and water cover in the landscape. Both species increased in density with increasing agriculture cover (sharply when agriculture dominated the landscape), and increasing amount of open water cover. Black-throated Blue Warbler was the only individual species to show strong positive response to urban cover and Lepidoptera abundance in the understory, similar to transient species as a whole.

All breeding migrant species showed a strong positive relationship with NDVI, similar to that of Neotropical migrants as a whole. Most of the breeding migrant species (4 out of 6 species) showed a negative relationship with arthropod abundance in the understory and a positive relationship with latitude. Unique among all individual species assessed, Acadian Flycatcher had a negative relationship with litter depth and proximity to bright areas, Wood Thrush had a negative relationship with ground vegetation cover, and White-eyed Vireo had a positive relationship with shrub habitat cover in the landscape.

Winter migrant species were the only individual species that showed strong positive responses to fruit abundance of American holly (4 out of 6), partridge berry (2 out of 6), and *Smilax* spp. (2 out of 6). They were also the only individual species to show a positive relationship with proximity to the Atlantic coastline (2 out of 6 species). Unique among all individual species assessed, Golden-crowned Kinglet had a positive relationship with arthropod abundance on the ground, Winter Wren had positive relationships with Diptera abundance in the understory and tree basal area, and Yellow-shafted Flicker had a positive relationship with fruit abundance of black gum.

Objective 4: Classifying stopover site function

We used data from 45 sites within the Mid-Atlantic and Gulf Coast regions to assess stopover functional types. We identified four well-defined groups from the cluster analysis (Figure 46). Based on the values of the four predictor variables (proportion of hardwood forest within sample volumes and within 5 km, distance to coast, insect density, Table 16), we assigned functional types to each cluster. We ended up with eight coastal fire escapes, 14 inland rest stops, 10 full service hotels, and 13 convenience stores. On average, coastal fire escapes were distinguished by having short stopover duration, were located closest to the coast, had the lowest amount of forest cover in the landscape, and the lowest insect density (Figure 47). Inland rest stops had moderate stopover duration, low insect density (intermediate but not statistically different from fire escapes and convenience stores), were located away from the coast, and had a moderate amount of forest cover in the landscape. Convenience store sites had the longest stopover duration, were located away from the coast, had moderate forest cover in the landscape, and moderate amounts of insects. Hotel sites had short stopover duration (not different from fire escapes), the highest amounts of forest cover and insect density, and were located farthest from the coast. All hotel sites were located within extensive forested wetlands and inland areas near the Gulf Coast (Figure 48). All fire escapes were located in coastal and highly urbanized areas of the Mid-Atlantic. Inland rest stops occurred primarily on the Delmarva Peninsula. Convenience stores were generally located along inland riparian forests within both Gulf Coast and Mid-Atlantic regions.

Discussion

Objective 1: Mapping stopover incidence with radar

The use of NEXRAD data to map stopover distributions of migrating birds is a relatively new application and new developments and refinements of the approach pioneered by Buler and Diehl (2009) continue to be made (e.g., Buler and Dawson 2014). We made two important advancements to the data screening and processing algorithms. We improved the objective determination of the flight speed and direction of animals at all radars (i.e., not just radars with affiliated radiosonde balloons) by using NARR data as a source of wind speed and direction aloft. Although coarser in height resolution than radiosonde, NARR provides a more accurate temporal match to radar data because it is measured every three hours instead of every twelve hours as for radiosonde. NARR covers the entire U.S. thus allowing us to incorporate wind data at radars that have no associated radiosonde. Additionally, because NARR is modeled at a finer spatial scale (approximately every 30 km), we can obtain average wind measures across the entire radar domain as opposed to just the point location where the radiosonde is launched. The end result is more accurate determination of the air speeds of targets for distinguishing birds from insects.

The second advancement to data processing that we developed during this study is the dynamic empirical determination of a suitable sampling time for each radar and night. We verified that the precise timing of the onset of migration varies among radars and days and represents an important potential source of sampling bias previously alluded to by Buler and Dawson (2014). The timing of the onset of migration ranged from roughly 24 to 80 minutes after sunset. This range of sampling times may be due to time of year, the species composition of migrating landbirds, and on individual departure decisions (Åkesson et al. 1996). Age and condition of individuals may also provide insight as to why we see this range of exodus timings. Smolinsky et al. (2013) found that the majority of radio-tagged Swainson's Thrushes (*Catharus ustulatus*) leaving after astronomical twilight were lean, hatch-year birds. Choosing to sample at the peak of exodus on a daily basis allows us to capture the variability in timing from day to day, yet standardizes the relative sampling time among days. The sampling times from the new algorithm are determined automatically, quantitatively, and consistently at the time when the rate of increase in the density of birds entering the airspace is greatest, typically about 5-10 minutes after the first birds begin to take off. The dynamic nature of the algorithm allows it to sample flight exodus at the same relative time point despite any systematic and/or stochastic changes in the precise timing of the onset of migratory flight among radars and days. This standardization is important since birds in the airspace can double every couple of minutes (Hebrard 1971). As a follow-up to this project, we plan to model the variability in the timing of exodus flights to improve our understanding of the factors that influence the onset of migration.

The correlations between radar measures of emigrant density aloft and migrant densities at the ground were weak to moderate in strength, likely due to several reasons. These include factors contributing to sampling error and differences in the quantification of bird density.

Factors contributing to sampling error include inconsistent calibration of NEXRAD sites, and spatial and temporal mismatches in sampling days between ground surveys and radar observations. By design, NEXRAD radars should be calibrated to produce similar values of reflectivity for the same density of birds aloft, but operational parameters can vary by radar (Crum and Alberty 1993). Additionally, the radars sample transects at a relatively coarser resolution than observers through field surveys. The radars likely enumerate birds that could have taken flight from outside the bounds of transects. Observations from radar and field surveys were also not temporally matched to the same days. These spatial and temporal mismatches can add to noise to the correlations.

Stopover duration of migratory landbirds is extremely variable and depends largely on how quickly birds can refuel (Moore and Kerlinger 1987, Lindström and Alerstam 1992). Since we conducted surveys approximately every four days, we may not have captured complete turnover of individual migrants since stopovers can last for many days. Thus, the possibility of recounting the same individuals on multiple surveys means that ground surveys really provide a measure of bird use days and not an explicit measure of unique individuals stopping over. Radar measures more explicitly measure individuals leaving stopover sites for flight and presumably they do not return to the same stopover sites once they leave. Therefore, the relationship between mean radar reflectivity of emigrating individuals and mean daily bird density (index of bird use days) on the ground is confounded if stopover length varies within and among sites.

The seven-year dataset that we used allowed us to quantify linear trends in the changes in stopover densities of migrants across years. While there was variability among areas that exhibited steep increases to no changes to steep decreases, the overall average trend indicated an annual decrease of 4% in stopover densities. When extended over the seven years of the analysis, there was a 29% decline in stopover densities of migrants. This is alarming, and must be considered seriously as a sign that aggregate populations of landbirds that migrate through Region 5 are experiencing rapid declines in their post-breeding population sizes since the radars comprehensively measure 25% of the land area within Region 5 in a systematic, consistent, and quantitative way. Although we did not find obvious indications of sampling bias, further investigation of how differences in the number of sampling nights among years might create bias should be pursued.

Objective 2: Modeling stopover incidence with radar

Validating the output of the NEXRAD-based BGAM models with ancillary radar data was not without challenges, mostly stemming from limited observed coverage areas by TDWR and NPOL. However, the compatibility of the NEXRAD-based predictive models with the observed TDWR data seems quite reasonable given the latter's lower range and sparser data set. The poorer than expected fit of our model results with the NPOL data, which ostensibly has even higher spatial resolution than the NEXRAD data, may stem from the limited overlap between the NEXRAD and NPOL coverages and clutter issues with the NPOL data (see Appendix A). This

highlights another benefit of our modeling approach in that measurement errors can be directly estimated and accounted for across regional scales.

A major strength in choosing an additive approach like BGAMs is the possibility to separate prevailing responses to geographic or flyway-scale spatial effects (X, Y) from sub-regional coastal and hardwood effects. However, sensitivities to edge effects and smoothing of the response functions remain to be fully quantified. We have made preliminary comparisons between the BGAM and GWR and STEM models. These indicate that the smoothed additive approach of the BGAMs slightly underperforms compared to the others within a dense observation network, but is more robust and accurate at remote locations, e.g. remote radar sites. We are exploring these differences more rigorously using both synthetic and NEXRAD data sets.

Our predicted patterns of stopover use based on the BGAM models, with lower density in New England and near the Great Lakes, is more consistent with recent radar studies focusing on airborne densities through the night (La Sorte et al. 2014, Farnsworth et al. 2016). Differences in predicted density and classification from Buler and Dawson (2014) are partly attributable to our more flexible and precise calculation of exodus peaks (all previous radar studies have considered static sun angles). For example, in the northeastern portion of the region, exodus times were typically relatively late so stopover densities based on a static sun angle would be under-predicted. Our models also benefitted from having a deeper dataset compiled across seven years.

The consistent importance of fractional hardwood forest cover in determining stopover density was naturally expected (e.g. Buler et al. 2007, Ktitorov et al. 2008), but the prevalence of cover within 50 km versus 1 or 5 km was noteworthy. Hardwood fractions at 5 km and 50 km are moderately correlated (0.77), so some caution in interpretation is warranted. However, the consistent importance of 50-km over 5-km scales suggests that density-dependence may not be a strong factor in determining stopover density, since VIR is then predicted to increase within each 1-km cell if fractional hardwood increases at 50 km. This further emphasizes the importance of conserving largely intact forested areas along migratory flyways.

The predicted decrease in density with increasing fraction of non-hardwood covers was striking (Figure 19). Regarding agricultural land cover, this is consistent with Buler and Dawson (2014) using localized linear regression (GWR). This study presents the first evidence that stopover density decreases with increasing extent of emergent marsh and coniferous forest. These effects could be related to inter-guild effects with lower numbers of birds utilizing these habitats compared with those stopping over in deciduous forests. Another possible confounding factor is that birds may make several nocturnal “test flights” on different nights during the course of a stopover bout at a single location, which may last up to several weeks (e.g. Mills et al. 2011). A test flight is where a bird flies high into the air but does not engage in a long distance flight and, instead, quickly returns near the point of departure. Lastly, the response to urban cover is consistent with the GWR findings in Buler and Dawson (2014), which predicted that stopover densities decreased with increasing urban cover in undeveloped regions up to when urban cover reaches 10% of the landscape, and then increased with urban cover in heavily developed areas where urban cover dominated the landscape (Figure 21).

Response in mean VIR to distance to bright lights consistently indicated higher stopover densities close to brightly lit (and therefore typically close to highly urbanized) areas. Although there is evidence dating back to the early 1800s of birds being attracted to sources of artificial lights (Gauthreaux and Belser 2006 and references therein), our study seems to be the first to provide evidence consistent with birds being drawn to urban glow. Olsen et al. (2014) estimates that the skyglow of large metropolitan areas can be perceived by an observer on the ground from up to 300 kilometers, and likely to greater distances for birds aloft. Positive phototaxis of birds while aloft has also been suggested as a possible explanation for large altitudinal shifts in migrants during flight (Bowlin et al. 2015). The fact that, unlike other landscape-scale variables, VIR was more variable with increasing urbanization and proximity to bright light indicates that migrants may be more likely to land near brightly-lit areas under certain conditions, e.g. poor atmospheric visibility or strong winds. The increased densities closer to brightly lit hardwood forests indicate that migrants can and do mitigate any negative effects on availability of suitable habitat. It remains to be quantified to what extent migrants might be impacted by broad-scale phototaxis. We are continuing to investigate artificial light effects, using higher-resolution light data and with fewer interactions between spatial co-ordinates and landscape scale predictors. We also have a doctoral student in the Aeroecology Lab at UD who is investigating the extent of light pollution along bird migration routes at different scales (worldwide and U.S.-wide), testing whether artificial lights at a landscape scale promote stopping over of nocturnal migrants, assessing whether migrating birds in active flight react to the presence of experimentally-controlled artificial lights, and, based on NEXRAD data, analyzing whether moon phase, cloud cover, and visibility play a role in modifying stopover concentrations of migrating birds in urban areas.

Objective 3: Explaining migratory landbird use of forests via field surveys

Migratory bird densities during autumn stopover within hardwood-dominated forests of the Mid-Atlantic region were associated with ecological data measured at patch, landscape, and regional spatial scales. Migrant densities also varied temporally with sampling period as breeding species left, transient species passed through, and wintering species arrived in the region over the course of the autumn. For most species (57%), sampling period was the most influential predictor of their habitat use. Therefore, it is important to view differences in the responses of bird habitat use to factors across all spatial scales with sampling period in mind. It is also important to keep in mind that since we surveyed unmarked individuals that may have stopped over long enough to be detected in more than one survey, that bird density measures from ground surveys reflect intensity of bird use rather than a measure of how many individual birds passed through a site. As an extreme example, one Wood Thrush detected per survey for three successive surveys at one site could reflect three individual thrushes that stopped over for short intervals between surveys or three detections of one individual thrush that stopped over for the duration of the three surveys. This means that bird density from surveys should be positively related to both the number of individuals passing through a site and to mean stopover duration

among individuals (i.e. the quantity that allows us to extract a measure of relative stopover duration by integrating radar and ground survey data for objective 4).

At the patch level, both food resources as well as habitat characteristics had an important effect on predicting migrant densities, with food resources more commonly identified as highly influential predictors. Total arthropod density was generally more important than individual arthropod taxa in explaining density for most migrant bird groups and species. The negative relationship between arthropod abundance and the density of most individual breeding species and breeding migrants as a group may seem counterintuitive. However, a possible explanation may reflect carry over effects of territorial breeding site selection earlier in the year. "Migrant" density of species known to breed in the region was at its seasonal peak during August and early September (period 1) when birds detected during this time were likely dominated by local breeders (some "migrants" were detected as singing males during this time) still using habitat within their breeding territories (Ryder et al. 2011, Stutchbury et al. 2011, Stanley et al. 2012, Mitchell et al. 2012). This sampling period also coincided with the seasonal low in arthropod abundance. Birds can suppress arthropod populations over time (Marquis and Whelan 1994). Thus, the negative relationship between breeding migrant density and insect abundance early in late summer/early fall may reflect depletion of insects within territories used during the breeding season.

Passage migrants (i.e., breeding species in the second half of the season and true transients) and wintering migrants, on the other hand, were positively related to arthropod density, consistent with other studies (Hutto 1985, Petit 2000, Buler et al. 2007). Lepidoptera larvae abundance was important in explaining total transient migrant density and, among individual species, had the greatest relative importance for the two transient migrant species analyzed (Black-throated Blue Warbler and American Redstart). Caterpillars are particularly important in the diet of these two warblers during stationary periods of the year (Rodenhouse and Holmes 1992, Lovette and Holmes 1995). However, numerous migrating warbler species in spring have been observed feeding almost exclusively on caterpillars in forests of the midwestern U.S. (Graber and Graber 1983). Thus, passage migrants appear to be particularly responsive to lepidopteran larva over other arthropod taxa. Wintering migrant species detections likely included some passage individuals, but also local residents making initial habitat selection of wintering territories and apparently settling in positive relation to arthropod density.

It is important to bear in mind that due to logistic constraints we only sampled arthropod density in the two lower strata of the forest (ground and understory), which does not necessarily reflect arthropod availability across all strata (including midstory and canopy). Thus, interpreting relationships of bird density with arthropod abundance must be done with caution. Moreover, sampling of arthropods was done without discrimination of palatability of arthropods. There is uncertainty in the proportion of arthropods sampled that may be consumed by birds. Fruit abundance was also important in explaining migrant bird densities, particularly for transient, frugivorous, and wintering species. Both transient species examined, American Redstart and Black-throated Blue Warbler, showed strong positive relationships with fruit abundance of grape

(*Vitis* spp.) and are frugivorous in late summer and fall (Holmes 2005, Sherry and Holmes 2016). Several wintering bird species showed positive relationships with fruit abundance of American holly, partridge berry, and/or *Smilax* spp. Holly and *Smilax* spp. were among the latest fruits to ripen, doing so late in the survey season when wintering migrants began arriving in large numbers. These fruits are usually consumed by birds during the fall (partridge berry), in late winter (holly), or steadily throughout the winter (*Smilax* spp.) (McCarty et al. 2002, Greenberg and Walter 2010). Further investigation into the relationships of individual bird species and fruiting plants is warranted as some of the migrant species associated with ripe fruits are not necessarily known to consume those fruit species. Hardwood forests are known to contain a higher level of fruiting species abundance and diversity than pine-dominated forests (Greenberg et al. 2012). While this may be the case, hardwoods should not be considered the only important forest type. There is great diversity in the types of fruiting species found between hardwood and pine forests, and preferences for food type must be considered on a species-by-species basis if assessments of habitat quality are to accurately represent their true value for migrant species (Moore et al. 1995, Greenberg et al. 2011).

The most common patch-scale habitat structure variables influencing migrant density were shrub cover and shrub stem density. Attraction to dense shrub cover was widespread among flycatchers, foliage gleaners including warblers, kinglets, and vireos, and a ground-foraging thrush (Wood Thrush). Although some researchers have found no or weak relationships between habitat structure and bird abundance during migration (Skagen et al. 1998, Somershoe and Chandler 2004, Buler et al. 2007), greater migrant abundance is often associated with greater understory cover (Deppe and Rotenberry 2008), often typical of tree-fall gaps within hardwood forests (Blake and Hoppes 1986, Martin and Karr 1986, Wilson and Twedt 2003, Rodewald and Brittingham 2004) where food resources are concentrated (Blake and Hoppes 1986, Martin and Karr 1986, Kilgo et al. 1999). Greater understory vegetation also provides cover from predators (Lindström 1990, Cimprich et al. 2005, Woodworth et al. 2014). Wood Thrush also responded strongly and negatively to forb ground cover, consistent with a preference for open litter for foraging (Roth et al. 2011). Winter Wren was unique in being the only species to respond strongly and positively to tree basal area. This is consistent with a preference for old growth forest where it probes bark and upturned roots of trees (Hejl et al. 2002).

Breeding migrants showed strong positive relationships to primary productivity (NDVI), which was likely driven by their distributions and selection of breeding territories earlier in the growing season. NDVI has proven to be a powerful predictor of bird species richness and abundance tied to greater rainfall, green vegetation and favorable conditions for insectivorous birds (e.g., Seto et al. 2004, Gordo 2007, Saino et al. 2010, Pettorelli et al. 2011 and references therein). The only other migrants that responded to NDVI were wintering migrants (Winter Wren and Northern Flicker) and their response was negative. NDVI was negatively related to sampling period, which may have contributed to the negative relationship with these two wintering migrants that peaked in abundance when NDVI was at its lowest.

At the landscape scale, landscape composition exhibited strong influence on migrant densities, particularly for passage migrants. Passage migrants' use of forested stopover sites increased when there was less forest in the landscape and more agriculture and urban development, similar to Strobl (2010). This is consistent with radar studies that demonstrate forest patches in highly developed landscapes support high densities of migrating birds (this study, Bonter et al. 2009, Buler and Dawson 2014). Buler and Dawson (2014) suggested the greater number of migrants stopping in forest patches may be due to a 'wicking effect' in which forest patches draw in migrants from the surrounding unsuitable landscape and concentrate them. Subsequently, food resources may decline relatively quickly (Moore and Wang 1991) and lead to increased stopover duration (Ktitorov et al. 2008). Increased stopover duration would also lead to increased observed bird use in ground surveys. The wicking effect of transitory migrants is also supported by the change from a positive response of breeding migrants to hardwood forest cover while local breeders were still present to a negative response to hardwood forest cover as the season progressed and transient individuals of breeding species passed through the region.

Regional scale variables were highly influential for some species. Latitude showed a highly-influential positive relationship with half of the species examined. However, White-eyed Vireo is the only species that had greater densities at lower latitudes. Part of this explanation could be that migrants tended to be more concentrated into the forests of the Delmarva Peninsula and are more diffuse on the mainland of Virginia that contains greater forest cover. Distance to the Atlantic Ocean tended to be more important for migrant groups than for individual species. Our hypothesis that proximity to the coast would be an influential region-scale factor is supported by previous studies that found regional-scale selection and use of near-coastal stopover sites within several regions within the eastern U.S. (Diehl et al. 2003, Buler et al. 2007, Buler and Dawson 2014, LaFleur et al. 2016, Archibald et al. 2017). This is the first study to show that breeding migrants use forests farther from the coast with greater intensity, particularly early in the fall migration season. Again, this may reflect the spring selection of breeding territories rather than habitat selection of transient migrants, since later in the season the relationship of breeding migrant species changed to be negative with distance from the Atlantic (similar to transients). Many near-coastal landings arguably result as a consequence of other influencing factors on migrants facing overwater crossings, such as adverse weather conditions (Gauthreaux and Belser 1999, Schaub et al. 2004), body condition (Moore and Aborn 2000, Moore et al. 2005), and even "morning flight" or dawn reorientation of migrants aloft over water (Van Doren et al. 2014, 2016, Archibald et al. 2017).

Although distance to bright areas had a strong influence on migrant distributions based on radar data, it usually only had a moderate to weak influence on migrants based on ground surveys. However, the density of transient migrants and breeding species late in the season was greater with proximity to bright areas, consistent with radar observations. Conversely, locally breeding species and wintering migrants (i.e., migrants in residence) tended to avoid bright areas. This is an intriguing result that suggests that attraction to light may only affect migrants while in

passage and not those that have/are established/ing long-term home ranges during stationary periods of the annual cycle.

Results of our study emphasize how truly variable stopover habitat use by migratory landbirds is, and how habitat factors across multiple spatial scales exhibit varying degrees of influence on site use (Buler et al. 2007, Deppe and Rotenberry 2008, LaFleur et al. 2016). Variability in habitat use is especially evident when considering the different needs and preferences of one migratory species versus another, and is apparent in noticeably different outcomes for top predictor variables from each density analysis. It, thus, highlights the need for using multi-scale approaches when comparing datasets to address ecological questions such as those presented here.

There are also numerous other habitat and individual factors that may be important to migrants and their choice of particular stopover sites that were not considered in this study. For example, age or sex differences within taxa may play an important role in migratory behavior. Juveniles are inexperienced in navigating their migratory route and this naïveté may manifest itself by the observation that large numbers of juvenile migrants move along coasts. This phenomenon, referred to as the coastal effect, may affect the importance and function of stopover sites used largely by juvenile birds (Ralph 1978). Following a coast is disadvantageous, generally involving a longer, less direct route that requires more energy expenditure. This tendency also may result in misdirected flight offshore, requiring more time or repeated attempts to cross an oceanic barrier and likely contributing significantly to annual juvenile mortality rates (Ralph 1978). Similarly, the predisposition to move along the coast demonstrates that migrant habitat use is constrained at a higher hierarchical level by location, and may not be as strongly influenced by fine-scale factors related to habitat quality per se. Although nearly impossible to address with an observational study such as this, individual decision-making events are a factor influencing stopover habitat use. For example, a Caribbean-bound migrant may choose to travel further south along the coast, shortening their overwater flight distance and duration, but increasing the length of the entire migratory journey. Other individuals of the same species may instead take advantage of conditions such as favorable winds and depart across the ocean earlier, the benefit being a much shorter migratory journey (Alerstam 2001).

Landscape-scale studies are logistically difficult to conduct, but are important for conservation planning. Increasing urbanization and habitat fragmentation, for example, reduces the availability of stopover habitat. Although fragmented forests in urbanized areas provide stopover habitat for migratory birds, they are usually not of the same quality as more extensive forests elsewhere (Moore et al. 1995, Faaborg et al. 2010a, Matthews and Rodewald 2010). Urbanized forest patches, for example, may have lower arthropod diversity and abundance, as well as a higher number of invasive plants, than contiguously forested areas (Matthews and Rodewald 2010). Additionally, we found evidence from radar and ground surveys that passage migrants appear attracted to bright urban areas due to the skyglow of artificial light at night. Thus, the enhanced competition for food in forested stopover sites with more limited resources may make the migratory journey even more difficult and dangerous (Askins and Askins 2002).

Fragmented urban landscapes also limit the potential for an individual to successfully locate more suitable habitats via morning flight, thus possibly extending stopover bouts and leading to even more time and energy being consumed (Moore et al. 1995).

Conducting an accurate and useful assessment of the influence of varying scale-dependent factors on migratory landbird selection and use of stopover sites requires that factors across multiple hierarchical levels are incorporated. Prior multi-scale analysis of stopover habitat use showed a positive association between landscape-scale hardwood forest cover and understory arthropod abundance, a patch-scale factor considered important to migrant bird use. This suggests that nearby surrounding hardwood forest could be an important cue of a high-quality site and may even convey cues for where to land (Buler et al. 2007). Our results reinforce the notion that a multi-scale analytical approach as we have done is paramount to effectively understand stopover habitat use by migratory landbirds.

Objective 4: Classifying stopover site function

Determining relative stopover duration by integrating radar and ground surveys, similar to O'Neal et al. (2012), with measures of food resources, proximity to the coast, and the fraction of hardwood forest cover in the landscape, allowed us to assess how migrants use specific stopover sites and classify sites into four categories similar to the framework outlined by Mehlman et al. (2005). Stopover duration varied in accordance with empirical data on the relationship between the propensity to leave a site and fuel deposition rate (Schaub et al. 2008). Namely, birds exhibited the shortest stopover duration in sites with the least amount of food (coastal fire escapes) and the most amount of food (full service hotels), while sites with moderate amounts of food (i.e. convenience stores) were associated with the longest stopover duration. The explanation of this is that birds that refuel quickly can spend less time at a stopover site. If there are only moderate amounts of food, it will take migrants longer to rebuild energy reserves to levels suitable for a long-distance migratory flight. This also begs the question as to whether convenience stores may be ecological traps and confer negative fitness consequences to migrants by delaying departure compared to higher quality (hotel) sites. Perhaps a more appropriate term for convenience store is "refueling trap"?

We could have lumped coastal fire escapes with inland rest stops in the category of "fire escape" because they both serve as temporary rest areas where birds likely cannot refuel due to low food resources. Collectively, they represented half of all stopover sites surveyed. However, the significant difference in their proximity to the coast is an importance distinction. Nocturnally-migrating birds will change flight direction to remain over land when approaching coastlines (Bruderer and Liechti 1998, Diehl et al. 2003, Horton et al. 2016). Furthermore, the phenomenon of redirected flights towards land of nocturnal migrants over water after dawn (i.e., morning flight) is widespread and frequent, leading to increased numbers of migrants stopping in coastal areas (Diehl et al. 2003, Van Doren et al. 2016, Horton et al. 2016, Archibald et al. 2017). Thus, coastal fire escapes offer a safe landing place for landbirds that may have just completed or delayed an open water crossing and tend to be used in greater and more consistent densities

than inland rest stops. The consistent migrant use of coastal “fire escape” sites runs counter to the original general description by Mehlman et al. (2005) that fire escapes are only used infrequently by migrants. We suggest relaxing the defining condition that fire escapes are used infrequently since the need for “emergency” resting areas near coasts is constant. Alternatively, the label of fire escape should be changed to “rest stop”, which removes the connotation of infrequent use.

Conservation Implications

Forests and other natural habitats on or near coastlines are conservation priorities because they provide resting or landing sites for birds before or after overwater crossings. Coastal habitats are also important for landbirds that migrate along the coast, which may disproportionately be juvenile birds on their first migration. Corroboration of the relationship of transient migrant attraction to light by radar and ground surveys strengthens the inference that migrants are affected by artificial light at night at broad spatial scales. Moreover, broad scale attraction of migrants to bright urban areas, particularly during fall, has been shown using eBird observations by citizen scientists (La Sorte et al. 2017). Migrants drawn to brightly lit areas in and around urban areas, where they may be exposed to various human-associated hazards (e.g. towers, cars, windows, cats), rely on forest tracts as well as tree canopy and shrub cover in parks and residential communities, so maintaining or enhancing these should be encouraged.

Maps of predicted stopover densities identify sites throughout the region with high or consistent use. Locally classified maps (e.g., 10-km or 50-km window, see Figure 30) could guide bird clubs, National Wildlife Refuges, and State or local governments to select sites for conservation, while regionally classified predicted stopover use and the mapped Cumulative Stopover Importance Index (Figure 33) may be more useful for broader conservation planning. The maps also show portions of the region with predicted low use by migrants. Migratory flights could be simulated or tracked to see if these areas are bypassed due to their relative location. Additionally, these areas could be examined either remotely or directly to determine if few suitable stopover sites exist and thus need conservation attention.

While the bird species composition of NEXRAD data cannot be determined, regionally-classified predicted bird stopover use mapped during bimonthly periods (Figure 31) can focus conservation actions on bird species groups of interest. In general, the two maps for September encompass predominantly Neotropical migrants while the October maps are dominated by temperate migrants. Banding, eBird or other observational data can be used to identify the bimonthly periods that coincide most closely with the migration schedules of species of particular conservation concern; overlaying mapped information on their breeding ranges and spatial distribution during migration would be an initial step to identify species-specific sites that are potentially important, although field surveys would be needed to provide confirmation.

The maps also can serve as a sampling frame to design field studies of migrants. More research is needed to both verify model predictions and better understand how migrants use sites in order to further prioritize sites for conservation and to identify ways to enhance habitats to

benefit migrants. With the limited conservation funding that typically is available, we suggest that it is critical to focus conservation efforts for migrating landbirds on areas where they likely will be most effective.

Finally, the associations of migrants with vegetation data collected in ground surveys should be examined further to develop prescriptions to manage forests to benefit fall migrants. Particularly in the southern portions of Region 5, managing forest and scrub habitats to improve vegetation structure and increase the diversity and abundance of fruit-bearing plants can provide benefits beyond the migration season since many temperate migrants winter at these latitudes. The strong relationships of overwintering migrants with late-season, long-lasting fruits merits further attention from forest managers, as relatively little other food is available in winter, when energy demands of birds are high (McCarty et al. 2002). Additionally, increasing understory vegetation cover by reducing deer herbivory can also benefit migratory birds outside the migratory season (Gill 1992, McShea and Rappole 2000, Fuller 2001, Gill and Fuller 2007).

Acknowledgments

We would like to acknowledge the field technicians who assisted in the collection and organization of field data: M. Buschow, E. Cali, J. Dacus, R. Hepner, C. Higgins, B. Hodgkins, A. Lamoreaux, D. Lipp, J. Martini, A. Moss, N. Weyandt, B. Zyla. We thank R. Lyon, D. Greene, J. LaFleur, L. Cruz, M. Levendosky, J. Antalffy, L. Young, and M. Atkinson for screening and processing radar data. We graciously thank all the private landowners and various groups for permitting access to their forested properties: Delaware Department of Natural Resources and Environmental Control, Isle of Wight Hunt Club, Anne Johnston and the Johnston family, Betsy Mapp, Maryland Department of Natural Resources, Maryland Ornithological Society, NASA, The Nature Conservancy, Bill Owens, Ellen Phillips, Salisbury, Md.'s city council, the U.S. Fish and Wildlife Service, Virginia Coastal Zone Management Program, Virginia Department of Conservation and Recreation, Virginia Department of Game and Inland Fisheries, and Virginia Natural Heritage Program. We are especially grateful for the assistance received on various aspects of the project from numerous individuals and groups: Alex Wilke, Bobby Clontz, Dave Harris, Deborah Landau, and John Graham with The Nature Conservancy; Becky Gwynn with the Virginia Department of Game and Inland Fisheries; Darren Loomis, Dot Field, Erik Molleen, Forrest Gladden and Theresa Duffy with Virginia Department of Conservation and Recreation; Joel Mitchell with NASA; John Moulis with the Maryland Department of Natural Resources; and Sue Rice with the U.S. Fish and Wildlife Service. This research project was only possible through immense support, chiefly in funding through grants, data collection / analysis, and project design and execution, from our dedicated sponsors and partners: Gwen Brewer and John Sherwell with the Maryland Department of Natural Resources, Walt Peterson and other staff at the NASA Wallops Flight Facility, Barry Truitt with The Nature Conservancy, the University of Delaware, Randy Dettmers with the U.S. Fish and Wildlife Service's Migratory Bird Program, Scott Schwenk with the U.S. Fish and Wildlife Service's North Atlantic LCC, Bill Thompson with the U.S. Fish and Wildlife Service's National Wildlife

Refuge System, Laura McKay and the Virginia Coastal Zone Management Program, and Ruth Boettcher with the Virginia Department of Game and Inland Fisheries.

Any use of trade, firm, or product names is for descriptive purposes only and does not imply endorsement by the U.S. Government.

Outcomes

Here is a list of 19 oral scientific presentations and 2 posters that have been made about the USFWS-funded project. The presenter(s) is underlined. Note that Andrew Arnold is the Master's student at Old Dominion University who worked on the project through support from Maryland DNR.

2013. Buler, J. J. Recent applications of weather radar for understanding the stopover ecology of migrating birds, Old Dominion University, Department of Biological Sciences, Norfolk, VA

2013. Arnold, A., J. J. Buler, T. Schreckengost, and E. L. Walters. Using radar-based data to predict forested hardwood habitat use by migrants along the Eastern Shore of Virginia and Maryland: A preliminary report, Coastal Upland Management Meeting, Eastern Shore of Virginia National Wildlife Refuge, Cape Charles, VA

2014. Arnold, J.A., E. L. Walters, T. Schreckengost, and J. J. Buler. 2014. Migratory bird use of forested stopover sites on the lower Delmarva Peninsula and a comparison with radar-based predictive models, Virginia Coastal Avian Partnership Meeting, Eastern Shore Community College, Melfa, VA

2014. Buler, J. J. Some revelations of bird migration and stopover ecology from weather surveillance radar observations, Villanova University, Department of Biology, Philadelphia, PA

2014. Arnold, J. A., T. Schreckengost, J. J. Buler, and E. L. Walters. Assessing habitat use and quality of stopover sites during fall migration, North American Congress for Conservation Biology, University of Montana, Missoula, MT

2014. Buler, J. J., D. Dawson, D. La Puma, J. Smolinksy, T. Schreckengost, A. Arnold, and E. Walters. Broad-scale mapping and monitoring of migratory landbird stopover sites using the national network of weather radars, Joint Meeting of the Northeast and Southeast Partners in Flight, Virginia Beach, VA

2014. Arnold, J. A., T. Schreckengost, J. J. Buler, and E. L. Walters. Assessing avian use of forested stopover habitat during fall migration along Virginia's Eastern Shore, Tidewater Student Research Poster Session, Christopher Newport University, Newport News, VA

2015. Schreckengost, T. and J. J. Buler. Update on validating weather radar observations to map migrating landbird stopover distributions in the northeastern. US, Virginia Coast Avian Partnership Meeting, Melfa, VA

2015. Schreckengost, T., A. Arnold, M. Boone, D. Dawson, J. Smolinsky, E. Walters, and J. J. Buler. When is the best time to sample migrating birds in the air with weather surveillance radar to determine their stopover density at the ground? Student Poster Session, Joint meeting of Society of Canadian Ornithologists, American Field Ornithologists, and Wilson Ornithological Society, Wolfville, Nova Scotia **Winner of best student poster

2015. Schreckengost, T., A. Arnold, M. Boone, D. Dawson, J. Smolinsky, E. Walters, J. J. Buler. When is the best time to sample migrating birds in the air with weather surveillance radar to determine their stopover density at the ground? Symposium: "Recent scientific applications of weather radar for advancing ornithology", Joint meeting of American Ornithologists' Union and Cooper Ornithological Society, Norman, OK

2015. McLaren, J., J. J. Buler, D. Dawson, J. Smolinsky, and M. Boone. Predictive models of stopover incidence by migrant landbirds, Symposium: "Recent scientific applications of weather radar for advancing ornithology", Joint meeting of American Ornithologists' Union and Cooper Ornithological Society, Norman, OK

2015. Buler, J. J., D. Dawson, J. Smolinsky, T. Schreckengost, M. Boone, A. Arnold, and E. Walters. Determining relative stopover duration for migrating forest birds by integrating ground surveys and weather radar observations, Symposium: "Recent scientific applications of weather radar for advancing ornithology", Joint meeting of American Ornithologists' Union and Cooper Ornithological Society, Norman, OK

2015. Arnold, J. A., T. Schreckengost, J. J. Buler, and E. L. Walters. Assessing avian use of forested stopover habitat during fall migration, Association of Southeastern Biologists annual meeting, Chattanooga, TN

2015. Buler, J. J. Recent insights into the stopover ecology of migrating landbirds from weather radar observations. Smithsonian Migratory Bird Center, Washington DC

2015. Arnold, J.A., T. Schreckengost, E. L. Walters, and J. J. Buler. Forested stopover habitat use by migratory landbirds during fall migration. Williamsburg Bird Club Monthly Meeting, Williamsburg, Virginia.

2015. Arnold, J. A., T. Schreckengost, J. J. Buler, and E. L. Walters. Assessing migratory landbird bird use of forested stopover habitat during fall migration, Virginia Society of Ornithology, Wintergreen, VA

2016. Buler, J. J., M. Boone, J. LaFleur, F. R. Moore, T. Schreckengost, J. Smolinsky, D. Dawson, J. A. Arnold, and E. Walters. Where and for how long do migrating landbirds stopover along the northern Gulf of Mexico? A radar perspective. Symposium: "Synthesizing Science to Inform Conservation of Songbird Migrants Around The Gulf of Mexico", North American Ornithological Conference VI. Washington D.C.

2016. Buler, J. J., M. Boone, D. Dawson, J. McLaren, *K. Rivera, T. Schreckengost, and J. Smolinsky. A macrosystems examination of stopover distributions of migrating landbirds using a network of weather surveillance radars. Symposium: "Macrosystems Ornithology–Scaling from Individuals to Ecosystems", North American Ornithological Conference VI. Washington D.C.

2016. McLaren, J., J. J. Buler, D. Dawson, T. Schreckengost, and J. Smolinsky. Predictive models of stopover incidence among migrating landbirds. Virginia Coastal Avian Partnership Annual Meeting, Wachapreague, VA.

2016. Arnold, J.A., T. Schreckengost, J. J. Buler, and E. L. Walters, Assessing avian use of forested stopover sites along the Delmarva Peninsula. Virginia Coastal Avian Partnership Annual Meeting, Wachapreague, VA.

2016. Buler, J. J., T. D. Schreckengost, J. Smolinsky, J. McLaren, D. K. Dawson, and E. L. Walters. Bird use of Delaware wetlands during fall migration based on weather radar observations. Delaware Wetlands Conference, Wilmington, DE

Literature Cited

Akaike, H. 1973. Information theory as an extension of the maximum likelihood principle. Pages 267–281 Second International Symposium on Information Theory. Akademiai Kiado, Budapest.

Åkesson, S., T. Alerstam, and A. Hedenström. 1996. Flight initiation of nocturnal passerine migrants in relation to celestial orientation conditions at twilight. Journal of Avian Biology 27:95–102.

Alerstam, T. 2001. Detours in bird migration. Journal of Theoretical Biology 209:319–331.

Alerstam, T. 2003. Bird migration speed. Pages 253–267 *in* P. Berthold, E. Gwinner, and E. Sonnenschein, editors. Avian Migration. Springer-Verlag, Berlin.

Alldredge, M. W., T. R. Simons, and K. H. Pollock. 2007. A Field Evaluation of Distance Measurement Error in Auditory Avian Point Count Surveys. The Journal of Wildlife Management 71:2759–2766.

Archibald, K. M., J. J. Buler, J. A. Smolinsky, and R. J. Smith. 2017. Migrating birds reorient toward land at dawn over the Great Lakes, USA. Auk 134:193–201.

Askins, R. A., and R. Askins. 2002. Restoring North America's birds: lessons from landscape ecology. Yale University Press.

Blake, J. G., and W. G. Hoppes. 1986. Influence of resource abundance on use of tree-fall gaps by birds in an isolated woodlot. Auk 103:328–340.

Bonter, D. N., S. A. Gauthreaux, and T. M. Donovan. 2009. Characteristics of important stopover locations for migrating birds: Remote sensing with radar in the Great Lakes Basin. Conservation Biology 23:440–448.

Bowlin, M. S., I.-A. Bisson, J. Shamoun-Baranes, J. D. Reichard, N. Sapir, P. P. Marra, T. H. Kunz, D. S. Wilcove, A. Hedenstrom, C. G. Guglielmo, S. Akesson, M. Ramenofsky, and M. Wikelski. 2010. Grand challenges in migration biology. Int Comp Biol 50:261–279.

Bowlin, M. S., D. A. Enstrom, B. J. Murphy, E. Plaza, P. Jurich, and J. Cochran. 2015. Unexplained altitude changes in a migrating thrush: Long-flight altitude data from radio-telemetry. Auk 132:808–816.

Bridge, E. S., K. Thorup, M. S. Bowlin, P. B. Chilson, R. H. Diehl, R. W. Fleron, P. Hartl, K. Roland, J. F. Kelly, W. D. Robinson, and M. Wikelski. 2011. Technology on the move: recent and forthcoming innovations for tracking migratory birds. Bioscience 61:689–698.

Bruderer, B., and F. Liechti. 1998. Flight behaviour of nocturnally migrating birds in coastal areas: crossing or coasting. Journal of Avian Biology 29:499–507.

Buler, J. J., and D. K. Dawson. 2012. Radar analysis of fall bird migration stopover sites in the northeastern U.S.: Final report. USGS Patuxent Wildlife Research Center, Laurel, MD, USA.

Buler, J. J., and D. K. Dawson. 2014. Radar analysis of fall bird migration stopover sites in the northeastern U.S. Condor 116:357–370.

Buler, J. J., and R. H. Diehl. 2009. Quantifying bird density during migratory stopover using weather surveillance radar. IEEE Transactions on Geoscience and Remote Sensing 47:2741–2751.

Buler, J. J., and F. R. Moore. 2011. Migrant–habitat relationships during stopover along an ecological barrier: extrinsic constraints and conservation implications. Journal of Ornithology 152:S101–S112.

Buler, J. J., F. R. Moore, and S. Woltmann. 2007. A multi-scale examination of stopover habitat use by birds. Ecology 88:1789–1802.

Buston, P. M., and J. Elith. 2011. Determinants of reproductive success in dominant pairs of clownfish: a boosted regression tree analysis. Journal of Animal Ecology 80:528–538.

Canty, A., and B. Ripley. 2014. boot: Bootstrap R (S-Plus) Functions. R package version 1.3–11. Vienna: R Foundation for Statistical Computing.

Chilson, P. B., W. F. Frick, P. M. Stepanian, J. R. Shipley, T. H. Kunz, and J. F. Kelly. 2012. Estimating animal densities in the aerosphere using weather radar: To Z or not to Z? Ecosphere 3:art72.

Cimprich, D. A., and F. R. Moore. 1999. Energetic constraints and predation pressure during stopover. Pages 834–846 Proceedings of the 22nd International Ornithological Congress. BirdLife South Africa, Johannesburg.

Cimprich, D., M. S. Woodrey, and F. R. Moore. 2005. Passerine migrants respond to variation in predation risk during stopover. Animal Behaviour 69:1173–1179.

Cohen, E. B., S. M. Pearson, and F. R. Moore. 2014. Effects of landscape composition and configuration on migrating songbirds: inference from an individual-based model. Ecological Applications 24:169–180.

Cooper, R. J., and R. C. Whitmore. 1990. Arthropod sampling methods in ornithology. Pages 29–37 Avian foraging: theory, methodology and applications. Cooper Ornithological Society, Lawrence, KS.

Cresswell, W. 2014. Migratory connectivity of Palaearctic–African migratory birds and their responses to environmental change: the serial residency hypothesis. Ibis 156:493–510.

Crum, T. D., and R. L. Alberty. 1993. The WSR-88D and the WSR-88D operational support facility. Bulletin of the American Meteorological Society 74:1669–1687.

De'Ath, G. 2007. Boosted trees for ecological modeling and prediction. Ecology 88:243–251.

Deppe, J. L., and J. T. Rotenberry. 2008. Scale-Dependent Habitat Use by Fall Migratory Birds: Vegetation Structure, Floristics, and Geography. Ecological Monographs 78:461–487.

Diehl, R. H., R. P. Larkin, and J. E. Black. 2003. Radar observations of bird migration over the Great Lakes. Auk 120:278–290.

Elith, J., J. R. Leathwick, and T. Hastie. 2008. Boosted regression trees—a new technique for modelling ecological data. Journal of Animal Ecology 77:802–813.

Faaborg, J., R. T. Holmes, A. D. Anders, K. L. Bildstein, K. M. Dugger, S. A. Gauthreaux, P. Heglund, K. A. Hobson, A. E. Jahn, D. H. Johnson, S. C. Latta, D. J. Levey, P. P. Marra, C. L. Merkord, E. Nol, S. I. Rothstein, T. W. Sherry, T. S. Sillett, F. R. Thompson, and N. Warnock. 2010a. Conserving migratory land birds in the New World: Do we know enough? Ecological Applications 20:398–418.

Faaborg, J., R. T. Holmes, A. D. Anders, K. L. Bildstein, K. M. Dugger, S. A. Gauthreaux, P. Heglund, K. A. Hobson, A. E. Jahn, D. H. Johnson, S. C. Latta, D. J. Levey, P. P. Marra, C. L. Merkord, E. Nol, S. I. Rothstein, T. W. Sherry, T. S. Sillett, F. R. Thompson, and N. Warnock. 2010b. Recent advances in understanding migration systems of New World land birds. Ecological Monographs 80:3–48.

Falchi, F., P. Cinzano, D. Duriscoe, C. C. M. Kyba, C. D. Elvidge, K. Baugh, B. A. Portnov, N. A. Rybnikova, and R. Furgoni. 2016. The new world atlas of artificial night sky brightness. Science Advances 2:e1600377.

Farnsworth, A., D. Sheldon, J. Geevarghese, J. Irvine, B. Van Doren, K. Webb, T. Dietterich, and S. Kelling. 2014. Reconstructing velocities of migrating birds from weather radar - A case study in computational sustainability. AI Magazine 35:31–48.

Farnsworth, A., B. M. Van Doren, W. M. Hochachka, D. Sheldon, K. Winner, J. Irvine, J. Geevarghese, and S. Kelling. 2016. A characterization of autumn nocturnal migration detected by weather surveillance radars in the northeastern USA. Ecological Applications 26:752–770.

Fink, D., W. M. Hochachka, B. Zuckerberg, D. W. Winkler, B. Shaby, M. A. Munson, G. Hooker, M. Riedewald, D. Sheldon, and S. Kelling. 2010. Spatiotemporal exploratory models for broad-scale survey data. Ecological Applications 20:2131–2147.

Fiske, I., and C. R. Chandler. 2011. unmarked: An R package for fitting hierarchical models of wildlife occurrence and abundance. Journal of Statistical Software 43:1–23.

Fuller, R. J. 2001. Responses of woodland birds to increasing numbers of deer: a review of evidence and mechanisms. Forestry 74:289–298.

Games, P. A., and J. F. Howell. 1976. Pairwise multiple comparison procedures with unequal n's and/or variances: a Monte Carlo study. Journal of Educational and Behavioral Statistics 1:113–125.

Gauthreaux, S. A., and C. G. Belser. 1998. Displays of bird movements on the WSR-88D: patterns and quantification. Weather and Forecasting 13:453–464.

Gauthreaux, S. A., and C. G. Belser. 1999. Bird migration in the region of the Gulf of Mexico. Pages 1931–1947 *in* N. J. Adams and R. H. Slotow, editors. Proceedings of the 22nd International Ornithological Congress. Birdlife South Africa, Durban.

Gauthreaux, S. A., and C. G. Belser. 2006. Effects of artificial night lighting on migrating birds. Pages 67–93 *in* C. Rich and T. Longcore, editors. Ecological consequences of artificial night lighting. Island Press, Washington, D. C.

Gauthreaux, S. A., J. E. Michi, and C. G. Belser. 2005. The temporal and spatial structure of the atmosphere and its influence on bird migration strategies. Pages 182–196 *in* R. Greenberg and P. P. Marra, editors. Birds of two worlds. Smithsonian Institution, Washington, D. C.

Gill, R., and R. J. Fuller. 2007. The effects of deer browsing on woodland structure and songbirds in lowland Britain. Ibis 149:119–127.

Gill, R. M. A. 1992. A review of damage by mammals in north temperate forests: 3. Impact on trees and forests. Forestry 65:363-a-388.

Gordo, O. 2007. Why are bird migration dates shifting? A review of weather and climate effects on avian migratory phenology. Climate Research 35:37–58.

Graber, J. W., and R. R. Graber. 1983. Feeding rates of warblers in spring. The Condor 85:139–150.

Greenberg, C. H., D. J. Levey, C. Kwit, J. P. Mccarty, S. F. Pearson, S. Sargent, and J. Kilgo. 2012. Long-term patterns of fruit production in five forest types of the South Carolina upper coastal plain. The Journal of Wildlife Management 76:1036–1046.

Greenberg, C. H., R. W. Perry, C. A. Harper, D. J. Levey, and J. M. McCord. 2011. The role of young, recently disturbed upland hardwood forest as high quality food patches. Pages 121–141 Sustaining Young Forest Communities. Springer.

Greenberg, C. H., and S. T. Walter. 2010. Fleshy fruit removal and nutritional composition of winter-fruiting plants: a comparison of non-native invasive and native species. Natural Areas Journal 30:312–321.

Hebrard, J. J. 1971. The nightly initiation of passerine migration in spring: A direct visual study. Ibis 113:8–18.

Hedenström, A., and T. Alerstam. 1997. Optimum fuel loads in migratory birds: Distinguishing between time and energy minimization. Journal of Theoretical Biology 189:227–234.

Hejl, S. J., J. A. Holmes, and D. E. Kroodsma. 2002. Winter Wren (*Troglodytes hiemalis*). Page *in* P. G. Rodewald, editor. The Birds of North America. Cornell Lab of Ornithology.

Hijmans, R. J., S. Phillips, J. Leathwick, and J. Elith. 2015. dismo: Species distribution modeling. R package version 1.0-12. The R Foundation for Statistical Computing, Vienna http://cran. r-project. org.

Holmes, R. T. 2005. Black-throated Blue Warbler (*Dendroica caerulescens*). Page *in* A. Poole and F. B. Gill, editors. The Birds of North America. The Academy of Natural Sciences; The American Ornithologist's Union.

Homer, C. G., J. A. Dewitz, L. Yang, S. Jin, P. Danielson, G. Xian, J. Coulston, N. D. Herold, J. D. Wickham, and K. Megown. 2015. Completion of the 2011 National Land Cover Database for the conterminous United States-Representing a decade of land cover change information. Photogrammetric Engineering and Remote Sensing 81:345–354.

Horton, K. G., B. M. Van Doren, P. M. Stepanian, W. M. Hochachka, A. Farnsworth, and J. F. Kelly. 2016. Nocturnally migrating songbirds drift when they can and compensate when they must. Scientific Reports 6:21249.

Hurvich, C. M., and C.-L. Tsai. 1989. Regression and time series model selection in small samples. Biometrika 76:297–307.

Hutto, R. L. 1985. Habitat selection by nonbreeding, migratory land birds. Pages 455–476 *in* M. L. Cody, editor. Habitat selection in birds. Academic Press, Inc., Orlando.

Hutto, R. L. 2000. On the importance of en route periods to the conservation of migratory landbirds. Studies in Avian Biology 20:109–114.

James, F. C., and H. H. Shugart. 1970. A quantitative method of habitat description. Audubon Field Notes 24:727–735.

Johnson, P. 2013. Migratory stopover of songbirds in the western Lake Erie Basin. The Ohio State University, Columbus, OH.

Keast, A., and E. S. Morton. 1980. Migrant birds in the Neotropics: ecology, behavior, distribution, and conservation. Smithsonian Institution Press, Washington, D. C.

Kilgo, J. C., K. V. Miller, and W. P. Smith. 1999. Effects of group-selection timber harvest in bottomland hardwoods on fall migrant birds. Journal of Field Ornithology 70:404–413.

Ktitorov, P., F. Bairlein, and M. Dubinin. 2008. The importance of landscape context for songbirds on migration: body mass gain is related to habitat cover. Landscape Ecology 23:169–179.

La Puma, D., and J. J. Buler. 2013. Radar analysis of bird migration stopover sites in the southeastern U.S: Final Report.

La Sorte, F. A., D. Fink, J. J. Buler, A. Farnsworth, and S. A. Cabrera-Cruz. 2017. Seasonal associations with urban light pollution for nocturnally migrating bird populations. Global Change Biology.

La Sorte, F. A., D. Fink, W. M. Hochachka, A. Farnsworth, A. D. Rodewald, K. V. Rosenberg, B. L. Sullivan, D. W. Winkler, C. Wood, and S. Kelling. 2014. The role of atmospheric conditions in the seasonal dynamics of North American migration flyways. Journal of Biogeography 41:1685–1696.

LaFleur, J. M., J. J. Buler, and F. R. Moore. 2016. Geographic position and landscape composition explain regional patterns of migrating landbird distributions during spring stopover along the northern coast of the Gulf of Mexico. Landscape Ecology 31:1697–1709.

Larkin, R. P. 1991. Flight speeds observed with radar, a correction: slow “birds” are insects. Behavioral Ecology and Sociobiology 29:221–224.

Li, J. 2016. Assessing spatial predictive models in the environmental sciences: Accuracy measures, data variation and variance explained. Environmental Modelling & Software 80:1–8.

Lindström, Å. 1990. The role of predation risk in stopover habitat selection in migrating bramblings *Fringilla montifringilla*. Behavioral Ecology 1:102–106.

Lindström, Å., and T. Alerstam. 1992. Optimal Fat Loads In Migrating Birds: A Test of the Time-Minimization Hypothesis. The American Naturalist 140:477–491.

Lovette, I. J., and R. T. Holmes. 1995. Foraging behavior of American Redstarts in breeding and wintering habitats: implications for relative food availability. Condor:782–791.

Maechler, M., P. Rousseeuw, A. Struyf, M. Hubert, and K. Hornik. 2016. cluster: Cluster Analysis Basics and Extensions. R package version 2.0.1.

Maloney, K. O., M. Schmid, and D. E. Weller. 2012. Applying additive modelling and gradient boosting to assess the effects of watershed and reach characteristics on riverine assemblages. Methods in Ecology and Evolution 3:116–128.

Marquis, R. J., and C. J. Whelan. 1994. Insectivorous bird increase growth of white oak through consumption of leaf- chewing insects. Ecology 75:2007–2014.

Martin, T. E., and J. R. Karr. 1986. Patch utilization by migrating birds: resource oriented? Ornis Scandinavica 17:165–174.

Matthews, S. N., and P. G. Rodewald. 2010. Movement behaviour of a forest songbird in an urbanized landscape: the relative importance of patch-level effects and body condition during migratory stopover. Landscape ecology 25:955–965.

McCabe, J. D., and B. J. Olsen. 2015. Landscape-scale habitat availability, and not local geography, predicts migratory landbird stopover across the Gulf of Maine. Journal of Avian Biology 46:395–405.

McCarty, J. P., D. J. Levey, C. H. Greenberg, and S. Sargent. 2002. Spatial and temporal variation in fruit use by wildlife in a forested landscape. Forest Ecology and Management 164:277–291.

McShea, W. J., and J. H. Rappole. 2000. Managing the abundance and diversity of breeding bird populations through manipulation of deer populations. Conservation Biology 14:1161–1170.

Mehlman, D. W., S. E. Mabey, D. N. Ewert, C. Duncan, B. Abel, D. Cimprich, R. D. Sutter, and M. S. Woodrey. 2005. Conserving stopover sites for forest-dwelling migratory landbirds. Auk 122:1281–1290.

Mesinger, F., G. DiMego, E. Kalnay, K. Mitchell, P. C. Shafran, W. Ebisuzaki, D. Jović, J. Woollen, E. Rogers, E. H. Berbery, M. B. Ek, Y. Fan, R. Grumbine, W. Higgins, H. Li, Y. Lin, G. Manikin, D. Parrish, and W. Shi. 2006. North American regional reanalysis. Bulletin of the American Meteorological Society 87:343–360.

Mills, A. M., B. G. Thurber, S. A. Mackenzie, and P. D. Taylor. 2011. Passerines use nocturnal flights for landscape-scale movements during migration stopover. The Condor 113:597–607.

Mineault, P. 2011. Boosted Generalized Additive Models (bgam) package. MATLAB Central File Exchange.

Mitchell, G. W., A. E. M. Newman, M. Wikelski, and D. Ryan Norris. 2012. Timing of breeding carries over to influence migratory departure in a songbird: an automated radiotracking study. Journal of Animal Ecology 81:1024–1033.

Moore, F. R., and D. A. Aborn. 2000. Mechanisms of en route habitat selection: How do migrants make habitat decisions during stopover? Studies in Avian Biology 20:34–42.

Moore, F. R., S. A. Gauthreaux, P. Kerlinger, and T. R. Simons. 1995. Habitat requirements during migration: important link in conservation. Pages 121–144 *in* T. E. Martin and D. M. Finch, editors. Ecology and management of neotropical migratory birds. Oxford University Press, New York, Oxford.

Moore, F. R., and P. Kerlinger. 1987. Stopover and fat deposition by North American wood-warblers (Parulinae) following spring migration over the Gulf of Mexico. Oecologia 74:47–54.

Moore, F. R., and P. Kerlinger. 1989. Atmospheric structure and avian migration. Current Ornithology 6:109–142.

Moore, F. R., P. Kerlinger, and T. R. Simons. 1990. Stopover on a Gulf Coast barrier island by spring trans-gulf migrants. Wilson Bulletin 102:487–500.

Moore, F. R., and Y. Wang. 1991. Evidence of food-based competition among passerine migrants during stopover. Behavioral Ecology and Sociobiology 28:85–90.

Moore, F. R., M. S. Woodrey, J. J. Buler, S. Woltmann, and T. R. Simons. 2005. Understanding the stopover of migratory birds: a scale dependent approach. Pages 684–689 *in* C. J. Ralph and T. D. Rich, editors. Bird Conservation Implementation and Integration in the Americas: Proceedings of the Third International Partners in Flight Conference. USDA Forest Service, Gen. Tech. Rep. PSW-GTR-191.

Newton, I. 2006. Can conditions experienced during migration limit the population levels of birds? Journal of Ornithology 147:146–166.

Olsen, R. N., T. Gallaway, and D. Mitchell. 2014. Modelling US light pollution. Journal of Environmental Planning and Management 57:883–903.

O'Neal, B. J., J. D. Stafford, and R. P. Larkin. 2010. Waterfowl on weather radar: applying ground-truth to classify and quantify bird movements. Journal of Field Ornithology 81:71–82.

O'Neal, B. J., J. Stafford, and R. P. Larkin. 2012. Stopover duration of fall-migrating dabbling ducks. Journal of Wildlife Management 76:285–293.

Paradis, E., J. Claude, and K. Strimmer. 2004. APE: Analyses of Phylogenetics and Evolution in R language. Bioinformatics 20:289–290.

Petit, D. R. 2000. Habitat use by landbirds along Neartic-Neotropical migration routes: Implications for conservation of stopover habitats. Studies in Avian Biology 20:15–33.

Pettorelli, N., S. Ryan, T. Mueller, N. Bunnefeld, B. Jędrzejewska, M. Lima, and K. Kausrud. 2011. The Normalized Difference Vegetation Index (NDVI):: unforeseen successes in animal ecology. Climate Research 46:15–27.

R Development Core Team. 2016. R: a language and environment for statistical computing. R Foundation for Statistical Computing, Vienna, Austria.

Ralph, C. J. 1978. Disorientation and possible fate of young passerine coastal migrants. Bird Banding 49:237–247.

Rappole, J. H. 1995. The ecology of migrant birds: a neotropical perspective. Smithsonian Institution Press, Washington, D.C.

Reynolds, A. P., G. Richards, B. de la Iglesia, and V. J. Rayward-Smith. 2006. Clustering Rules: A Comparison of Partitioning and Hierarchical Clustering Algorithms. Journal of Mathematical Modelling and Algorithms 5:475–504.

Rich, T. D., C. J. Beardmore, H. Berlanga, P. J. Blancher, M. S. W. Bradstreet, G. S. Butcher, D. W. Demarest, E. H. Dunn, W. C. Hunter, E. E. Iñigo-Elias, J. A. Kennedy, A. M. Martell, A. O. Panjabi, D. N. Pashley, K. V. Rosenberg, C. M. Rustay, J. S. Wendt, and T. C. Will. 2004. Partners in Flight North American Landbird Conservation Plan. Cornell Lab of Ornithology, Ithaca, NY.

Ridgeway, G. 2006. gbm: Generalized boosted regression models. R package version 1:55.

Rodenhouse, N. L., and R. T. Holmes. 1992. Results of experimental and natural food reductions for breeding Black-throated Blue Warblers. Ecology 73:357–372.

Rodewald, P. G., and M. C. Brittingham. 2004. Stopover habitats of landbirds during fall: use of edge-dominated and early-successional forests. Auk 121:1040–1055.

Rodewald, P. G., and M. C. Brittingham. 2007. Stopover habitat use by spring migrant landbirds: the roles of habitat structure, leaf development, and food availability. The Auk 124:1063–1074.

Rodewald, P. G., and S. N. Matthews. 2005. Landbird use of riparian and upland forest stopover habitats in an urban landscape. Condor 107:259–268.

Roth, R. R., M. S. Johnson, and T. J. Underwood. 2011. Wood Thrush (*Hylocichla mustelina*). Page The Birds of North America. The Academy of Natural Sciences; The American Ornithologist's Union.

Ruth, J. M., R. H. Diehl, and R. K. Felix Jr. 2012. Migrating birds' use of stopover habitat in the Southwestern United States. The Condor 114:698–710.

Ryder, T. B., J. W. Fox, and P. P. Marra. 2011. Estimating migratory connectivity of gray catbirds (*Dumetella carolinensis*) using geolocator and mark—recapture data. The Auk 128:448–453.

Saino, N., D. Rubolini, J. Von Hardenberg, R. Ambrosini, A. Provenzale, M. Romano, and F. Spina. 2010. Spring migration decisions in relation to weather are predicted by wing morphology among trans-Mediterranean migratory birds. Functional Ecology 24:658–669.

Schaub, M., L. Jenni, and F. Bairlein. 2008. Fuel stores, fuel accumulation, and the decision to depart from a migration stopover site. Behavioral Ecology 19:657–666.

Schaub, M., F. Liechti, and L. Jenni. 2004. Departure of migrating European robins, *Erithacus rubecula*, from a stopover site in relation to wind and rain. Anim Behav 67.

Schmaljohann, H., and B. Naef-Daenzer. 2011. Body condition and wind support initiate the shift of migratory direction and timing of nocturnal departure in a songbird. Journal of Animal Ecology 80:1115–1122.

Seto, K. C., E. Fleishman, J. P. Fay, and C. J. Betrus. 2004. Linking spatial patterns of bird and butterfly species richness with Landsat TM derived NDVI. International Journal of Remote Sensing 25:4309–4324.

Sheehy, J., C. M. Taylor, and D. R. Norris. 2011. The importance of stopover habitat for developing effective conservation strategies for migratory animals. Journal of Ornithology 152:161–168.

Sherry, T. W., and R. T. Holmes. 2016. American Redstart (*Setophaga ruticilla*). Page *in* A. Poole and F. B. Gill, editors. The Birds of North America. The Academy of Natural Sciences; The American Ornithologist's Union.

Sillett, T. S., and R. T. Holmes. 2002. Variation in survivorship of a migratory songbird throughout its annual cycle. Journal of Animal Ecology 71:296–308.

Skagen, S. K., C. P. Melcher, W. H. Howe, and F. L. Knopf. 1998. Comparative use of riparian corridors and oases by migrating birds in southeast Arizona. Conservation Biology 12:896–909.

Smith, S. B., and S. R. McWilliams. 2009. Dietary macronutrients affect lipid metabolites and body composition of a migratory passerine, the White-throated Sparrow (*Zonotrichia albicollis*). Physiological and Biochemical Zoology 82:258–269.

Smolinsky, J., R. Diehl, T. Radzio, D. Delaney, and F. Moore. 2013. Factors influencing the movement biology of migrant songbirds confronted with an ecological barrier. Behavioral Ecology and Sociobiology 67:2041–2051.

Somershoe, S. G., and C. R. Chandler. 2004. Use of oak hammocks by Neotropical migrant songbirds: the role of area and habitat. Wilson Bulletin 116:56–63.

Stanley, C. Q., M. MacPherson, K. C. Fraser, E. A. McKinnon, and B. J. Stutchbury. 2012. Repeat tracking of individual songbirds reveals consistent migration timing but flexibility in route. PloS one 7:e40688.

Strobl, E. 2010. Vegetation characterization for the Lake Ontario stopover project. Rochester Institute of Technology, Rochester, NY.

Strong, A. M. 2000. Divergent foraging strategies of two Neotropical migrant warblers: Implications for winter habitat use. Auk 117:381–392.

Stutchbury, B. J., E. A. Gow, T. Done, M. MacPherson, J. W. Fox, and V. Afanasyev. 2011. Effects of post-breeding moult and energetic condition on timing of songbird migration into the tropics. Proceedings of the Royal Society of London B: Biological Sciences 278:131–137.

Suthers, H. B., J. M. Bickal, and P. G. Rodewald. 2000. Use of successional habitat and fruit resources by songbirds during autumn migration in central New Jersey. Wilson Bulletin 112:249–260.

The Mathworks. 2016. MATLAB. Natick, Massachusetts, USA.

Valcu, M., and B. Kempenaers. 2010. Spatial autocorrelation: an overlooked concept in behavioral ecology. Behavioral Ecology 21:902–905.

Van Doren, B. M., K. G. Horton, P. M. Stepanian, D. S. Mizrahi, and A. Farnsworth. 2016. Wind drift explains the reoriented morning flights of songbirds. Behavioral Ecology 27:1122–1131.

Van Doren, B. M., D. Sheldon, J. Geevarghese, W. M. Hochachka, and A. Farnsworth. 2014. Autumn morning flights of migrant songbirds in the northeastern United States are linked to nocturnal migration and winds aloft. The Auk 132:105–118.

Warkentin, I. G., and D. Hernández. 1996. The conservation implications of site fidelity: a case study involving Nearctic-Neotropical migrant songbirds wintering in a Costa Rican mangrove. Biological Conservation 77:143–150.

Watts, B. D., and S. E. Mabey. 1994. Migratory landbirds of the lower Delmarva: habitat selection and geographic distribution. Report No. NA37OZ0360-01, Virginia Department of Environmental Quality Coastal Resource Management Program, Richmond, VA.

Wilson, R. R., and D. J. Twedt. 2003. Spring bird migration in Mississippi Alluvial Valley forests. American Midland Naturalist 149:163–175.

Woodworth, B. K., C. M. Francis, and P. D. Taylor. 2014. Inland flights of young red-eyed vireos Vireo olivaceus in relation to survival and habitat in a coastal stopover landscape. Journal of Avian Biology 45:387–395.

Table 1. Predictor variables included in the final boosted generalized additive model (BGAM) of seasonal mean landbird density at migration stopover sites (as measured by vertically integrated reflectivity) across the northeastern U.S. 'Category' groups variables according to the scale at which they apply; 'corrective predictors' dRdr and relelev were used to fit models but not for estimating regional densities.

Name	Category	Description (units)	Range measured
hwood	Landscape	hardwood fraction within 1 km	0 - 1
hw5km	Landscape	hardwood fraction within 5 km	0 - 1
hw50	Landscape	hardwood fraction within 50 km	0.08 - 0.88
cnf5km	Landscape	coniferous fraction within 5 km	0 - 0.86
emmarsh5km	Landscape	Non-forested wetlands fraction within 5 km	0 – 1
ag5km	Landscape	agricultural fraction within 5 km	0 - 0.89
urb5km	Landscape	urban fraction within 5 km	0 - 1
ndvimean	Landscape	mean fall NDVI	-0.16 - 0.86
ndvistd	Landscape	standard deviation NDVI	0 - 0.31
X	Regional	distance to seaboard (km)	$-2.8\ 10^5 - 1.1\ 10^$
Y	Regional	distance down seaboard (km)	$4.0\ 10^6 - 5.3\ 10^6$
Lat	Regional	latitude (degrees)	36.5 – 47.4
dAtl	Coastal	distance to Atlantic coast (km)	0 - 150
dGtL	Coastal	distance to Great Lakes coast (km)	0 - 150
dBrL	Coastal	distance to bright light (km)	0 - 208
dRdr	Corrective	distance from radar (km)	6 - 64
relelev	Corrective	elevation versus radar (m)	-873 - 1660

Table 2. Independent variables available for use in boosted regression tree (BRT) analyses of ground survey data to identify site or survey characteristics that influence density of landbirds on migratory stopovers. For each variable, the spatial scale (P = Patch, L = Landscape, R = Regional) is given as well as a brief description, mean untransformed value of continuous variables, range of values, whether it was log transformed (Y= yes, N= no), and if it was included in the ensemble models used for the BRT analysis (Y= yes, N= no).

Variable Name	Scale	Variable Description	Mean value	Value range	Transformed Data	Used In Final Models
Date	-	Dates of patch-scale data collection	-	-	N	N
Transect	P	Survey sites; random effect in ALL models	-	-	N	N
Region	R	a = AKQ , b = ESVA , c = MD , d = DE	-	-	N	N
Year	-	a = 2013 , b = 2014	-	-	N	Y
Period	-	21 days each; 1 = 15Aug-4Sept , 2 = 5Sept-25Sept , 3 = 26Sept-16Oct , 4 = 17Oct-7Nov	-	-	N	Y
InvPerGrBr	P	Invertebrates per gram of branch, all species	0.09	0 – 2.02	Y	Y
InvVism2	P	Invertebrates per m2 ground surveyed, all species	10.70	0 – 214.67	Y	Y
InvBrAR	P	Arachnids per gram of branch	0.06	0 – 1.87	Y	N
InvVisAR	P	Arachnids per m2 ground surveyed	3.76	0 – 213.33	Y	Y
InvBrLep	P	Lepidoptera per gram of branch	0.00	0 – 0.65	Y	Y
InvVisLep	P	Lepidoptera per m2 ground surveyed	0.05	0 – 2.67	Y	Y
InvBrDI	P	Diptera per gram of branch	0.01	0 – 0.17	Y	Y
InvVisDI	P	Diptera per m2 ground surveyed	2.32	0 – 20.00	Y	Y
InvBrOR	P	Orthoptera per gram of branch	1.00	0.99 – 1.16	Y	Y
InvVisOR	P	Orthoptera per m2 ground surveyed	4.57	0.99 – 785.76	Y	Y
FrtAllm2	P	Ripe fruit per m2 for all species	0.68	0 – 16.76	Y	Y
FrtBGum	P	Ripe Black Gum per m2	0.07	0 – 6.04	Y	Y
FrtHolly	P	Ripe American Holly per m2	0.16	0 – 10.42	Y	Y
FrtBlueB	P	Ripe Blueberry per m2	0.00	0 – 0.31	Y	Y
FrtDogw	P	Ripe Flowering Dogwood per m2	0.00	0 – 0.44	Y	Y
FrtGrape	P	Ripe Grape per m2	0.09	0 – 8.40	Y	Y
FrtParB	P	Ripe Partridge Berry per m2	1.00	0.99 – 1.67	Y	Y
FrtSmilax	P	Ripe Greenbrier per m2	0.04	0 – 3.79	Y	Y
Latitude	R	Latitude (decimal)	37.88	36.58 – 39.27	N	Y
CanopyC	P	Average canopy cover (%)	93.1	79.3 – 96	N	Y
LitterDep	P	Average litter depth	27.8	8.2 – 55.5	N	Y
CtGrLeaf	P	Ocular tube litter count (out of 20)	19.1	4.3 – 20	N	Y
CtGrVeg	P	Ocular tube ground vegetation count (out of 20)	7.1	0.5 – 16.5	N	Y
CtMidstory	P	Ocular tube midstory count (out of 20)	17.6	10.8 – 20	N	N
CtVine	P	Ocular tube vine count (out of 20)	1.2	0 – 6.5	N	Y
CtGrShrub	P	Ocular tube shrub count (out of 20)	16.0	4 – 20	N	Y
ShrubStemCt	P	Count of total shrub stems	278	3 – 2186	N	Y

ShrubDiv	P	Number of shrub species	8.7	1 – 17	N	N
BlueBShrub	P	Blueberry shrubs present (Y/N)	-	-	N	N
PrivetShrub	P	Privet shrubs present (Y/N)	-	-	N	N
WaxShrub	P	Wax Myrtle shrubs present (Y/N)	-	-	N	N
LgTreeDiv	P	Number of tree species (>8cm DBH)	-	-	N	N
LgTreeSp	P	Most abundant tree; a = Holly , b = Pine , c = Gum , d = Maple , e = Sweetgum , f = Oak , g = Poplar	-	-	N	N
basalarea	P	Total basal area for each site	591	332 – 1569	N	Y
skybright	P	Sky brightness ratio	0.42	0.05 – 4.47	N	N
NDVI	P	Normalized Difference Vegetation Index	7548	2325 - 9402	N	Y
distcoast	R	Distance to nearest coast	16.7	0.2 – 71.4	N	N
distatl	R	Distance to Atlantic Ocean	37.3	1.3 – 115.9	N	Y
dist_sky_5	R	Distance to areas of sky brightness > 5	59.5	0 – 120.2	N	Y
impurban1km	L	Impervious urbanization within buffer	0.05	0.00 – 0.65	N	Y
water1km	L	Permanent water within buffer	0.06	0 – 0.36	N	Y
ag1km	L	Agriculture / pasture within buffer	0.24	0 – 0.68	N	Y
hrdwood1km	L	Deciduous forest within buffer	0.43	0.07 – 0.91	N	Y
pine1km	L	Evergreen forest within buffer	0.11	0 – 0.53	N	N
shrub1km	L	Scrub / shrubland within buffer	0.05	0 – 0.24	N	Y
wetlnd1km	L	Marsh / wetland within buffer	0.04	0 – 0.23	N	Y
grassurb1km	L	Grassland / urban lawns within buffer	0.08	0 – 0.39	N	N
impurban5km	L	Impervious urbanization within buffer	0.05	0.00 – 0.65	N	N
water5km	L	Permanent water within buffer	0.13	0 – 0.61	N	N
ag5km	L	Agriculture / pasture within buffer	0.35	0 – 0.67	N	N
hrdwood5km	L	Deciduous forest within buffer	0.31	0.05 – 0.75	N	N
pine5km	L	Evergreen forest within buffer	0.07	0 – 0.26	N	N
shrub5km	L	Scrub / shrubland within buffer	0.04	0.00 – 0.19	N	N
wetlnd5km	L	Marsh / wetland within buffer	0.06	0.00 – 0.44	N	N
grassurb5km	L	Grassland / urban lawns within buffer	0.07	0.02 – 0.20	N	N

Table 3. Cross-correlation strength of potential explanatory variables. Values are Pearson correlation coefficients, and only those with moderate to strong correlations (strength < -0.7 or >0.7) are presented.

Variable 1	Variable 2	Correlation
impurban5km	skybright	0.97369894
skybright	urban5km	0.962902399
impurban5km	urban5km	0.961383704
impurban1km	urban1km	0.937281273
impurban1km	urban5km	0.919006943
pine5km	shrub5km	0.90989301
impurban1km	impurban5km	0.905324636
impurban1km	skybright	0.898904694
urban1km	urban5km	0.868620007
distcoast	distatl	0.861922637
grassurb1km	urban1km	0.85018663
water1km	water5km	0.834572192
pine1km	pine5km	0.823974503
InvPerGrBr	InvBrAR	0.820847392
distcoast	shrub5km	0.819132513
grassurb5km	urban5km	0.818769297
skybright	urban1km	0.812702184
distatl	shrub5km	0.810212851
impurban5km	urban1km	0.792868347
hrdwood1km	hrdwood5km	0.790221065
impurban5km	grassurb5km	0.752109572
ag1km	ag5km	0.736922164
grassurb5km	skybright	0.734510288
grassurb5km	urban1km	0.712981486
CtMidstory	pine1km	0.723955281

Table 4. Number of suitable sampling nights for each radar and year for the autumn migration season. The percent of suitable nights out of all screened nights by radar across years is also presented.

	Radar	Year							Total	%
		2008	2009	2010	2011	2012	2013	2014		
NEXRAD	AKQ	9	9	9	6	5	15	7	60	10
	BGM	13	9	13	2	5	7	16	65	11
	BOX	13	7	11	10	17	24	16	98	16
	BUF	11	7	4	3	4	9	21	59	10
	CBW	7	5	15	11	21	15	11	85	14
	CCX	5	11	18	12	19	17	11	93	16
	DIX	9	2	11	13	6	18	7	66	11
	DOX	13	17	22	8	11	12	10	93	16
	ENX	17	10	12	11	6	16	21	93	16
	FCX	15	10	27	12	16	14	16	110	18
	GYX	16	11	18	18	28	30	18	139	23
	LWX	12	25	21	16	25	25	13	137	23
	OKX	19	7	19	13	7	26	14	105	18
	PBZ	15	22	17	16	13	26	26	135	23
	RLX	14	15	4	5	8	9	13	68	11
	TYX	7	9	17	13	12	12	15	85	14
TDWR	TJFK	n/a	21	25	12	18	17	32	125	25
	TPHL	n/a	30	31	24	29	41	34	189	37
	TBWI	n/a	21	14	11	20	22	20	108	21
	TDCA	n/a	17	24	16	18	29	23	127	25
Total		195	265	332	232	288	384	344	2040	18

Table 5. Interactions between predictors selected by Boosted Regression Trees for mean and variability in reflectivity (see text and Table 1 for names and descriptions of predictors)

Interaction
X*Y
X*hw50
Y*hw50
Y*dAtl
Y*dGtL
dAtl*ndvistd
dAtl* hw50
dBrLt* hw50
cnf5km*hw50
hw5km*hw50
ndvimean*std

Table 6. List of transect sites, nearby radar (KAKQ = Wakefield, VA; KDOX= Dover, DE; Outside = Outside radar range), State (ES = Eastern Shore of Virginia, VA = Inland SE Virginia), number of visits, detection probabilities, and detection-corrected migrant bird densities within 50 m of the transect centerline during fall 2013 and 2014.

Transect	Radar	Location of Site	# of Visits (2013 / 2014)	% detected within 50 m (2013 / 2014)	Density (birds/ha/visit) (2013 / 2014)
CBSN	KAKQ	VA	19 / 19	0.48 / 0.63	1.6 / 1.41
CPSP	KAKQ	VA	20 / 17	0.54 / 0.52	2.38 / 2.47
CSNA	KAKQ	VA	19 / 17	0.57 / 0.57	2.92 / 1.87
GDNW	KAKQ	VA	14 / 16	0.4 / 0.58	2.35 / 1.16
GDSE	KAKQ	VA	19 / 17	0.48 / 0.42	2.21 / 1.26
GDSW	KAKQ	VA	13 / -	0.51 / -	1.35 / -
HCWP	KAKQ	VA	19 / 17	0.52 / 0.46	2.22 / 1.73
MSBT	KAKQ	VA	20 / 17	0.58 / 0.66	2.87 / 1.69
PACP	KAKQ	VA	19 / 17	0.23 / 0.31	4.25 / 2.22
RACP	KAKQ	VA	19 / 18	0.45 / 0.56	3.43 / 2.06
SOQU	KAKQ	VA	15 / 17	0.49 / 0.59	2.78 / 3.07
WADI	KAKQ	VA	- / 12	- / 0.62	- / 0.97
ZUNI	KAKQ	VA	16 / 17	0.48 / 0.52	4.19 / 2.59
BFLP	KDOX	DE	17 / 15	0.57 / 0.51	1.85 / 2.54
BHNW	KDOX	DE	14 / 15	0.67 / 0.67	3.74 / 2.38
BLWA	KDOX	DE	17 / 15	0.72 / 0.69	2.55 / 2.74
CHSP	KDOX	DE	18 / 15	0.71 / 0.57	2.54 / 4.57
FBNP	KDOX	DE	17 / 15	0.68 / 0.59	2.78 / 3.87
IDYL	KDOX	MD	18 / 16	0.62 / 0.41	2.49/ 3.51
KPSP	KDOX	MD	17 / 15	0.68 / 0.59	2.57 / 2.84
MAHO	KDOX	MD	18 / 16	0.38 / 0.45	3.43 / 3.23
MASP	KDOX	DE	18 / 16	0.43 / 0.40	2.55 / 2.30
MCWS	KDOX	DE	16 / 15	0.63 / 0.51	1.09 / 3.00
MNWA	KDOX	DE	16 / 15	0.57 / 0.63	4.55 / 2.66
NWWA	KDOX	DE	17 / 15	0.63 / 0.73	2.86 / 1.17
PHWA	KDOX	DE	17 / 15	0.67 / 0.19	2.14 / 8.69
THWO	KDOX	DE	16 / 15	0.63 / 0.61	2.62 / 2.91
TUSP	KDOX	DE	17 / 15	0.73 / 0.64	3.28 / 2.66
BROW	Outside	ES	17 / 16	0.54 / 0.64	1.78 / 2.54
CACH	Outside	ES	18 / 16	0.45 / 0.41	2.55 / 2.88
EAVA	Outside	MD	17 / 16	0.62 / 0.37	2.09 / 2.36
FOES	Outside	MD	17 / 16	0.56 / 0.54	2.29 / 2.51
KIPT	Outside	ES	16 / 16	0.55 / 0.37	2.51 / 8.88
MAFA	Outside	ES	15 / 15	0.35 / 0.41	3.09 / 3.57
MARU	Outside	MD	17 / 16	0.62 / 0.56	1.41 / 1.80
MILA	Outside	MD	17 / 16	0.72 / 0.60	1.92 / 1.63
MUHU	Outside	ES	18 / 16	0.42 / 0.46	3.17 / 2.32
NAMI	Outside	MD	19 / 16	0.46 / 0.57	2.12 / 1.33
NASS	Outside	MD	18 / 16	0.60 / 0.57	1.85 / 1.85
OAGR	Outside	ES	18 / 15	0.41 / 0.43	3.82 / 6.00
PHFA	Outside	ES	17 / 15	0.29 / 0.55	3.51 / 2.63
PIHA	Outside	ES	18 / 16	0.48 / 0.37	3.61 / 5.58
POSF	Outside	MD	18 / 15	0.54 / 0.53	3.48 / 3.89
PRAN	Outside	MD	17 / 15	0.40 / 0.51	4.06 / 1.96
PUDD	Outside	ES	18 / 16	0.44 / 0.49	3.17 / 3.34
QUIN	Outside	ES	16 / 14	0.60 / 0.51	1.27 / 1.91
SANE	Outside	ES	18 / 16	0.39 / 0.52	5.23 / 2.46
WAIS	Outside	ES	14 / 14	0.55 / 0.58	3.11 / 1.66
WICO	Outside	MD	16 / 16	0.58 / 0.38	1.61 / 3.21

Table 7. Complete list of bird species and species groups detected during fall 2013 and fall 2014 among 48 transect locations. Migration status classifications (mi – transient, su – summer breeder, wi – winter resident, yr – year-round) and total detections are also presented. Species are ordered by declining number of detections.

Common Name	Species Code	Scientific Name	Migration Status	Total Detections
Carolina Wren	CARW	*Thryothorus ludovicianus*	yr	1538
(Eastern) Tufted Titmouse	ETTI	*Baeolophus bicolor*	yr	1210
Northern Cardinal	NOCA	*Cardinalis cardinalis*	yr	1104
Red-bellied Woodpecker	RBWO	*Melanerpes carolinus*	yr	1033
Carolina Chickadee	CACH	*Poecile carolinensis*	yr	1010
American Robin	AMRO	*Turdus migratorius*	yr	861
Blue Jay	BLJA	*Cyanocitta cristata*	yr	805
Downy Woodpecker	DOWO	*Picoides pubescens*	yr	600
Unknown Bird				594
Yellow-shafted Flicker	YSFL	*Colaptes auratus*	wi	542
Golden-crowned Kinglet	GCKI	*Regulus satrapa*	wi	439
American Crow	AMCR	*Corvus brachyrhynchos*	yr	438
Unknown Warbler				424
Pileated Woodpecker	PIWO	*Dryocopus pileatus*	yr	418
Red-eyed Vireo	REVI	*Vireo olivaceus*	su	395
Eastern Wood-Pewee	EAWP	*Contopus virens*	su	345
White-breasted Nuthatch	WBNU	*Sitta carolinensis*	yr	293
Yellow-rumped Warbler	MYWA	*Setophaga coronata*	wi	270
Pine Warbler	PIWA	*Setophaga pinus*	yr	268
Acadian Flycatcher	ACFL	*Empidonax virescens*	su	240
American Goldfinch	AMGO	*Spinus tristis*	yr	240
Hairy Woodpecker	HAWO	*Picoides villosus*	yr	199
Hermit Thrush	HETH	*Catharus guttatus*	wi	193
Mourning Dove	MODO	*Zenaida macroura*	yr	140
Black-throated Blue Warbler	BTBW	*Setophaga caerulescens*	mi	138
Common Grackle	COGR	*Quiscalus quiscula*	yr	132
Unknown Woodpecker				132
American Redstart	AMRE	*Setophaga ruticilla*	mi	127
Wood Thrush	WOTH	*Hylocichla mustelina*	su	117
Ruby-crowned Kinglet	RCKI	*Regulus calendula*	wi	112
Great Crested Flycatcher	GCFL	*Myiarchus crinitus*	su	105
Winter Wren	WIWR	*Troglodytes hiemalis*	wi	94
White-eyed Vireo	WEVI	*Vireo griseus*	su	90
Red-shouldered Hawk	RSHA	*Buteo lineatus*	yr	85
Eastern Towhee	EATO	*Pipilo erythrophthalmus*	yr	83
Yellow-billed Cuckoo	YBCU	*Coccyzus americanus*	su	80
Black-and-white Warbler	BAWW	*Mniotilta varia*	su	76
Cedar Waxwing	CEDW	*Bombycilla cedrorum*	yr	74
Eastern Bluebird	EABL	*Sialia sialis*	yr	73

White-throated Sparrow	WTSP	*Zonotrichia albicollis*	wi	70
Veery	VEER	*Catharus fuscescens*	mi	68
Brown Creeper	BRCR	*Certhia americana*	wi	67
Unknown Blackbird				65
Gray Catbird	GRCA	*Dumetella carolinensis*	su	62
Ovenbird	OVEN	*Seiurus aurocapilla*	su	59
Turkey Vulture	TUVU	*Cathartes aura*	yr	58
Canada Goose	CAGO	*Branta canadensis*	yr	54
Red-winged Blackbird	RWBL	*Agelaius phoeniceus*	yr	51
Yellow-throated Vireo	YTVI	*Vireo flavifrons*	su	50
Hooded Warbler	HOWA	*Setophaga citrina*	su	45
Scarlet Tanager	SCTA	*Piranga olivacea*	su	42
Summer Tanager	SUTA	*Piranga rubra*	su	37
Red-headed Woodpecker	RHWO	*Melanerpes erythrocephalus*	yr	34
Chimney Swift	CHSW	*Chaetura pelagica*	su	30
Barred Owl	BDOW	*Strix varia*	yr	28
Northern Parula	NOPA	*Setophaga americana*	mi	28
Brown Thrasher	BRTH	*Toxostoma rufum*	yr	27
Wild Turkey	WITU	*Meleagris gallopavo*	yr	26
Yellow-bellied Sapsucker	YBSA	*Sphyrapicus varius*	wi	25
Bobolink	BOBO	*Dolichonyx oryzivorus*	mi	23
Fish Crow	FICR	*Corvus ossifragus*	yr	23
Ruby-throated Hummingbird	RTHU	*Archilochus colibris*	su	20
Blackpoll Warbler	BLPW	*Setophaga striata*	mi	19
Eastern Phoebe	EAPH	*Sayornis phoebe*	su	18
Swainson's Thrush	SWTH	*Catharus ustulatus*	mi	16
Wood/Catharus Thrush				16
Unknown Empidonax		*Empidonax* sp.		15
Brown-headed Nuthatch	BHNU	*Sitta pusilla*	yr	14
Dark-eyed (Slate-colored) Junco	SCJU	*Junco hyemalis*	wi	14
Worm-eating Warbler	WEWA	*Helmitheros vermivorum*	su	14
Blue-headed Vireo	BHVI	*Vireo solitarius*	mi	12
Brown-headed Cowbird	BHCO	*Molothrus ater*	yr	12
European Starling	EUST	*Sturnus vulgaris*	yr	12
Great Blue Heron	GBHE	*Ardea herodias*	yr	12
House Finch	HOFI	*Carpodacus mexicanus*	yr	12
Purple Martin	PUMA	*Progne subis*	su	12
Bald Eagle	BAEA	*Haliaeetus leucocephalus*	yr	11
Chestnut-sided Warbler	CSWA	*Setophaga pensylvanica*	mi	10
Common Yellowthroat	COYE	*Geothlypis trichas*	su	10
Gray-cheeked Thrush	GCTH	*Catharus minimus*	mi	10
Indigo Bunting	INBU	*Passerina cyanea*	su	10
Northern Mockingbird	NOMO	*Mimus polyglottos*	yr	10

Red-tailed Hawk	RTHA	*Buteo jamaicensis*	yr	10
Killdeer	KILL	*Charadrius vociferus*	yr	9
Magnolia Warbler	MAWA	*Setophaga magnolia*	mi	9
Northern (Baltimore) Oriole	BAOR	*Icterus galbula*	su	9
Prothonotary Warbler	PROW	*Protonotaria citrea*	su	9
Eastern Screech-Owl	EASO	*Megascops asio*	yr	8
Field Sparrow	FISP	*Spizella pusilla*	su	8
Rose-breasted Grosbeak	RBGR	*Pheucticus ludovicianus*	mi	8
Tree Swallow	TRES	*Tachycineta bicolor*	su	8
Belted Kingfisher	BEKI	*Megaceryle alcyon*	yr	7
Great Horned Owl	GHOW	*Bubo virginianus*	yr	7
Northern Waterthrush	NOWA	*Parkesia noveboracensis*	mi	7
Unknown Vireo		*Vireo* sp.		7
Blue Grosbeak	BLGR	*Passerina caerulea*	su	6
Pine Siskin	PISI	*Spinus pinus*	wi	6
Unknown Hawk				6
American Woodcock	AMWO	*Scolopax minor*	yr	5
Black Vulture	BLVU	*Coragyps atratus*	yr	5
Black-throated Green Warbler	BTNW	*Setophaga nigrescens*	mi	5
Blue-gray Gnatcatcher	BGGN	*Polioptila caerula*	su	5
Cooper's Hawk	COHA	*Accipiter cooperii*	yr	5
Herring Gull	HERG	*Larus argentatus*	yr	5
Snow Goose	SNGO	*Chen caerulescens*	wi	5
Song Sparrow	SOSP	*Melospiza melodia*	yr	5
Unknown Accipiter		*Accipiter* sp.	yr	5
Unknown Gull				5
Barn Swallow	BARS	*Hirundo rustica*	su	4
Fox Sparrow	FOSP	*Passerella iliaca*	wi	4
House Wren	HOWR	*Troglodytes aedon*	su	4
Red-breasted Nuthatch	RBNU	*Sitta canadensis*	wi	4
Sharp-shinned Hawk	SSHA	*Accipiter striatus*	yr	4
Black-billed Cuckoo	BBCU	*Coccyzus erythropthalmus*	mi	3
Blackburnian Warbler	BLBW	*Setophaga fusca*	mi	3
Caspian Tern	CATE	*Hydroprogne caspia*	su	3
Great Egret	GREG	*Ardea alba*	yr	3
Greater Yellowlegs	GRYE	*Tringa melanoleuca*	mi	3
Northern Bobwhite	NOBO	*Colinus virginianus*	yr	3
Osprey	OSPR	*Pandion haliaetus*	su	3
Rusty Blackbird	RUBL	*Euphagus carolinus*	wi	3
Swamp Sparrow	SWSP	*Melospiza georgiana*	wi	3
Unknown Catharus		*Catharus* sp.	mi	3
Warbling Vireo	WAVI	*Vireo gilvus*	su	3
Wood Duck	WODU	*Aix sponsa*	yr	3

Yellow-breasted Chat	YBCH	*Icteria virens*	su	3
American Pipit	AMPI	*Anthus rubescens*	wi	2
Bay-breasted Warbler	BBWA	*Setophaga castanea*	mi	2
Canada Warbler	CAWA	*Cardellina canadensis*	mi	2
Cape May Warbler	CMWA	*Setophaga tigrina*	mi	2
Chipping Sparrow	CHSP	*Spizella passerina*	su	2
Horned Lark	HOLA	*Eremophila alpestris*	yr	2
Laughing Gull	LAGU	*Leucophaeus atricilla*	su	2
Unknown Buteo		*Buteo* sp.		2
Unknown Icterid		*Icterid* sp.	su	2
Unknown Owl			yr	2
Bank Swallow	BANS	*Riparia riparia*	su	1
Barn Owl	BANO	*Tyto alba*	yr	1
Blue-winged Warbler	BWWA	*Vermivora cyanoptera*	mi	1
Palm Warbler	PAWA	*Setophaga palmarum*	mi	1
Swainson's Warbler	SWWA	*Limnothlypis swainsonii*	su	1
Unknown Crow		*Crow* sp.	yr	1
Unknown Hummingbird			su	1
Unknown Oriole		*Icterus* sp.	su	1
Unknown Wren				1
Unknown Kinglet		*Regulus* sp.	wi	1
Yellow-bellied Flycatcher	YBFL	*Empidonax flaviventris*	mi	1

Table 8. Parameters and predictive performance metrics for all BRT models used in analysis of ground survey data, obtained from 10-fold cross-validation and using the 31 predictor variables detailed in Table 2. Table values indicate: the response variable for each model, each model's optimal learning rate, number of trees fitted for the final ensemble model, proportion of total deviance explained of the training data; and cross validation correlation. For all models, bag fraction was left at 0.5 and tree complexity at 2. Note: See Table 10 for species codes.

Response Variable (Model)	Learning Rate	No. of Trees	Proportion Deviance Explained	CV Correlation
AllMigPerHa	0.015	1100	0.38	0.43
FrugMigPerHa	0.0025	1400	0.24	0.39
TransMigPerHa	0.005	1700	0.27	0.37
BreedMigPerHa	0.015	1900	0.64	0.64
WinterMigPerHa	0.0025	1200	0.41	0.62
ACFL	0.015	1300	0.50	0.56
AMRE	0.005	1600	0.31	0.34
BTBW	0.01	1100	0.30	0.34
EAWP	0.005	1500	0.46	0.54
GCFL	0.0025	1100	0.25	0.35
GCKI	0.0025	1700	0.39	0.57
HETH	0.001	1600	0.28	0.40
MYWA	0.001	1500	0.16	0.38
RCKI	0.001	1600	0.13	0.31
REVI	0.015	1200	0.62	0.59
WEVI	0.025	1200	0.59	0.63
WIWR	0.005	1700	0.38	0.48
WOTH	0.0025	1200	0.26	0.30
YSFL	0.005	1800	0.30	0.39

Table 9. Summary table for the relative contributions (%) of each predictor variable included in boosted regression tree models developed to identify which factors were most influential in determining migrant density for 14 bird species. Species codes defined in Table 8.

	Predictor	Response Variable (%)													
		ACFL	AMRE	BTBW	EAWP	GCFL	GCKI	HETH	MYWA	RCKI	REVI	WEVI	WIWR	WOTH	YSFL
Patch / Food Resources	InvPerGrBr	**5.40**	2.10	2.04	**7.11**	1.99	0.74	0.30	4.56	**5.31**	**13.02**	1.61	1.74	**5.30**	4.83
	InvVism2	2.08	1.36	1.69	0.96	1.66	0.53	0.09	**5.00**	0.17	0.83	1.89	2.07	**21.09**	1.60
	InvVisAR	0.94	1.67	2.29	0.72	0.30	**7.22**	0.34	1.81	0.15	0.65	1.19	1.04	0.57	3.36
	InvBrLep	0.88	2.69	**8.20**	0.21	0.33	0.12	0.00	0.00	0.00	0.21	1.58	0.05	0.37	2.15
	InvVisLep	0.03	0.00	0.00	0.27	0.20	0.00	0.00	0.00	0.00	0.00	0.78	0.00	0.00	0.00
	InvBrDI	3.88	0.09	0.65	0.15	0.16	2.56	2.29	0.07	0.97	0.00	1.30	**5.29**	0.89	0.99
	InvVisDI	0.57	2.46	0.39	0.14	0.86	0.17	0.04	0.03	0.28	0.38	0.28	0.34	0.08	0.93
	InvBrOR	0.22	0.17	0.20	1.37	0.92	0.00	0.00	0.00	0.00	1.49	0.86	0.00	0.00	0.06
	InvVisOR	0.39	0.02	0.65	0.70	0.26	0.00	0.00	0.00	0.00	2.18	0.63	0.00	0.00	0.30
	FrtAllm2	2.15	**19.87**	3.21	0.62	4.67	0.37	0.98	0.40	1.12	2.21	2.86	1.84	0.43	**5.79**
	FrtBGum	0.23	0.09	2.23	0.34	3.25	0.16	0.00	1.25	0.00	1.66	0.50	2.23	3.06	**7.10**
	FrtHolly	0.56	2.50	1.36	0.02	0.01	**5.58**	**16.96**	0.91	**11.50**	0.00	0.23	4.60	0.07	**6.29**
	FrtBlueB	0.78	0.00	0.00	0.91	0.13	0.00	0.00	0.00	0.00	0.16	0.35	0.00	0.00	0.00
	FrtDogw	0.14	0.00	0.15	0.00	0.00	0.00	0.00	0.00	0.00	0.00	1.44	0.00	0.00	0.01
	FrtGrape	0.20	**8.66**	**8.30**	0.00	0.00	0.13	0.00	**5.83**	0.00	0.00	0.38	0.00	0.00	1.70
	FrtParB	0.80	0.18	4.49	0.24	0.45	1.96	**13.33**	1.39	**14.36**	0.01	0.46	0.84	2.71	2.35
	FrtSmilax	0.00	0.61	2.44	0.00	0.03	4.19	0.20	0.68	3.00	0.00	2.46	**19.49**	0.18	**7.06**
Patch / Habitat Features	CanopyC	1.00	0.05	1.60	0.42	2.99	1.37	0.05	0.61	3.03	0.06	2.77	1.80	0.00	0.16
	LitterDep	**10.11**	0.96	1.05	3.24	0.45	2.30	1.49	0.33	0.33	0.98	1.37	2.13	1.01	1.22
	CtGrLeaf	0.72	0.26	0.05	0.25	2.95	0.09	0.02	0.04	0.00	0.03	0.06	0.06	0.00	0.89
	CtGrVeg	2.04	0.51	3.74	0.26	0.58	0.34	0.23	0.08	0.87	1.38	0.28	2.06	**9.29**	3.10
	CtVine	0.26	0.71	0.30	0.68	0.00	0.64	0.49	0.01	0.11	0.13	0.05	0.00	0.03	0.83
	CtGrShrub	2.33	0.55	4.30	1.97	**5.45**	1.64	4.43	0.11	**11.34**	**9.52**	0.44	1.47	**18.89**	0.83
	ShrubStemCt	**5.19**	1.41	1.15	0.76	**7.07**	3.75	0.20	**10.59**	2.98	0.99	0.72	0.37	0.69	0.32
	basalarea	2.75	0.65	0.99	2.67	0.38	0.67	0.01	0.86	0.06	1.64	0.70	**18.27**	1.49	1.49
	NDVI	**15.20**	3.61	3.07	**23.85**	**23.26**	2.37	0.16	2.47	0.92	**30.42**	**11.70**	**10.06**	**8.90**	**5.34**

Landscape	impurban1km	2.64	1.18	**5.24**	0.11	1.10	0.21	1.31	0.06	0.02	1.03	3.95	0.35	1.50	0.62
	water1km	0.00	4.89	**5.08**	0.35	0.05	0.03	0.00	2.89	0.00	1.56	0.00	1.70	4.16	2.49
	ag1km	0.25	**25.48**	**7.98**	0.15	2.41	0.56	0.02	1.03	1.32	0.49	0.63	0.32	0.02	2.49
	hrdwood1km	4.92	0.51	1.14	0.49	4.86	1.25	0.03	0.09	0.76	4.07	0.74	0.37	2.11	1.38
	shrub1km	1.53	0.22	0.19	0.17	0.53	0.24	2.63	2.04	0.01	0.40	**27.50**	0.02	0.24	2.33
	wetlnd1km	0.18	0.12	0.84	0.56	0.03	0.07	4.86	1.14	0.01	2.25	0.28	0.54	0.08	1.63
Regional	Latitude	2.60	1.26	4.94	**18.84**	**8.68**	2.71	1.94	0.12	**18.13**	4.82	**6.42**	4.40	1.59	0.77
	distatl	0.34	1.73	2.15	2.94	0.28	2.66	**10.75**	**7.93**	1.76	2.52	2.71	2.68	4.48	2.19
	dist_sky_5	**5.81**	0.83	0.88	0.31	0.32	3.04	2.40	0.96	0.14	1.82	3.00	0.03	1.97	2.82
Temporal	Year	0.44	1.59	1.18	3.29	1.52	0.08	0.01	0.62	0.83	3.21	0.04	0.10	1.88	0.45
	Period	**22.25**	**10.85**	**15.67**	**24.73**	**21.67**	**52.11**	**34.26**	**45.93**	**20.37**	**9.71**	**17.66**	**13.59**	**6.78**	**23.99**

Note: All numbers in **bold** represent variables whose contributions accounted for at least 5% of the respective model's total, and were considered the most influential predictor variables for determining migrant density.

Table 10. Summary table for the relative contributions (%) of each predictor variable included in boosted regression tree models developed to identify which factors were most influential in determining migrant density for several species groups (defined in text).

	Predictor	Response Variable (%)				
		AllMigPerHa	FrugMigPerHa	BreedMigPerHa	TransMigPerHa	WinterMigPerHa
Patch / Food Resources	InvPerGrBr	2.55	4.64	**7.91**	3.53	1.85
	InvVism2	1.32	**5.03**	3.04	1.29	0.43
	InvVisAR	2.04	0.51	1.22	1.81	0.89
	InvBrLep	0.35	0.02	0.48	4.63	0.00
	InvVisLep	0.00	0.00	0.23	0.00	0.00
	InvBrDI	0.88	0.12	0.59	0.35	0.16
	InvVisDI	0.98	0.90	0.32	1.30	0.01
	InvBrOR	0.15	0.00	2.94	0.11	0.00
	InvVisOR	0.00	0.00	1.65	0.17	0.00
	FrtAllm2	**5.50**	**7.36**	0.91	**9.72**	0.41
	FrtBGum	**8.23**	3.13	**5.89**	3.36	0.02
	FrtHolly	**5.95**	2.32	0.25	3.31	4.25
	FrtBlueB	0.07	0.00	0.25	0.00	0.00
	FrtDogw	0.01	0.00	0.09	0.00	0.00
	FrtGrape	0.93	2.76	0.87	1.86	0.94
	FrtParB	**11.08**	**5.80**	0.05	0.98	4.02
	FrtSmilax	3.64	2.26	0.24	0.67	1.16
Patch / Habitat Features	CanopyC	1.44	1.20	0.38	0.39	0.75
	LitterDep	0.76	2.82	2.75	0.28	0.10
	CtGrLeaf	0.06	0.01	0.18	0.16	0.00
	CtGrVeg	2.23	0.75	1.42	0.70	0.09
	CtVine	0.09	0.06	0.16	0.16	0.04
	CtGrShrub	**5.20**	3.00	**6.26**	**5.23**	2.68
	ShrubStemCt	1.63	1.71	1.08	0.39	2.71
	basalarea	0.62	0.84	1.26	0.59	0.05
	NDVI	2.74	2.80	**18.52**	2.30	1.36

Landscape	impurban1km	0.86	0.37	2.78	3.30	0.22
	water1km	**6.47**	4.13	2.24	**7.96**	1.02
	ag1km	2.99	1.01	0.63	**16.60**	1.63
	hrdwood1km	1.80	0.96	2.89	1.29	0.65
	shrub1km	1.14	0.54	1.32	0.49	0.01
	wetlnd1km	0.54	1.82	0.95	0.81	0.12
Regional	Latitude	**5.32**	1.11	2.27	1.17	2.50
	distatl	**6.83**	**7.23**	2.75	2.96	**5.16**
	dist_sky_5	0.86	1.44	0.94	2.41	0.13
Temporal	Year	0.90	0.30	1.19	0.26	0.19
	Period	**13.66**	**32.88**	**22.91**	**19.30**	**66.29**

Note: All numbers in **bold** represent variables whose contributions accounted for at least 5% of the respective model's total, and were considered the most influential predictor variables for determining migrant density.

Table 11. Ranked interaction sizes for the ten most influential predictor variable interactions for the BRT analysis of winter migrant density.

Rank	Variable 1	Variable 2	Interaction Size
1	distatl	Period	12.37
2	ShrubStemCt	Period	12.07
3	FrtParB	Period	10.08
4	InvPerGrBr	Period	5.86
5	ag1km	Period	3.71
6	Latitude	Period	2.65
7	CtGrShrub	Period	2.22
8	FrtGrape	Period	1.68
9	InvVisAR	Period	1.02
10	Latitude	FrtHolly	0.94

Note: Interactions presented that include the variable "Period" likely reflect changes in the relationships with predictors when winter landbird migrants were generally absent.

Table 12. Ranked interaction sizes for the ten most influential predictor variable interactions for the BRT analysis of transient migrant density.

Rank	Variable 1	Variable 2	Interaction Size
1	ag1km	Period	1.37
2	FrtAllm2	Period	0.41
3	FrtAllm2	InvPerGrBr	0.35
4	FrtBGum	FrtAllm2	0.23
5	ag1km	InvBrLep	0.20
6	ag1km	FrtAllm2	0.19
7	water1km	FrtBGum	0.15
8	ag1km	FrtHolly	0.15
9	impurban1km	Period	0.15
10	ag1km	InvVisDI	0.14

Note: Interactions presented that include the variable "Period" likely reflect changes in the relationships with predictors when transient landbird migrants were generally absent.

Table 13. Ranked interaction sizes for the ten most influential predictor variable interactions for the BRT analysis of breeding migrant density.

Rank	Variable 1	Variable 2	Interaction Size
1	hrdwood1km	InvPerGrBr	12.05
2	FrtBGum	Period	9.93
3	LitterDep	NDVI	8.58
4	InvVism2	Period	8.32
5	CtGrShrub	Period	6.99
6	InvPerGrBr	NDVI	5.44
7	NDVI	Year	5.15
8	distatl	FrtBGum	3.58
9	InvVisAR	NDVI	3.09
10	CtGrShrub	FrtBGum	2.73

Note: Interactions presented that include the variable "Period" likely reflect changes in the relationships with predictors when breeding landbird migrants were generally absent.

Table 14. Ranked interaction sizes for the ten most influential predictor variable interactions for the BRT analysis of frugivorous migrant density.

Rank	Variable 1	Variable 2	Interaction Size
1	distatl	Period	4.09
2	FrtGrape	Period	2.76
3	InvVism2	Period	1.98
4	FrtParB	Period	1.42
5	wetlnd1km	Period	0.59
6	FrtParB	NDVI	0.56
7	FrtBGum	InvVisDI	0.47
8	water1km	FrtBGum	0.44
9	InvPerGrBr	Period	0.39
10	dist_sky_5	Period	0.36

Note: Interactions presented that include the variable "Period" likely reflect changes in the relationships with predictors when frugivorous landbird migrants were generally absent.

Table 15. Ranked interaction sizes for the ten most influential predictor variable interactions for the BRT analysis of all nocturnal migrant density.

Rank	Variable 1	Variable 2	Interaction Size
1	water1km	FrtBGum	16.31
2	ag1km	distatl	15.91
3	FrtParB	Period	9.27
4	distatl	Period	7.79
5	water1km	Latitude	7.53
6	hrdwood1km	CtGrShrub	3.06
7	InvVism2	Period	3.02
8	FrtGrape	Period	2.42
9	FrtHolly	InvBrDI	2.23
10	distatl	Latitude	2.17

Note: Interactions presented that include the variable “Period” likely reflect changes in the relationships with predictors when nocturnal landbird migrants were generally absent.

Table 16. Values of predictor variables to determine stopover functional type classification of 45 transects sites in the mid-Atlantic and Gulf Coast regions. All sites with 4-letter acronyms are from mid-Atlantic region.

Transect	Relative stopover duration	Proportion hardwood forest within sample volumes	Proportion hardwood forest within 5km	Distance to coast (km)	Insect density (#/g veg)	Residual stopover duration	Functional type
BFLP	0.65	0.77	0.29	4.1	0.051	-0.92	1) Coastal fire escape
BHNW	0.91	1.00	0.05	5.8	0.077	-0.16	1) Coastal fire escape
BLWA	1.21	0.88	0.35	20.8	0.066	-0.23	2) Inland fire escape
CBSN	2.69	0.83	0.36	52.8	0.190	0.53	3) Store
CHSP	1.08	0.65	0.21	2.1	0.063	-0.46	1) Coastal fire escape
CPSP	0.84	0.88	0.38	26.3	0.236	-0.60	2) Inland fire escape
CSNA	1.75	0.94	0.30	60.0	0.364	0.19	3) Store
FBNP	0.93	0.90	0.35	14.7	0.024	-0.48	2) Inland fire escape
GDNW	0.75	0.99	0.61	21.7	0.475	-0.51	2) Inland fire escape
GDSE	0.78	0.88	0.65	24.2	0.173	-0.67	2) Inland fire escape
GDSW	0.97	0.95	0.61	36.3	0.234	-0.37	2) Inland fire escape
HCWP	1.55	0.41	0.11	0.7	0.307	-0.18	1) Coastal fire escape
IDYL	1.96	0.99	0.41	39.7	0.095	0.45	3) Store
KPSP	1.53	0.96	0.28	17.0	0.046	0.09	2) Inland fire escape
MAHO	2.93	0.79	0.28	30.8	0.151	0.60	3) Store
MASP	3.72	0.59	0.24	24.9	0.129	0.76	3) Store
MCWS	0.95	0.84	0.17	9.6	0.040	-0.50	1) Coastal fire escape
MNWA	0.36	1.00	0.38	3.3	0.043	-1.14	1) Coastal fire escape
MSBT	6.07	0.56	0.38	27.8	0.275	1.23	3) Store
NE3	0.09	0.87	0.53	56.5	2.114	-2.80	4) Hotel
NE4	0.18	0.94	0.76	51.3	2.835	-2.07	4) Hotel
NE5	0.69	0.75	0.69	45.0	2.185	-0.86	4) Hotel
NW1	0.51	0.92	0.39	52.9	1.800	-1.05	4) Hotel
NW2	0.38	0.92	0.31	37.8	1.525	-1.36	2) Inland fire escape
NW3	7.29	0.96	0.33	32.6	2.208	1.67	3) Store
NW4	0.35	1.00	0.73	53.9	3.868	-1.08	4) Hotel
NW5	0.33	0.98	0.79	45.6	2.187	-1.37	4) Hotel
NW6	0.19	1.00	0.76	41.0	1.757	-1.69	4) Hotel
NWWA	2.36	0.95	0.51	22.6	0.027	0.51	2) Inland fire escape
PACP	3.95	0.23	0.01	13.1	0.094	0.69	1) Coastal fire escape
PHWA	0.53	0.97	0.29	3.8	0.038	-0.93	1) Coastal fire escape
RACP	2.04	0.93	0.27	71.4	0.091	0.34	3) Store
SE1	45.88	0.88	0.18	19.1	1.126	3.40	3) Store
SE2	57.70	1.00	0.17	17.8	1.191	4.03	3) Store
SE3	0.96	0.98	0.19	17.2	0.832	-0.30	2) Inland fire escape
SE4	0.12	0.98	0.80	24.1	1.770	-2.38	4) Hotel
SOQU	1.74	0.71	0.37	50.0	0.460	0.04	3) Store
SW1	7.51	0.80	0.31	8.5	1.039	1.54	3) Store
SW2	1.81	0.61	0.37	12.7	1.413	0.04	2) Inland fire escape
SW3	9.04	0.91	0.35	16.2	1.095	1.80	3) Store
SW4	3.40	1.00	0.85	22.8	2.447	1.20	4) Hotel
SW6	2.15	1.00	0.89	20.2	2.244	0.74	4) Hotel
THWO	4.46	0.98	0.28	5.9	0.022	1.20	1) Coastal fire escape
TUSP	1.45	0.88	0.21	21.7	0.043	-0.05	2) Inland fire escape
ZUNI	4.49	0.93	0.32	32.5	0.333	1.12	3) Store

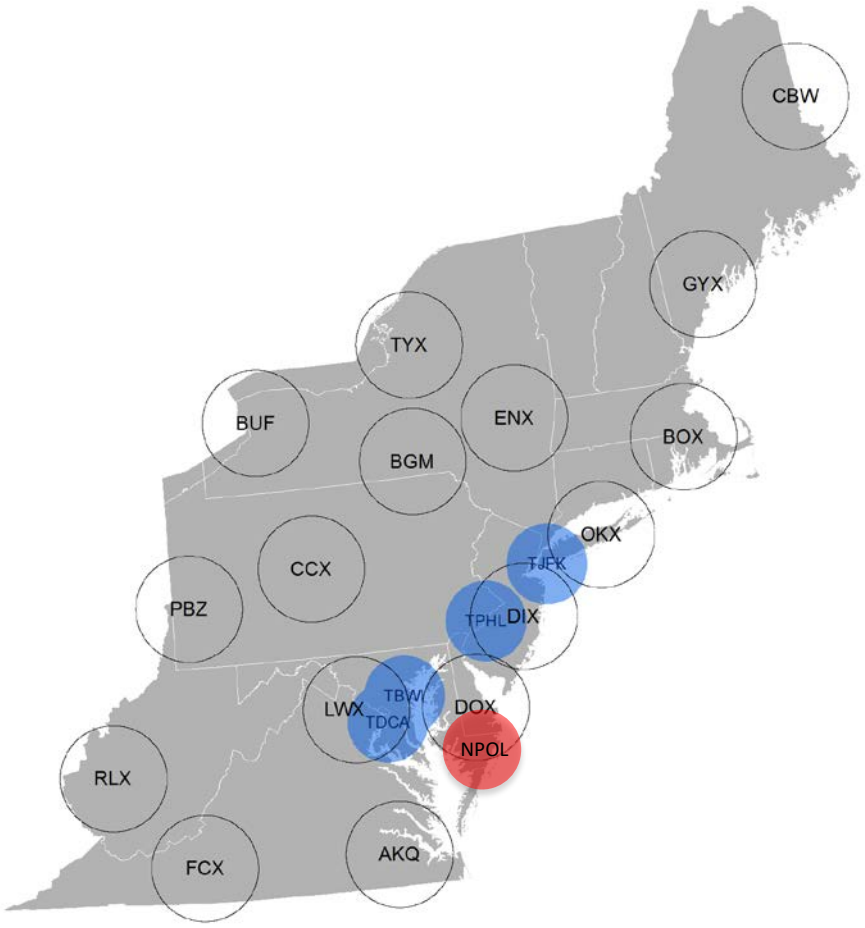

Figure 1. Location, short name, and radar coverage area (80-km radius) of 16 NEXRAD stations used in the study within USFWS Region 5. Coverage area (60-km radius) of NASA's NPOL radar (red) and the four TDWR stations (blue) used in the study are also denoted and labeled by radar name.

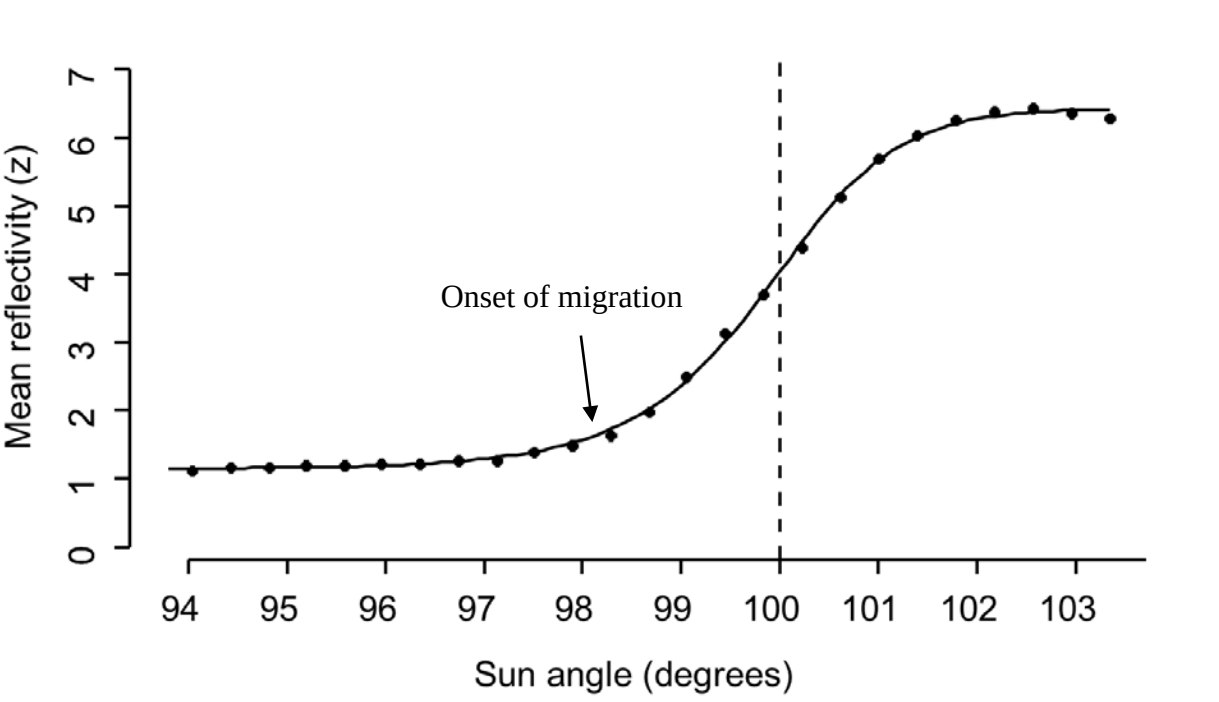

Figure 2. Example scatterplot of the increase in mean total reflectivity through time at the onset of a nocturnal bird-dominated flight. Vertical dashed line at the sun angle (100° [i.e., 10° below the horizon]) indicates where the point of the maximum rate of increase in reflectivity occurs. This would be the sun angle at which radar data were sampled for quantifying bird distributions aloft at this radar on this night.

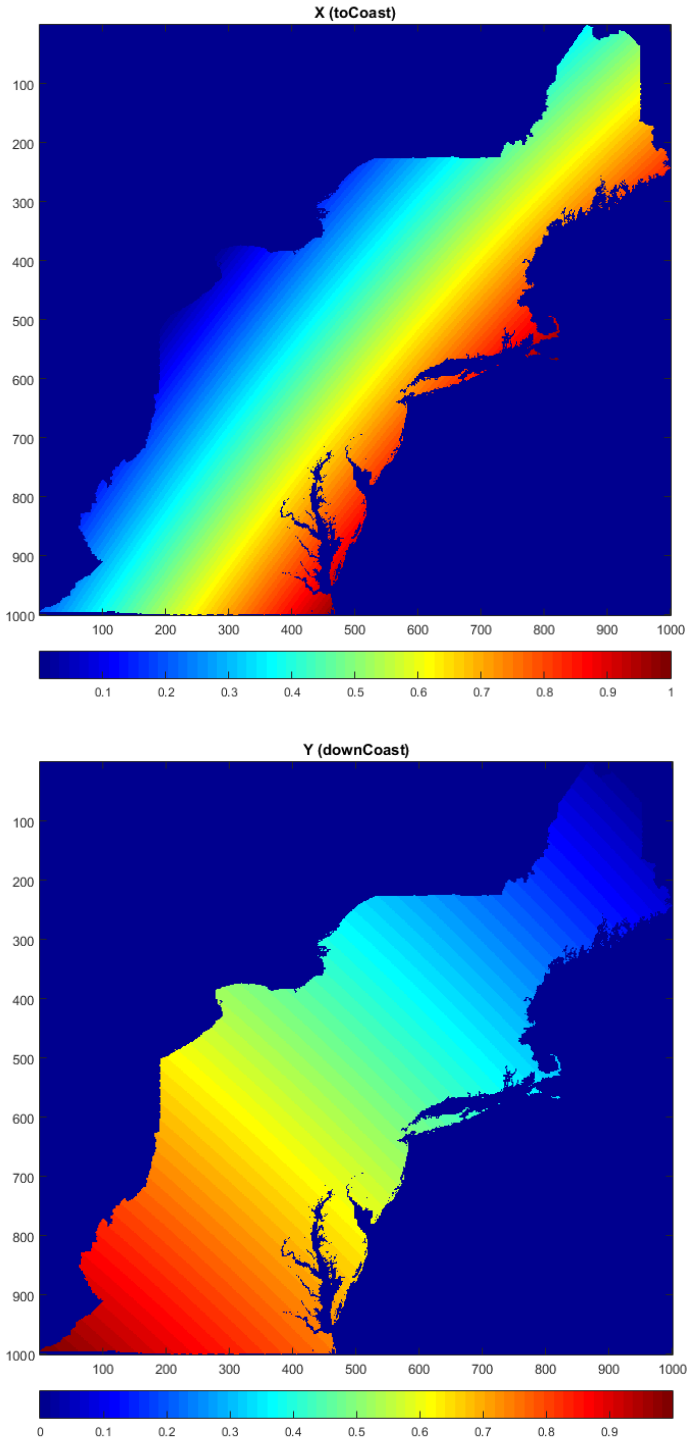

Figure 3. Normalized spatial axes towards (top) and along (bottom) the Atlantic Seaboard, rotated 42° clockwise compared to Easting and Northing variables, respectively.

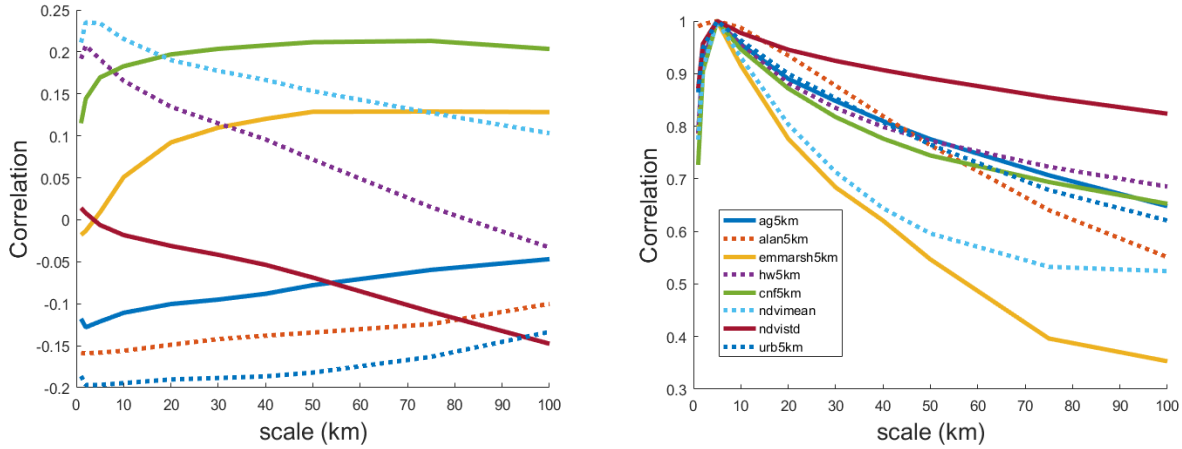

Figure 4. Correlation coefficients (left) between mean VIR and 8 landscape-scale predictors at 1-100-km scales (X axis), and (right) between the same predictor at each scale with that at the nominal 5-km scale.

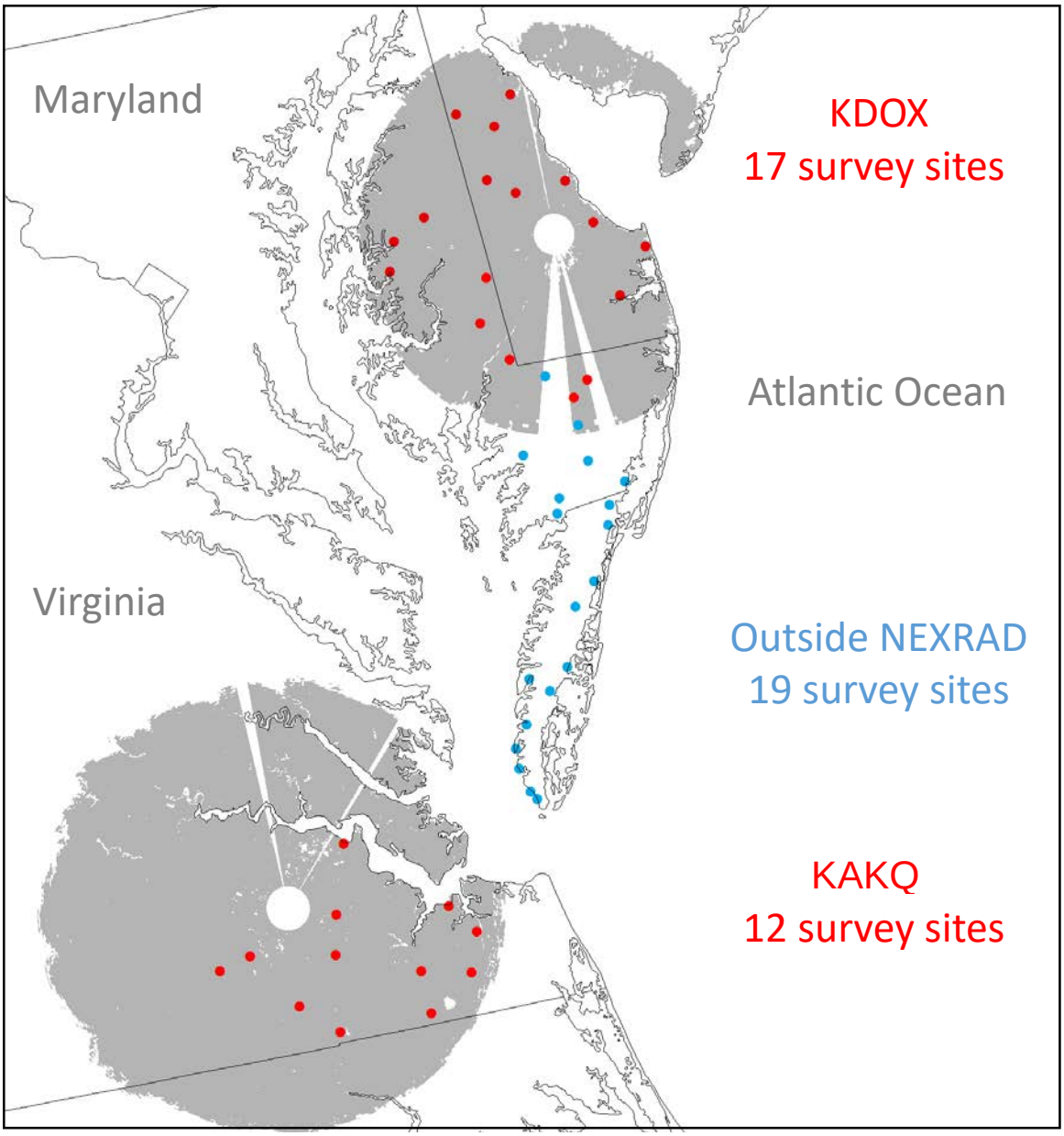

Figure 5. Locations of 48 hardwood forest transect survey sites within (red) and outside (blue) of NEXRAD coverage areas (gray shaded areas) where bird surveys were conducted.

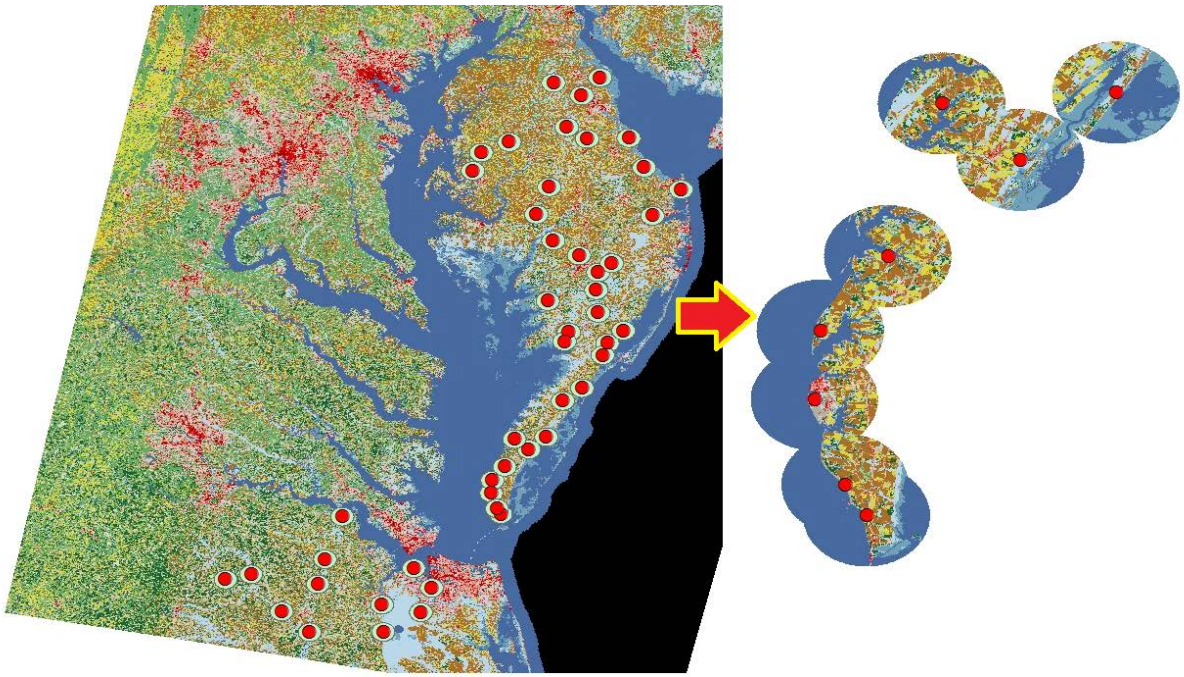

Figure 6. Visualization of steps for land cover data extraction in ArcGIS. The first image (left of the arrow) shows buffers around all 48 sites, while the second (right) shows the 5-km buffers around eight Eastern Shore of Virginia sites after using 'extract by mask' tool.

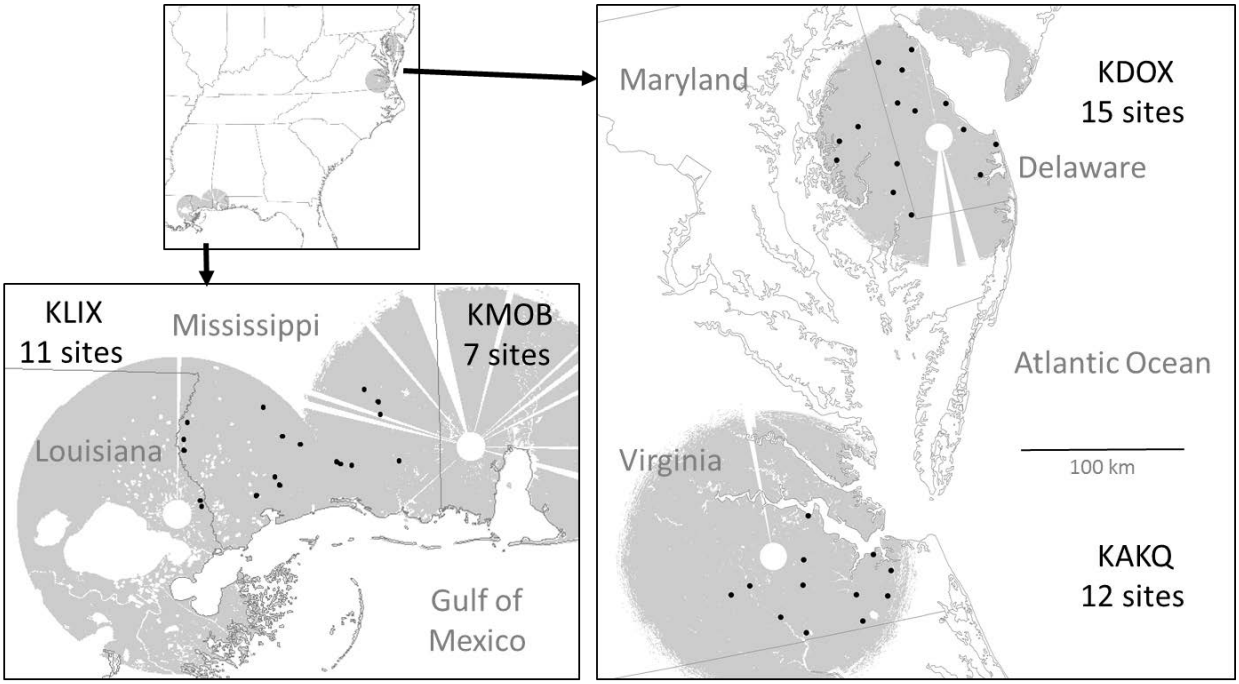

Figure 7. Locations of 45 hardwood forest transect sites where bird surveys were conducted for determination of stopover duration and the coverage areas (shaded in gray) and names of four associated NEXRAD stations.

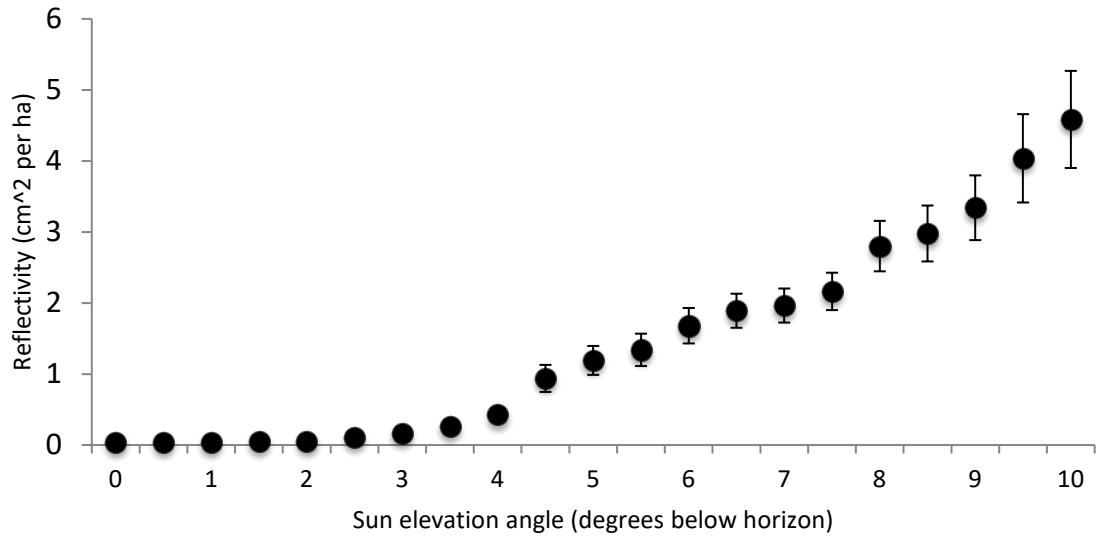

Figure 8. Radar measures of bird density at static sun elevation angles from 0 - 10° below the horizon. The change in mean reflectivity pooled across radars (KAKQ and KDOX) in autumns 2013 and 2014. Error bars denote ±1 standard error of the mean.

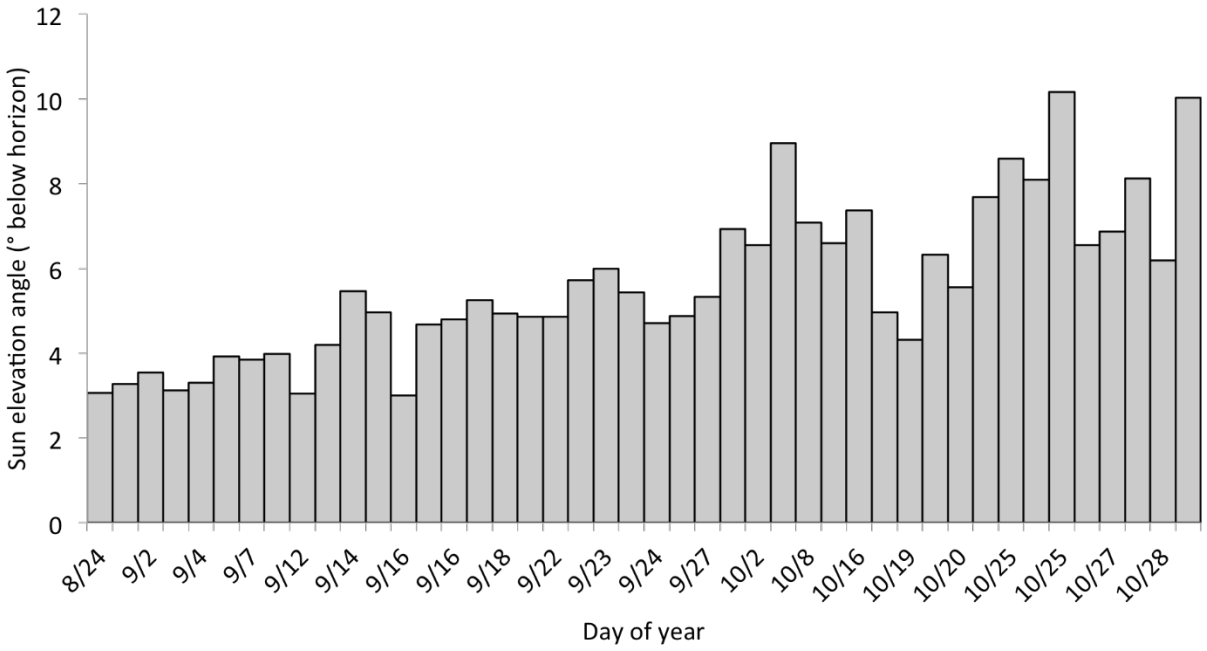

Figure 9. Bars indicate the sun elevation angle at the inflection point of flight exodus for individual sampling nights during autumn 2013 and 2014 at KDOX and KAKQ. Sampling days are sorted by increasing day of year.

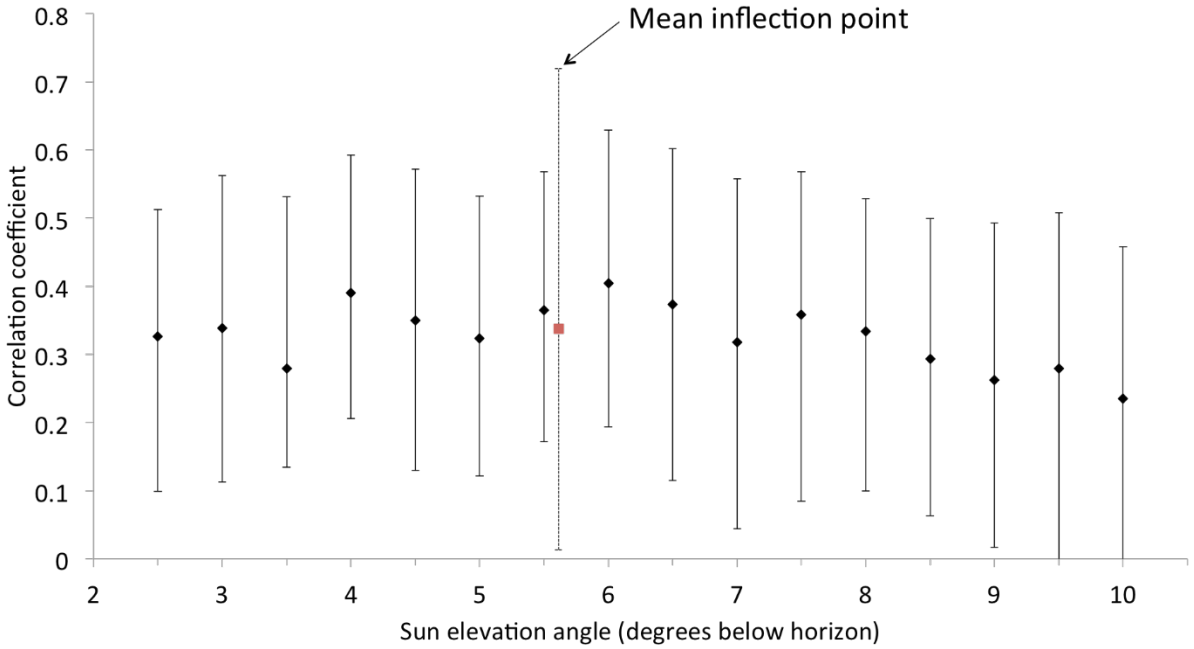

Figure 10. Pearson correlations between seasonal average migrant density at the ground and aloft sampled at a series of fixed sun angles and at the daily inflection point of exodus among days. Error bars are bootstrapped 95% CI.

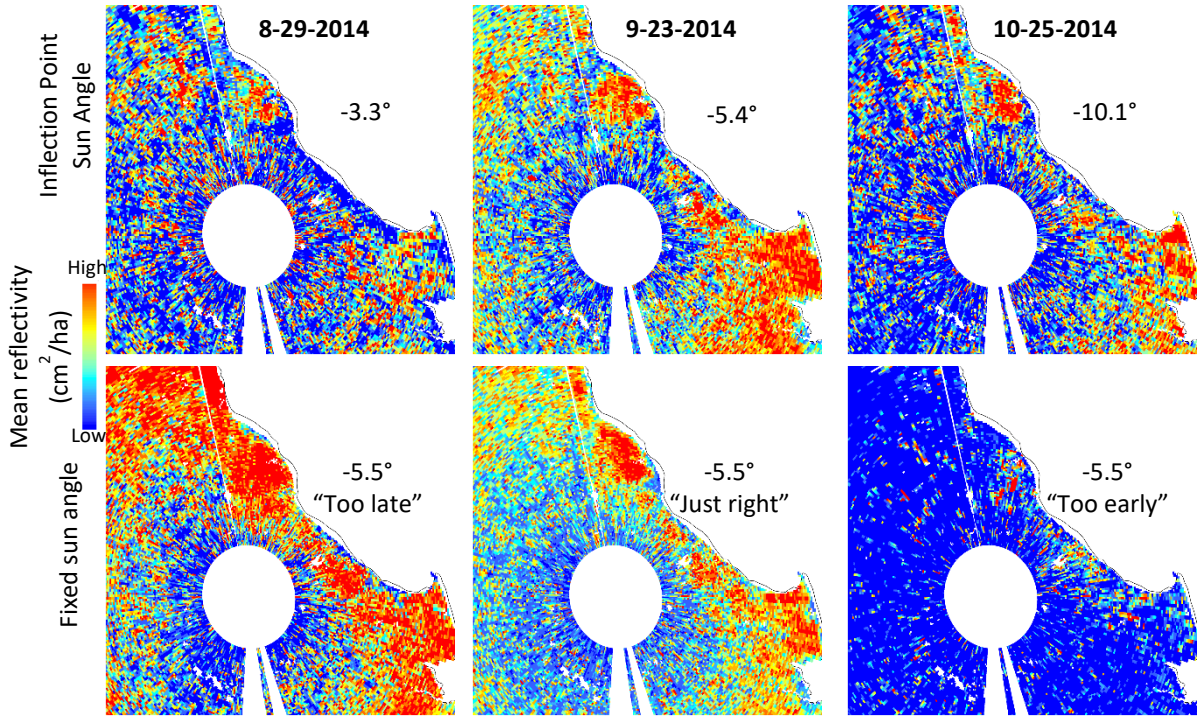

Figure 11. Mapped bird stopover density (mean reflectivity) on three nights sampled at either the daily inflection point of exodus (top) or a fixed sun angle of -5.5° (bottom) at the KDOX NEXRAD radar station.

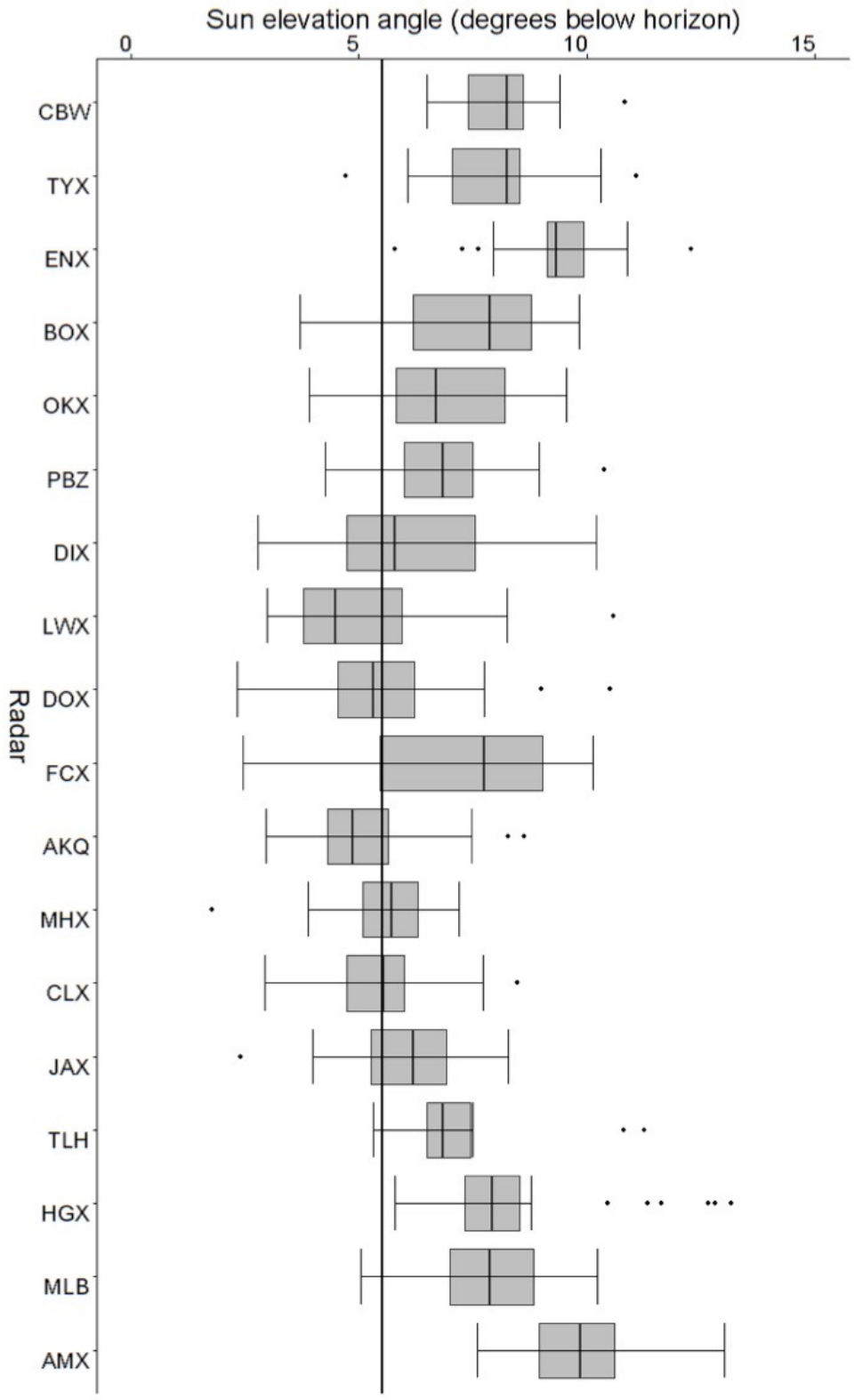

Figure 12. Boxplots of the distribution of the nightly sun angles at the inflection point of flight exodus curves for sampling nights at 18 radar stations in the eastern U.S. Radars decrease in latitude from top to bottom. Vertical line denotes the sampling sun angle of -5.5° of Buler and Dawson (2014).

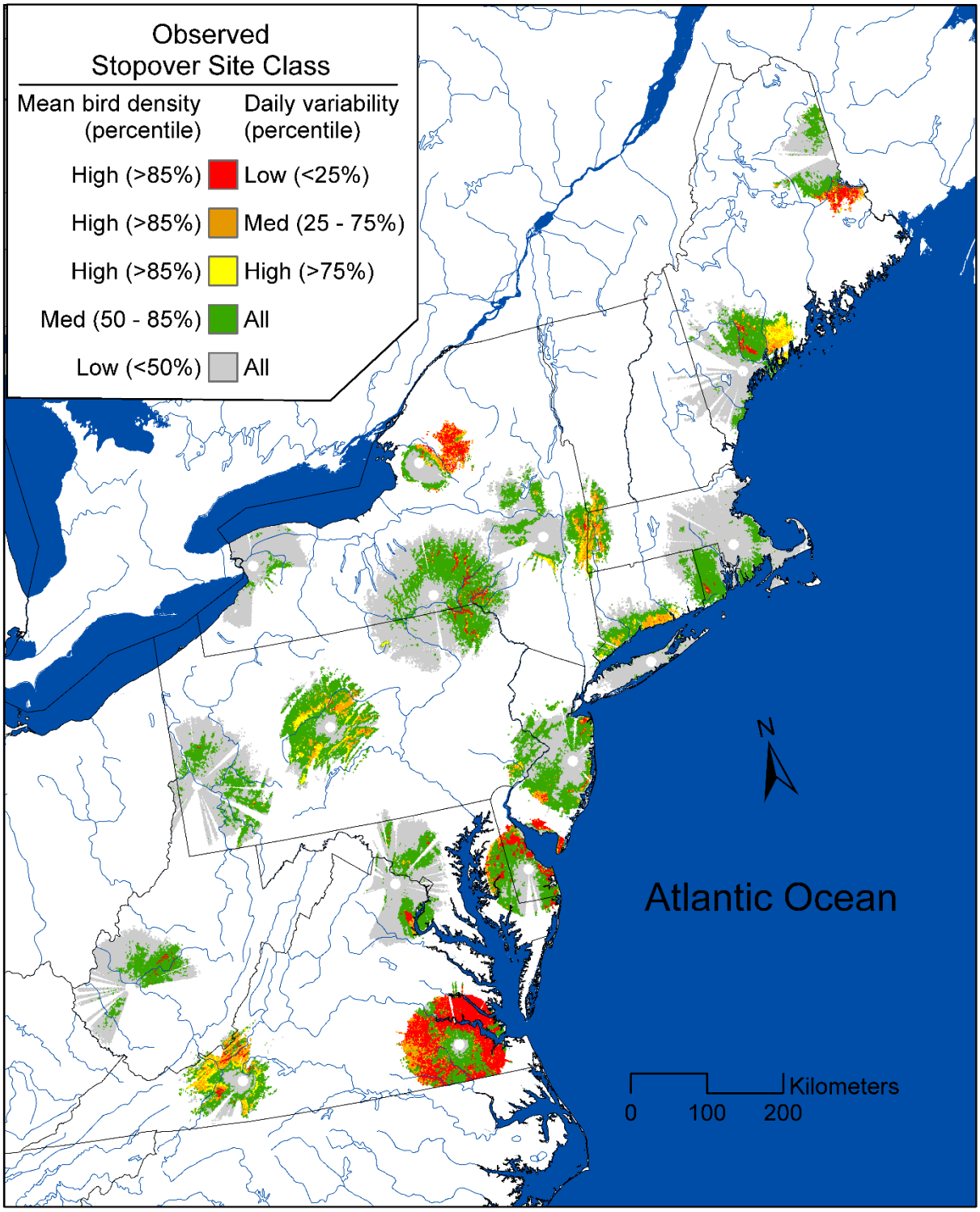

Figure 13. Map of regionally-classified (i.e., data pooled across radars) radar-observed bird stopover use during autumn 2008 - 2014 among 16 NEXRAD coverage areas within USFWS Region 5.

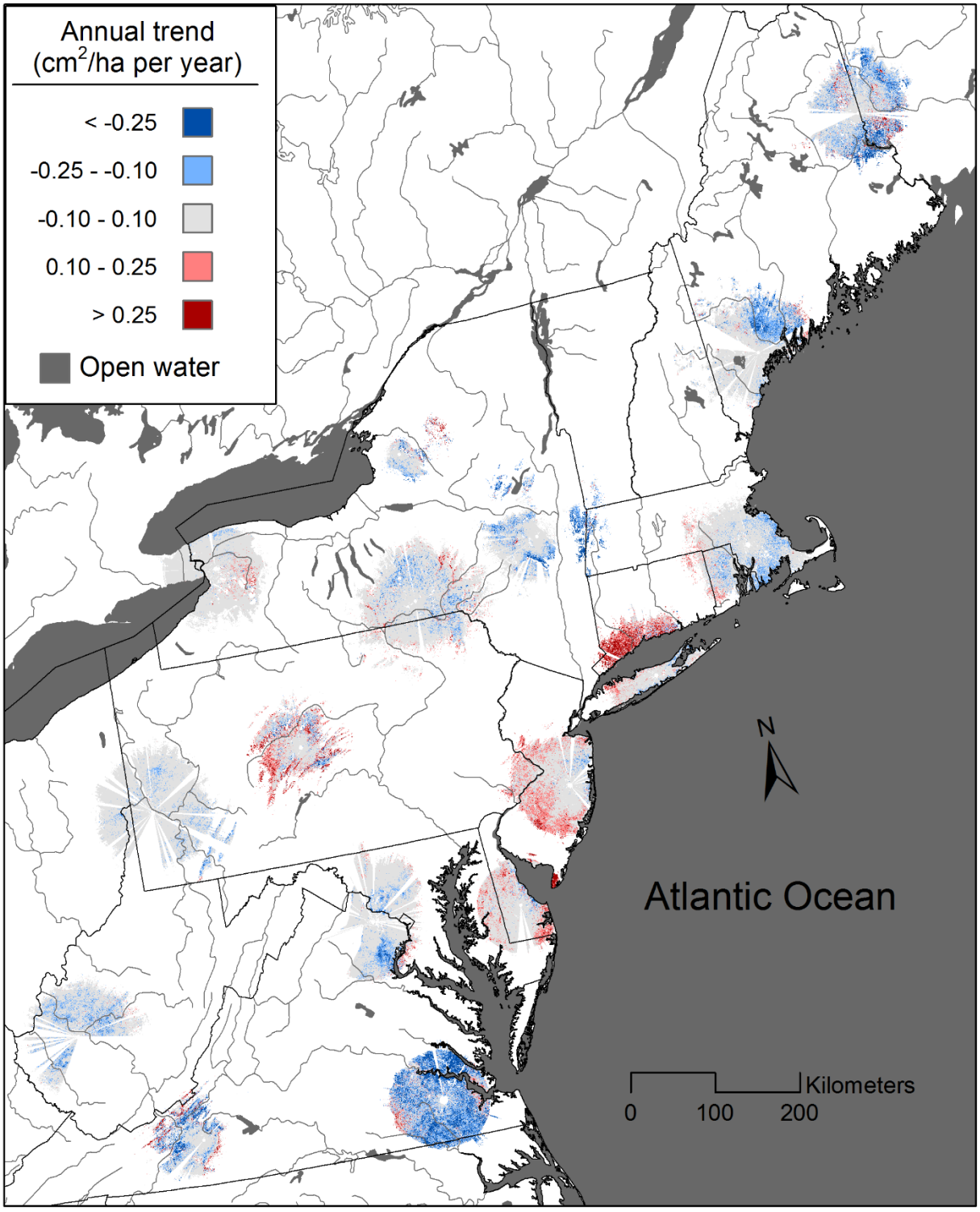

Figure 14. Map of coefficient of annual linear trend in mean autumn radar-observed bird stopover density (cm^2/ha per year) during autumn from 2008 - 2014 for 16 individual NEXRAD coverage areas within USFWS Region 5.

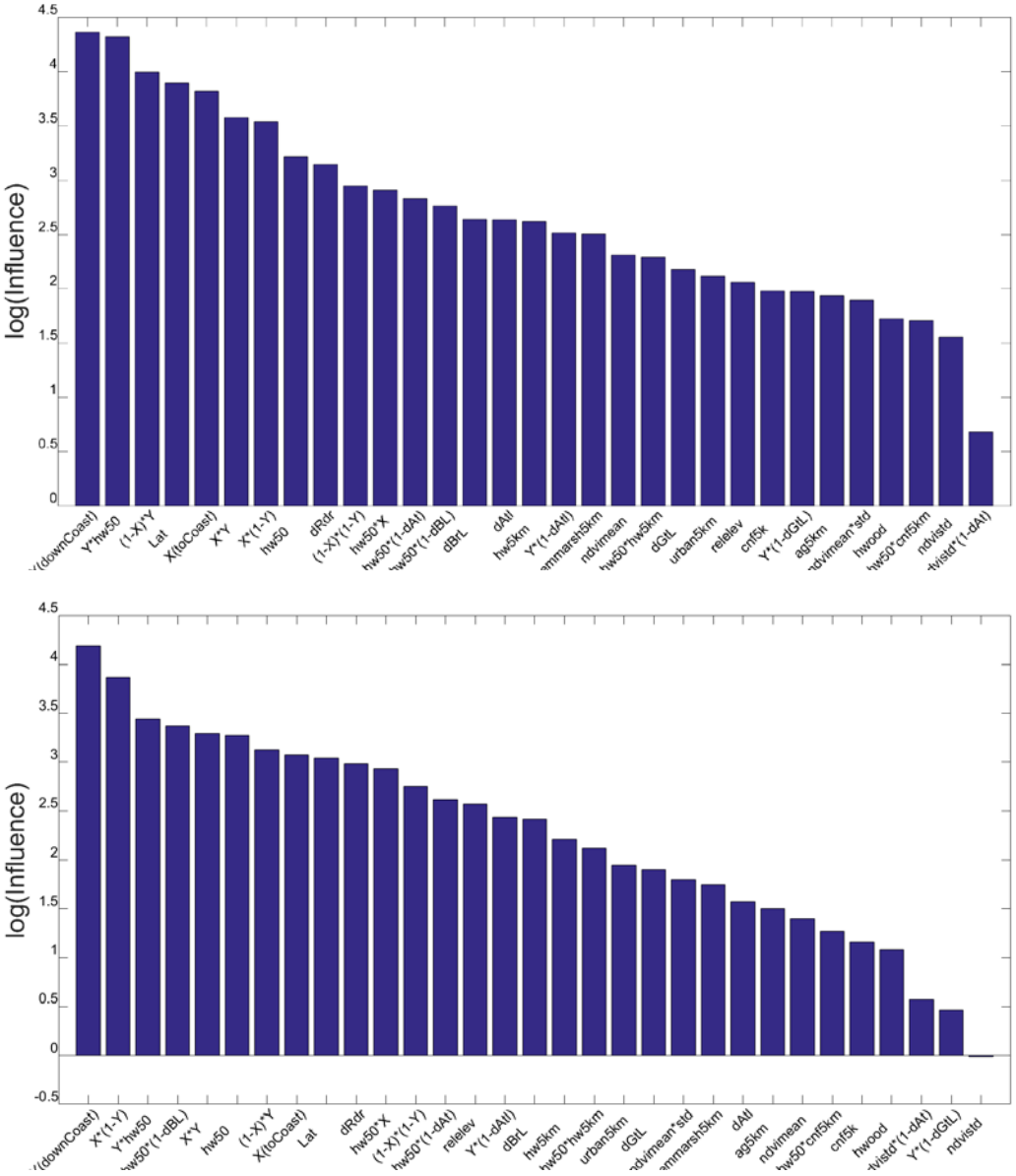

Figure 15. Predicted influence of each predictor on (top) mean fall stopover density and (bottom) daily variability in fall stopover density, based on the BGAM model and log-transformed seasonal mean VIR. See Table 1 for predictor names and descriptions.

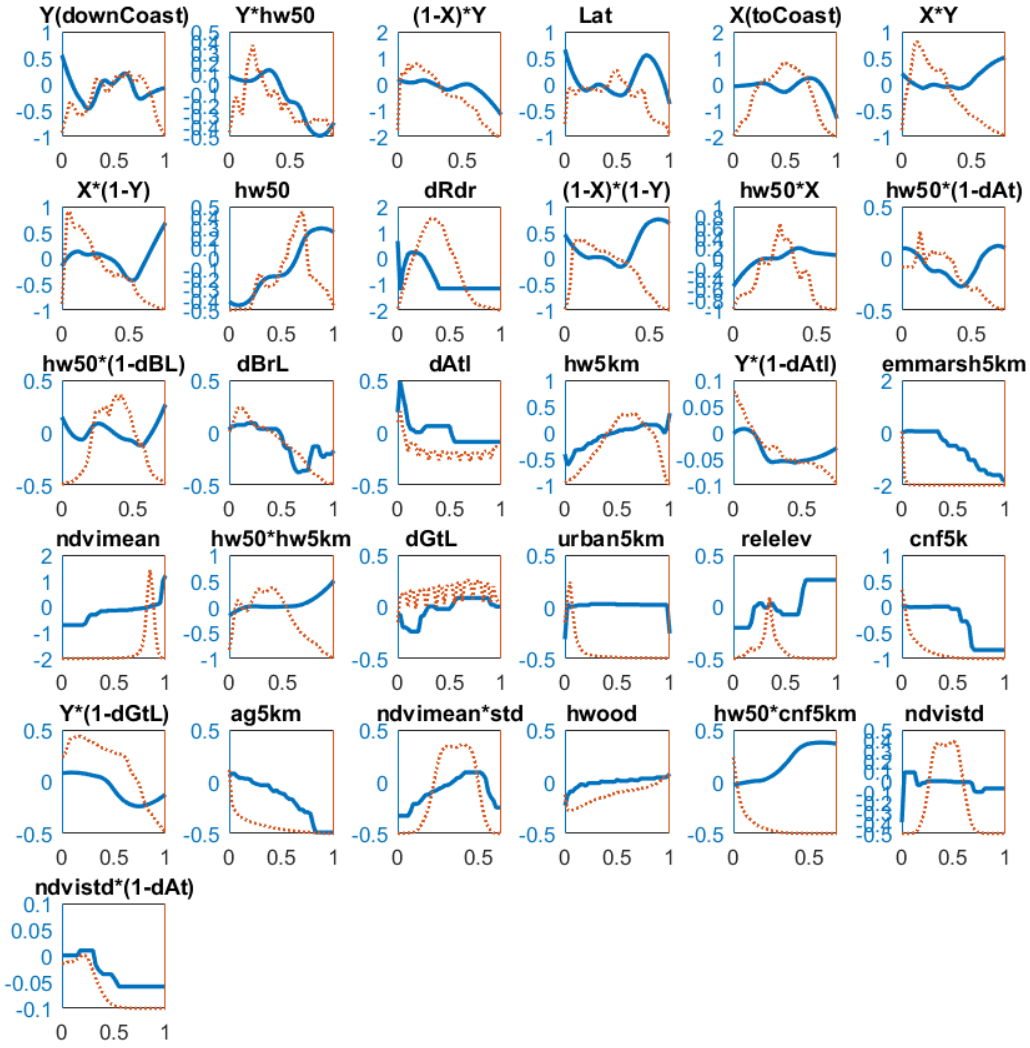

Figure 16. Predicted response to each (normalized) predictor on log-transformed mean VIR, as proxy for stopover density. Rug plots (red lines) indicate coverage of normalized values of each predictor (or interaction term) among the measured data.

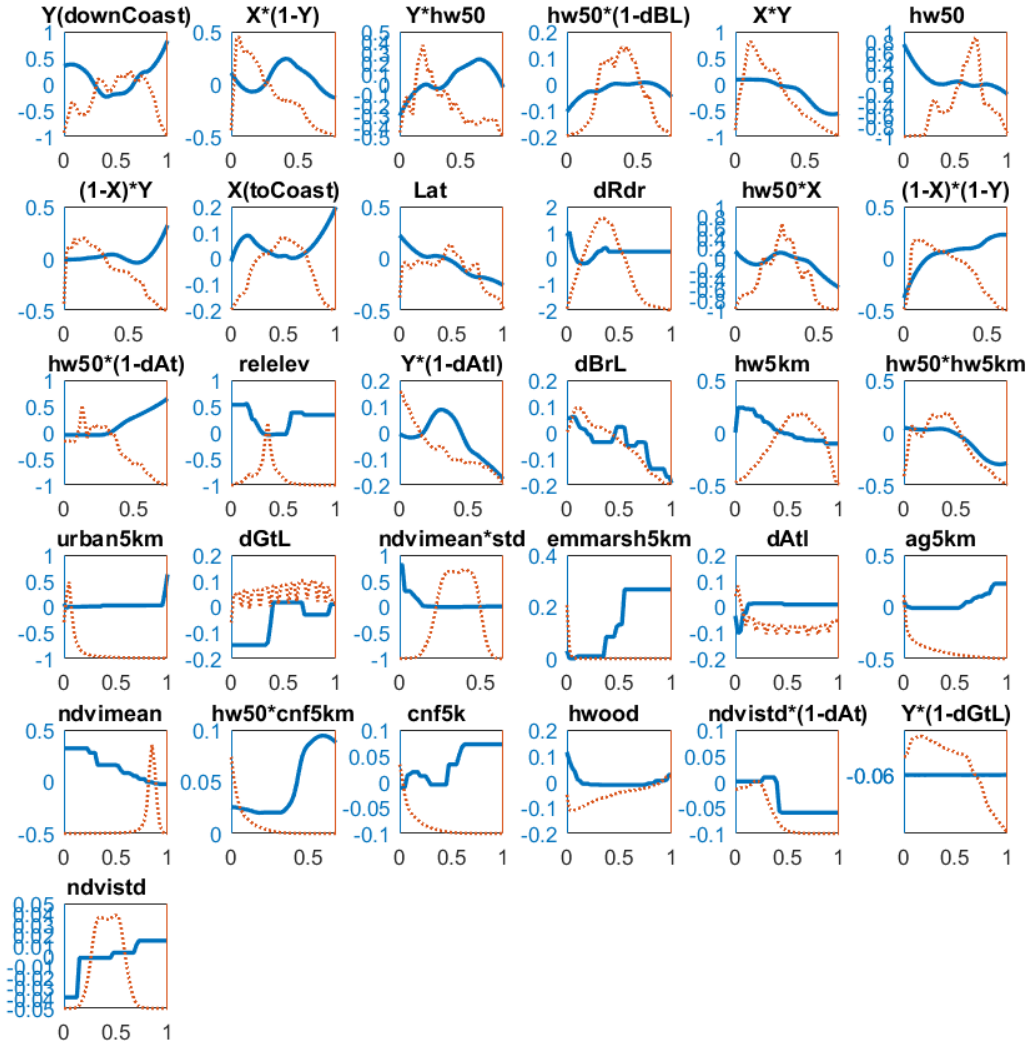

Figure 17. Predicted response to each (normalized) predictor on coefficient of variation in VIR, as proxy for variability in stopover density. Rug plots (red lines) indicate coverage of normalized values of each predictor (or interaction term) among the measured data.

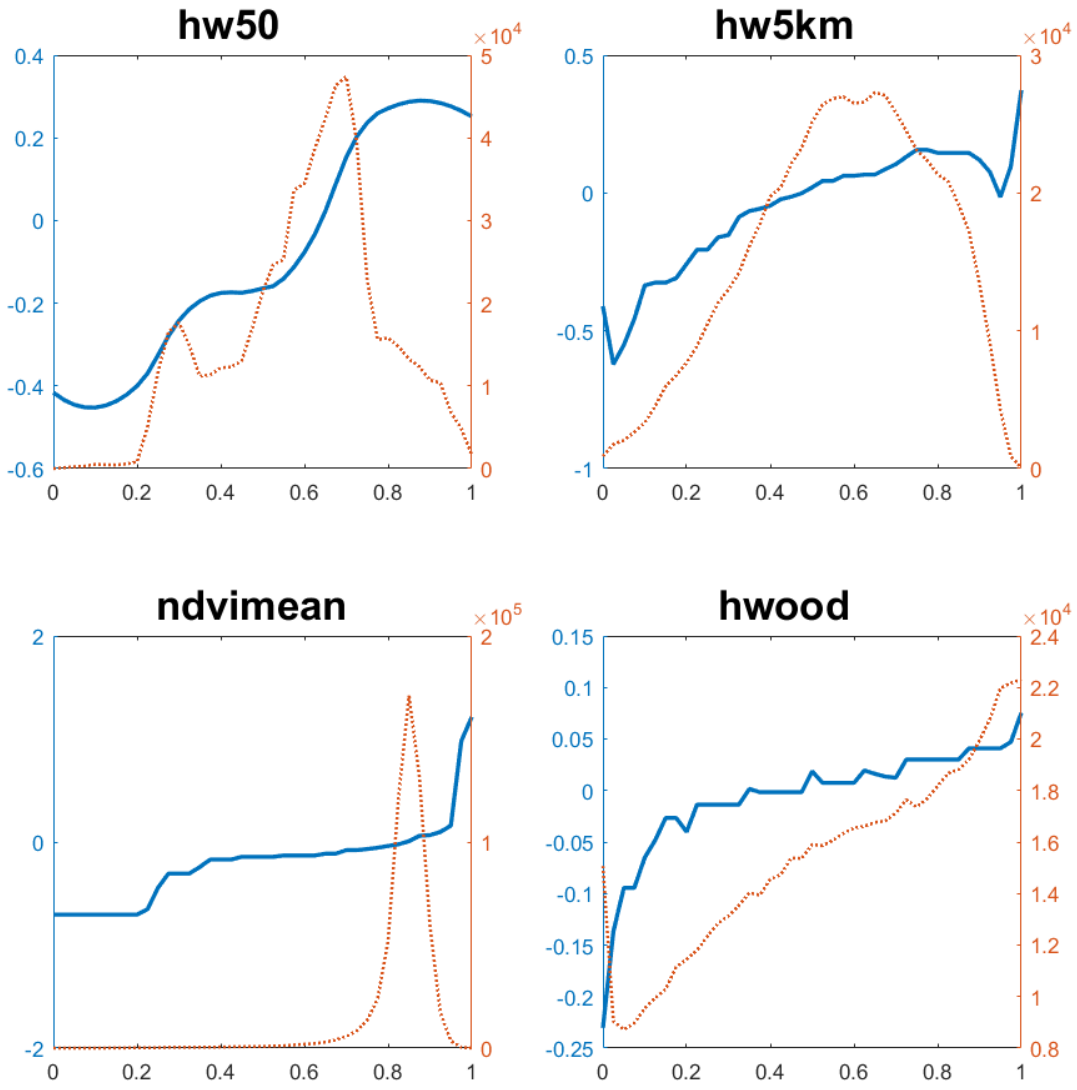

Figure 18. Predicted response (solid blue lines) in mean stopover to, and frequency distribution (dotted red lines) of, fractional hardwood cover at 50-km scales (upper left), 5 km (upper right), to mean NDVI (Normalized Difference Vegetation Index; lower left) and to hardwood at 1 km scales (lower right). The vertical axis represents additive factors in log-transformed stopover density, i.e. multiplicative factors in stopover density. Dotted red lines indicate frequency of normalized values of each predictor (or interaction term) among grid cells.

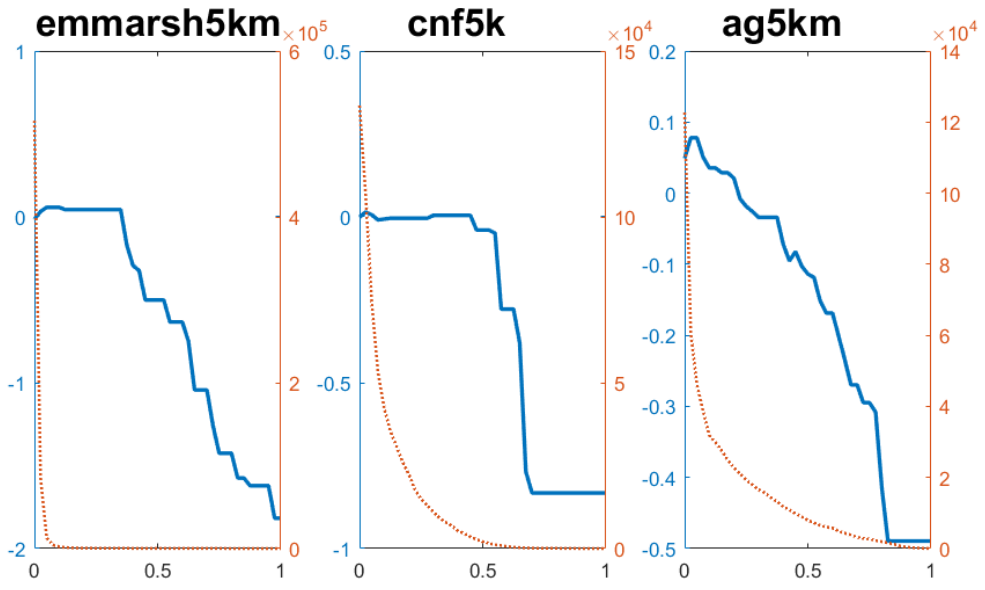

Figure 19. Predicted response (solid blue lines) in mean stopover to, and frequency distribution (dotted red lines) of, fraction of emergent marsh (left), coniferous forest and (middle) and agricultural landcover (right), all at 5-km scales. Panels are presented in descending order of model influence.

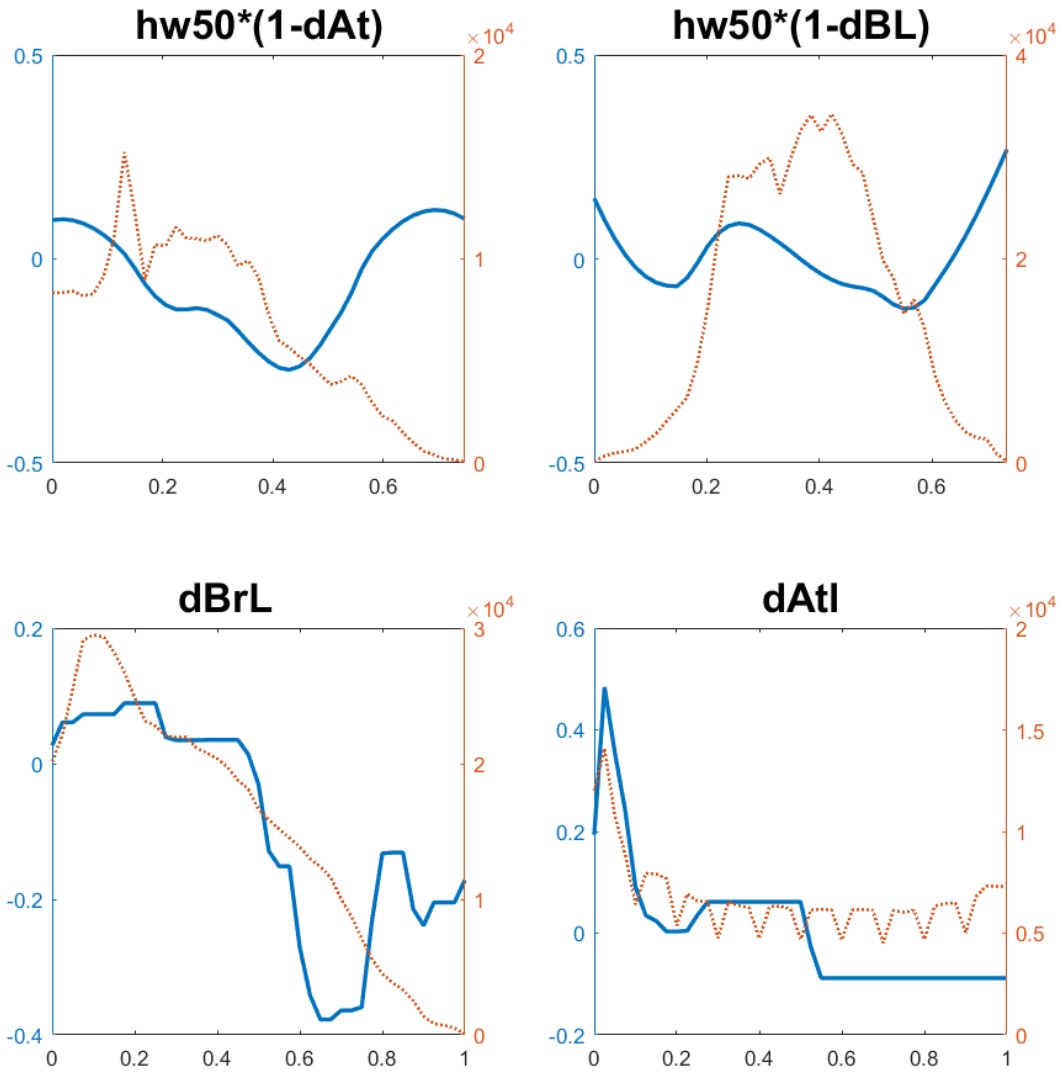

Figure 20. Predicted response (solid blue lines) in mean stopover to, and frequency distribution (dotted red lines) of, distance to the Atlantic coast (within 150 km) and to the brightest (4%) light sources, and their interactions with fractional hardwood cover at 50 km. Panels are presented in order of descending model influence (upper left, upper right, lower left, lower right.

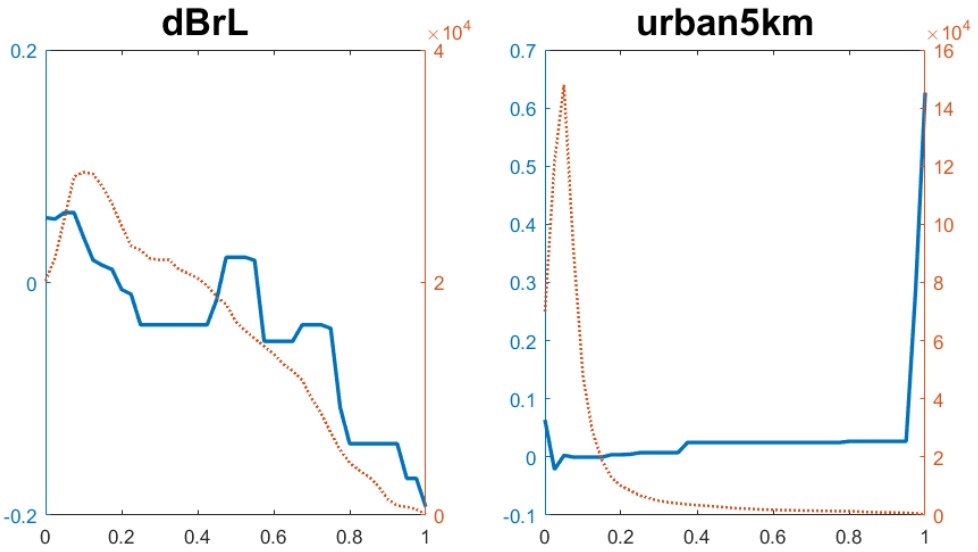

Figure 21. Predicted response (solid blue lines) in mean stopover to, and frequency distribution (dotted red lines) of, distance from bright lights (left) and fractional developed (urban) cover within 5 km (right). Panels are presented in descending order of model influence.

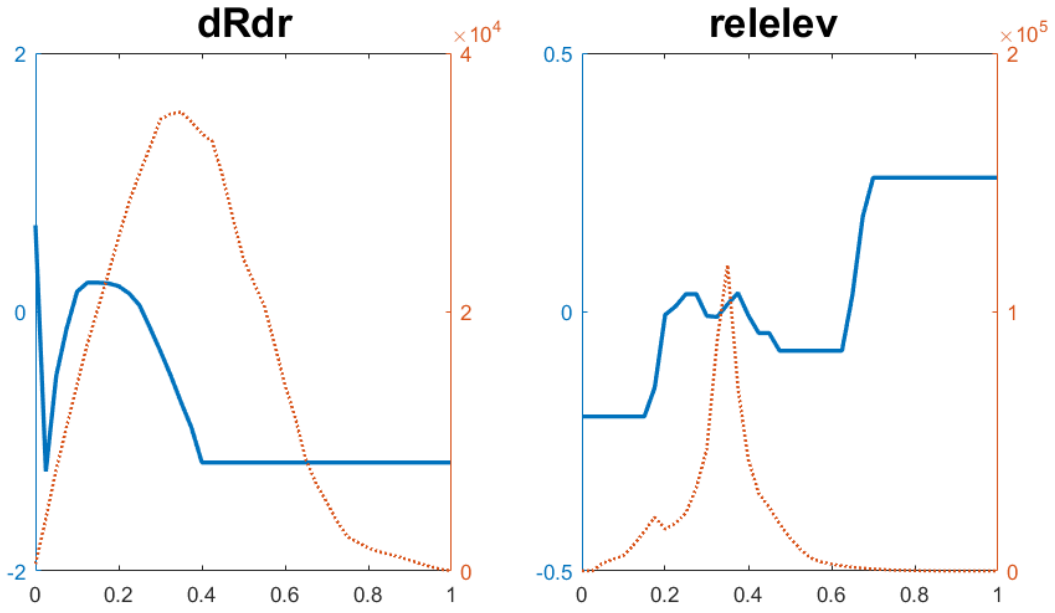

Figure 22. Predicted response (solid blue lines) in mean stopover to, and frequency distribution (dotted red lines) of, distance to the radar (left) and elevation relative to the radar (right). Panels are presented in descending order of model influence.

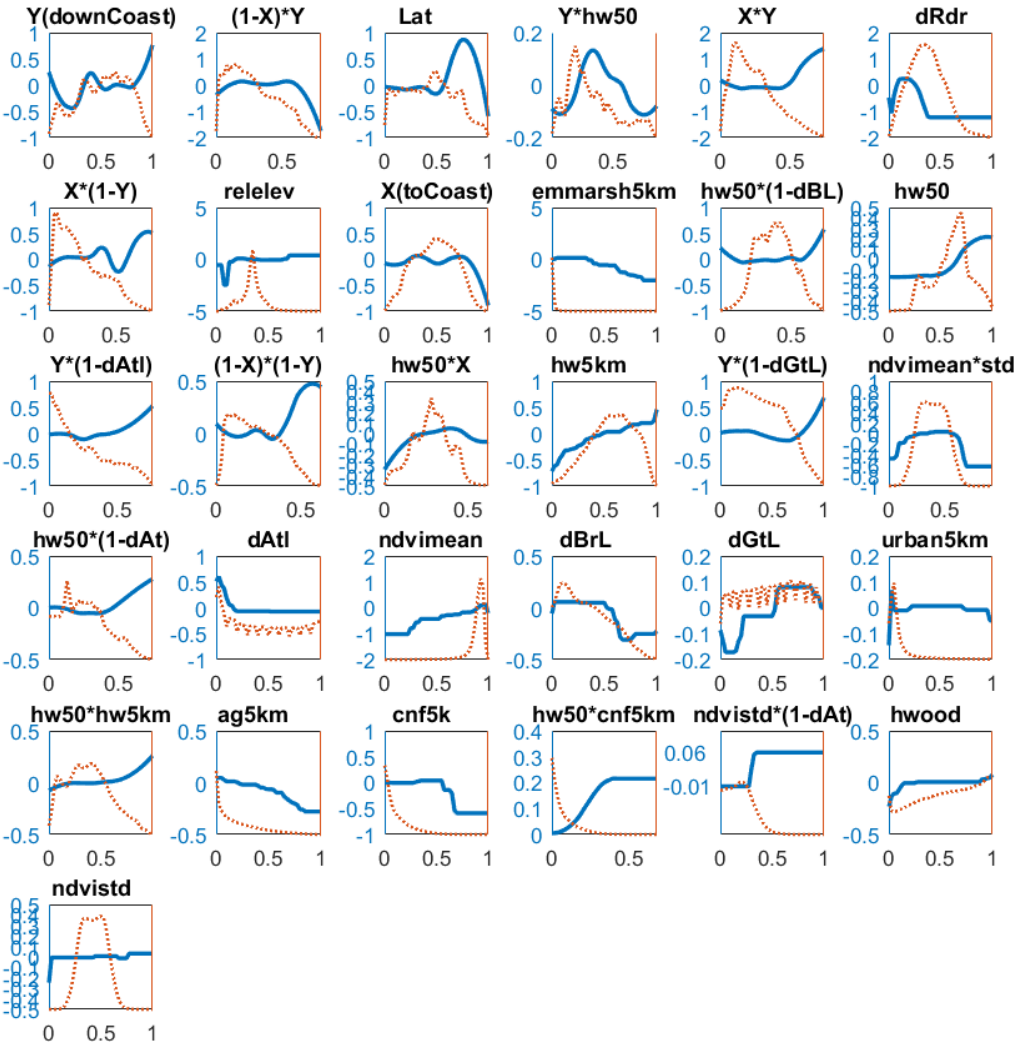

Figure 23. Predicted response to each (normalized) predictor on mean VIR in weeks 1-2, as proxy for stopover density. Rug plots (red lines) indicate coverage of normalized values of each predictor (or interaction term) among the measured data.

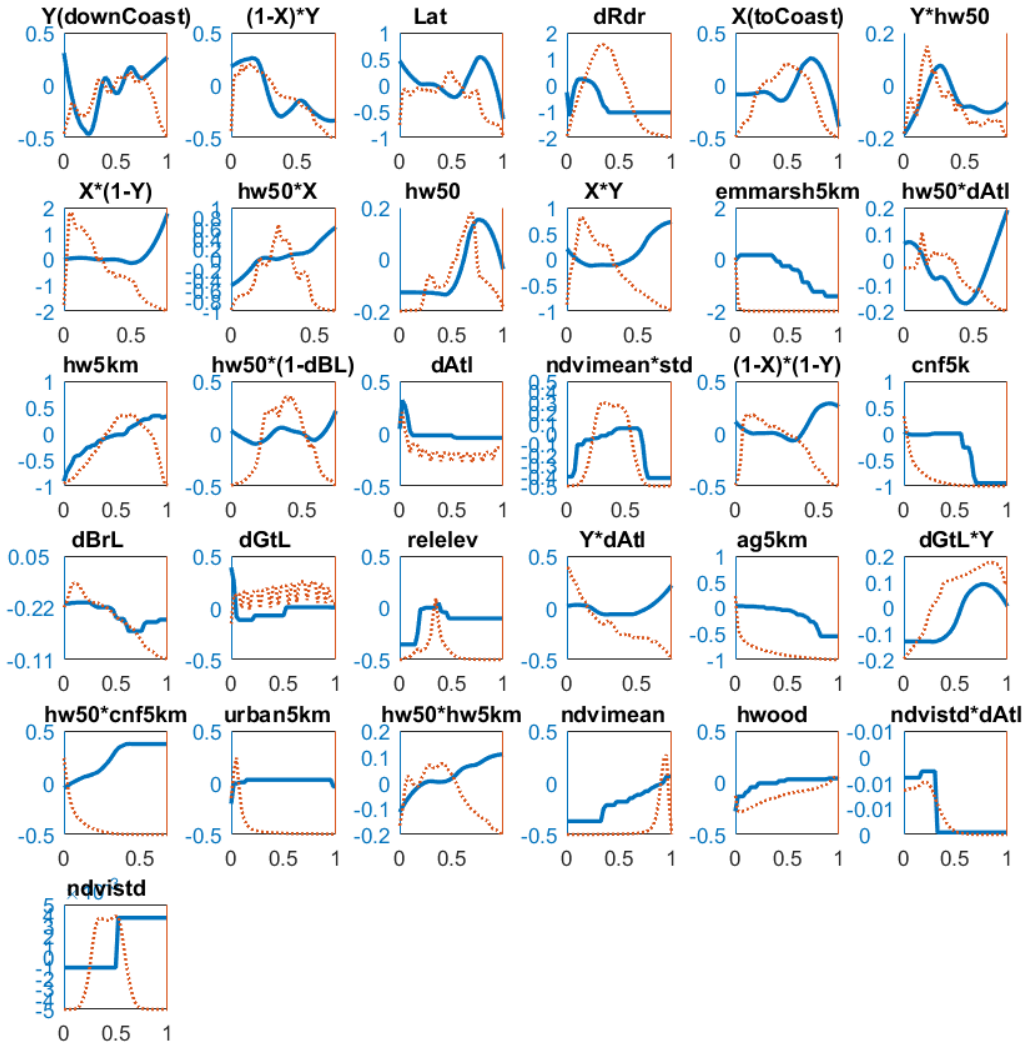

Figure 24. Predicted response to each (normalized) predictor on mean VIR in weeks 3-4, as proxy for stopover density. Rug plots (red lines) indicate coverage of normalized values of each predictor (or interaction term) among the measured data.

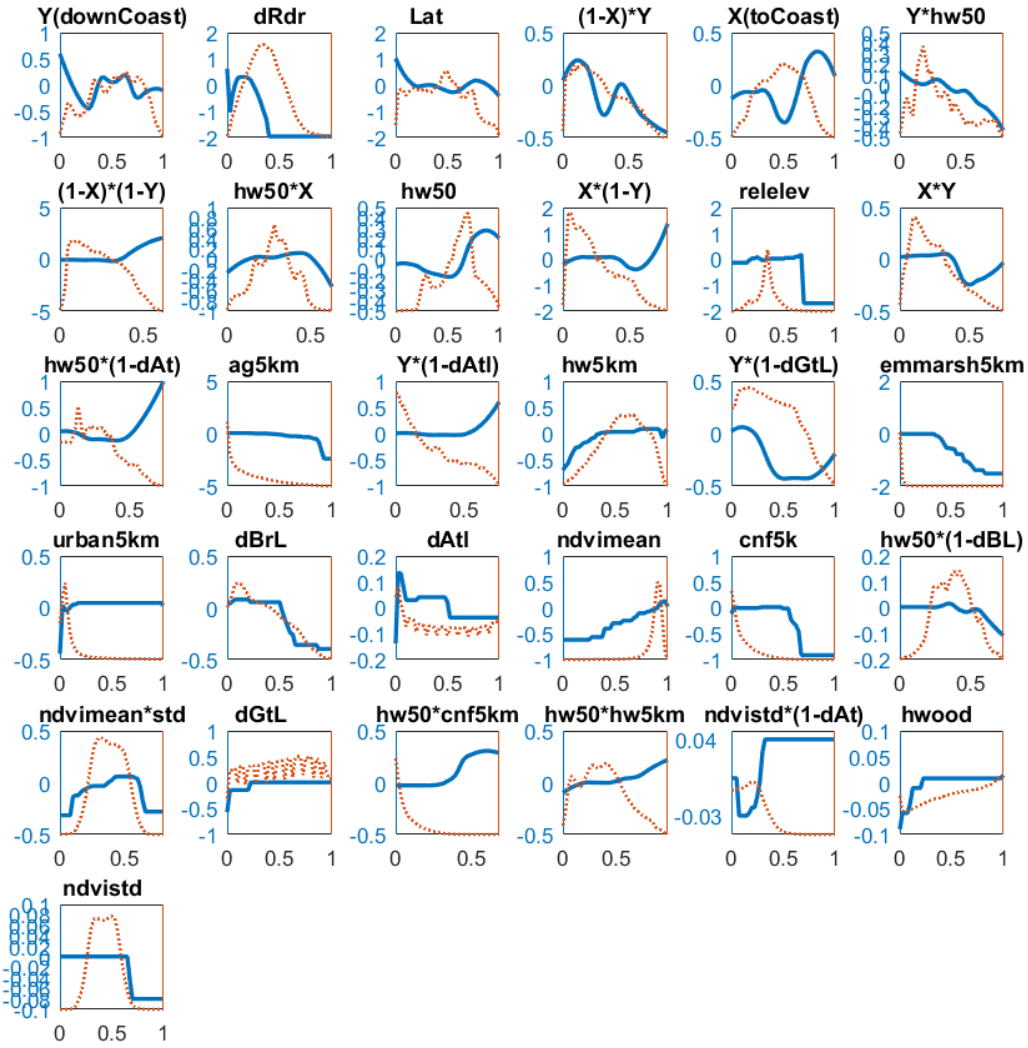

Figure 25. Predicted response to each (normalized) predictor on mean VIR in weeks 5-6, as proxy for stopover density. Rug plots (red lines) indicate coverage of normalized values of each predictor (or interaction term) among the measured data.

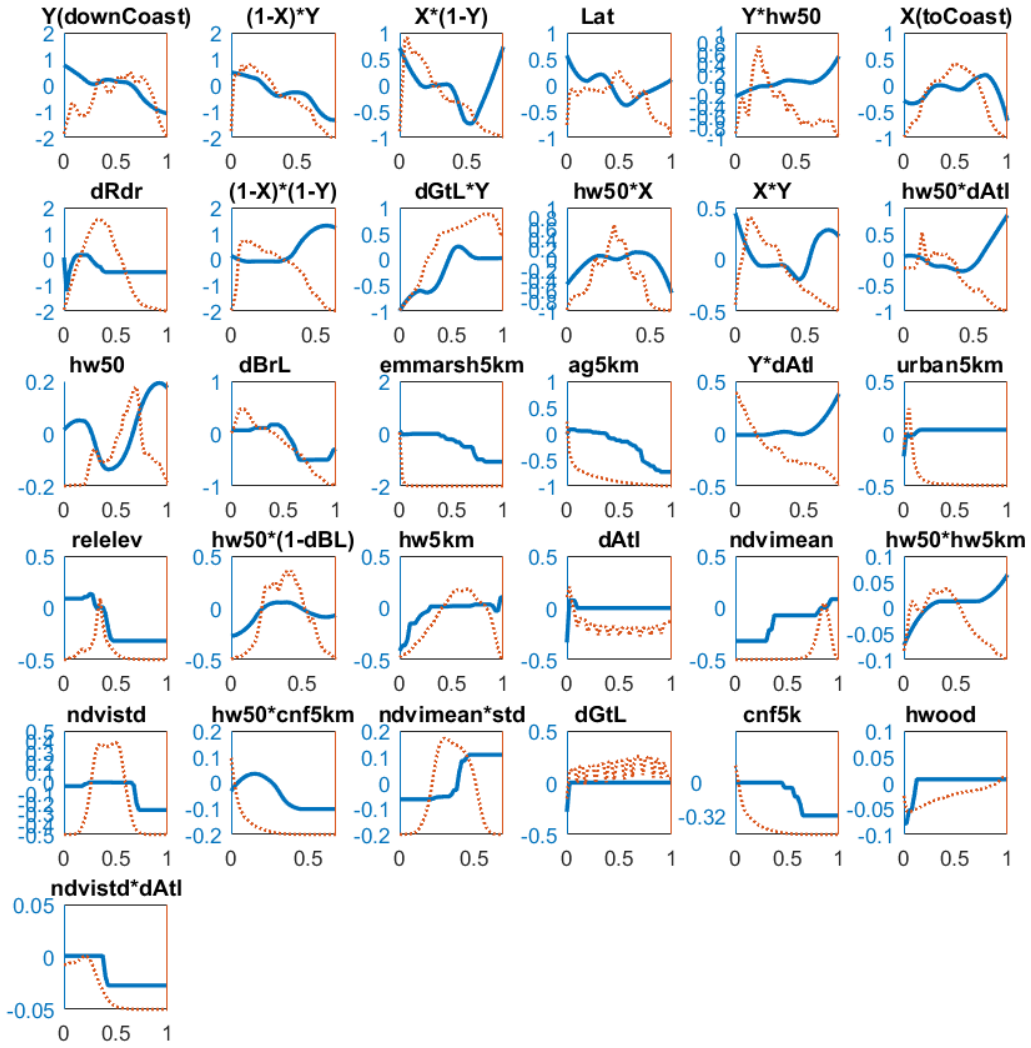

Figure 26. Predicted response to each (normalized) predictor on mean VIR in weeks 7-8, as proxy for stopover density. Rug plots (red lines) indicate coverage of normalized values of each predictor (or interaction term) among the measured data.

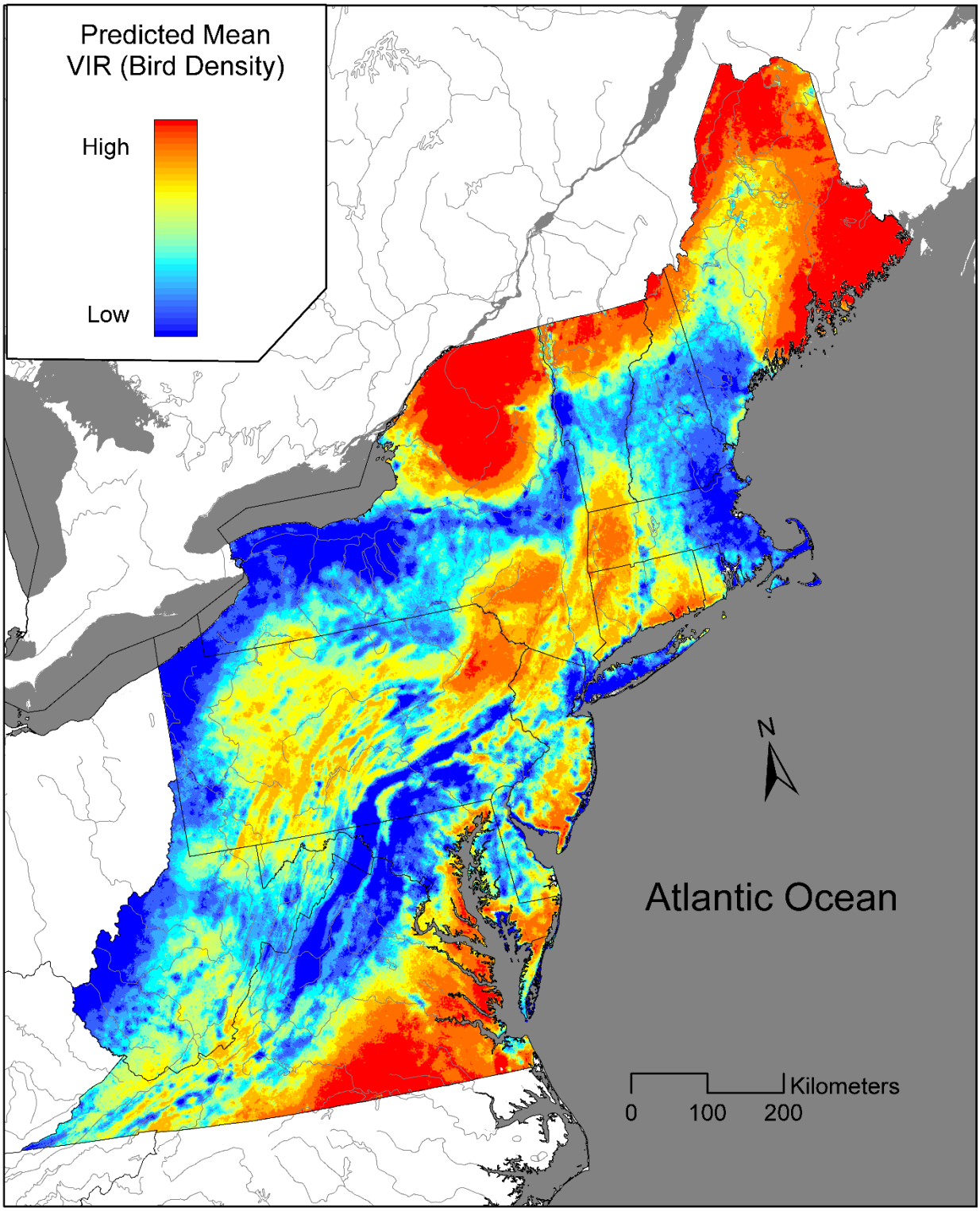

Figure 27. Predicted mean VIR during autumn 2008 – 2014 within USFWS Region 5 as proxy for mean stopover density, based on the BGAM model.

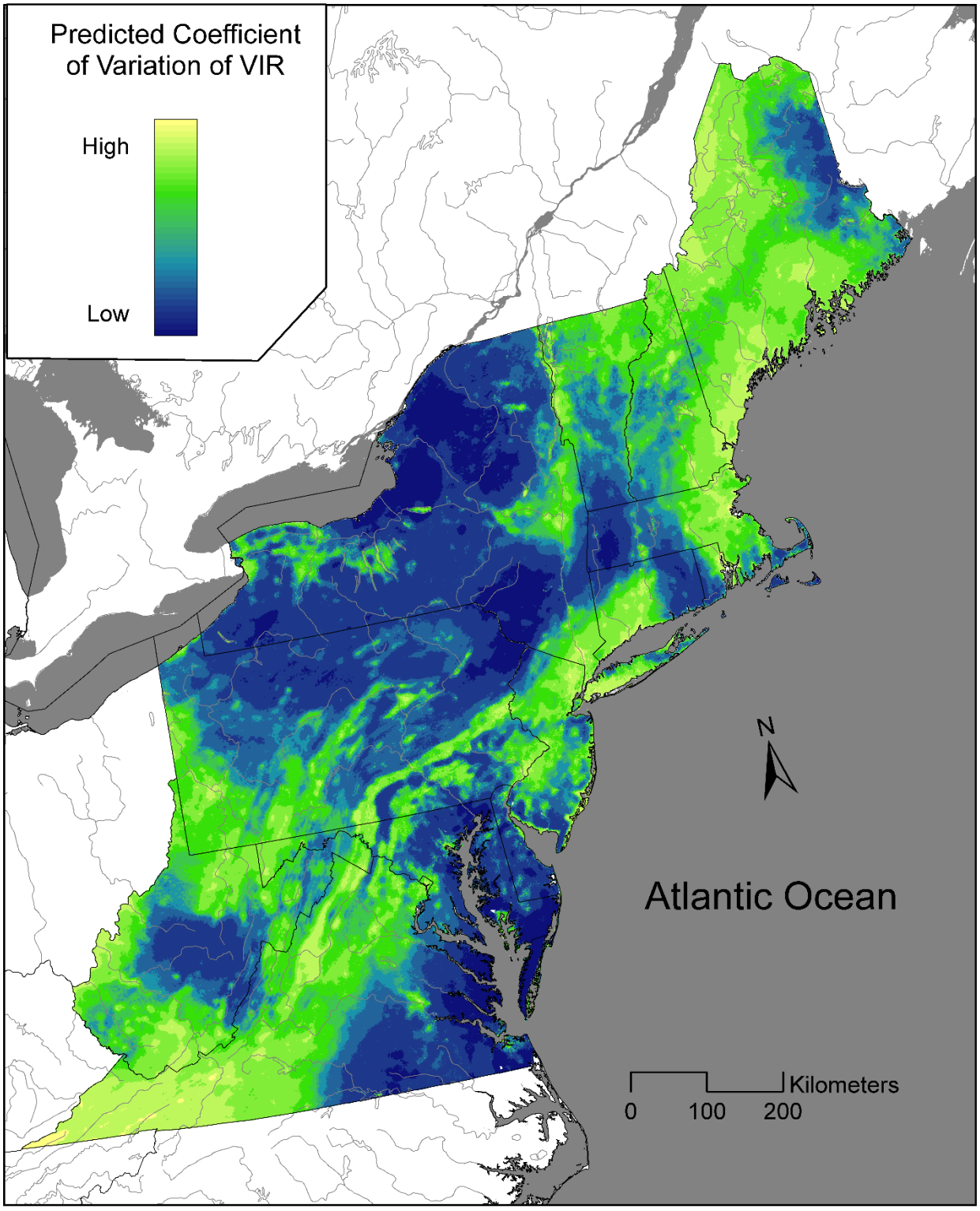

Figure 28. Predicted coefficient of variation in VIR during autumn 2008 – 2014 within USFWS Region 5 as proxy for daily variability in stopover density, based on the BGAM model.

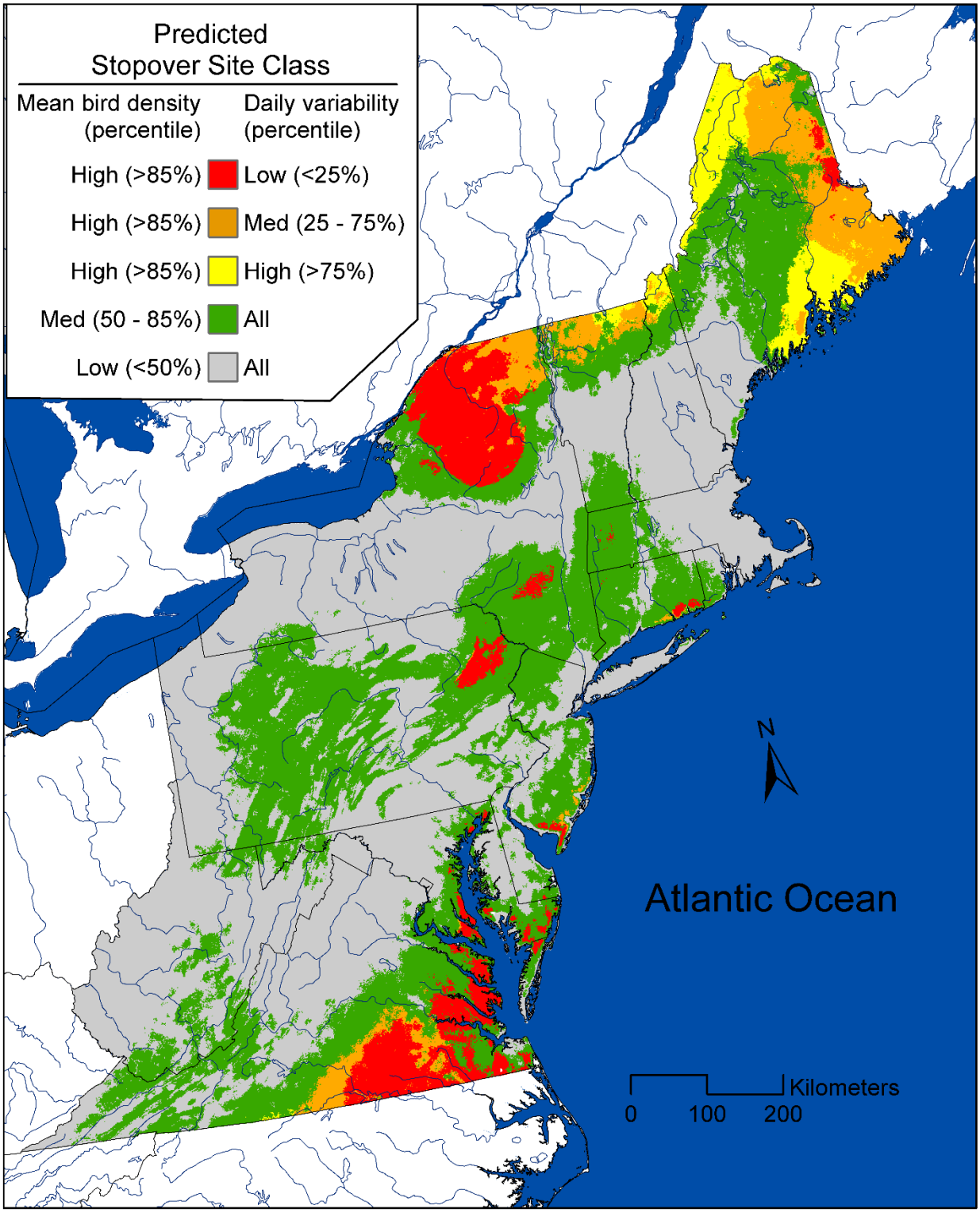

Figure 29. Map of regionally-classified predicted bird stopover use during autumn 2008 - 2014 within USFWS Region 5.

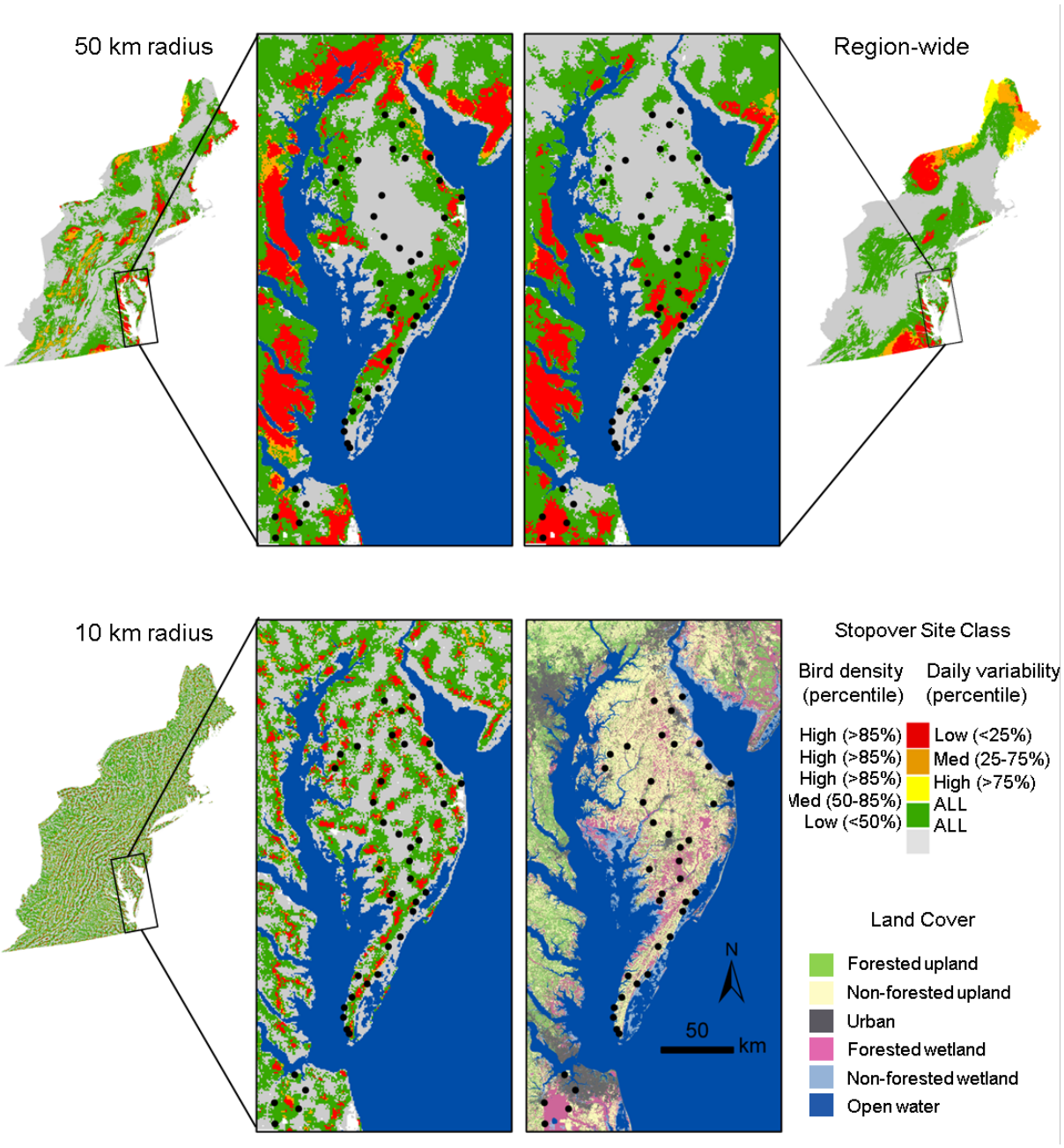

Figure 30. Maps depicting predicted stopover use classified at various window sizes (e.g. 10-km radius, 50-km radius, and region-wide) during autumn 2008 – 2014 within USFWS Region 5. Inset region of the Delmarva Peninsula is also shown with the locations of transect survey sites (black dots). Land cover of the Delmarva Peninsula is shown for reference.

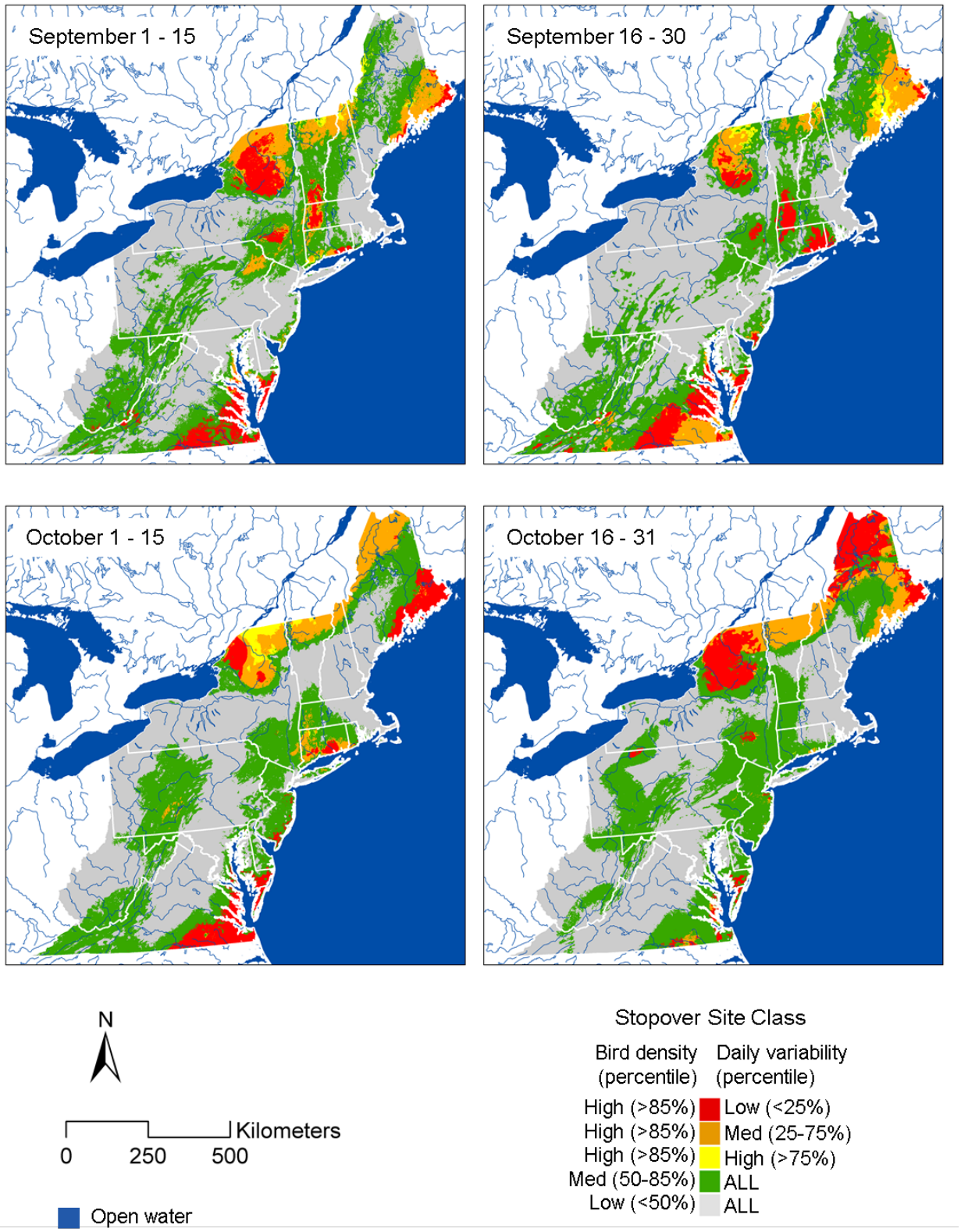

Figure 31. Map of regionally-classified predicted bird stopover use during four bimonthly periods averaged across autumn 2008 - 2014 within USFWS Region 5.

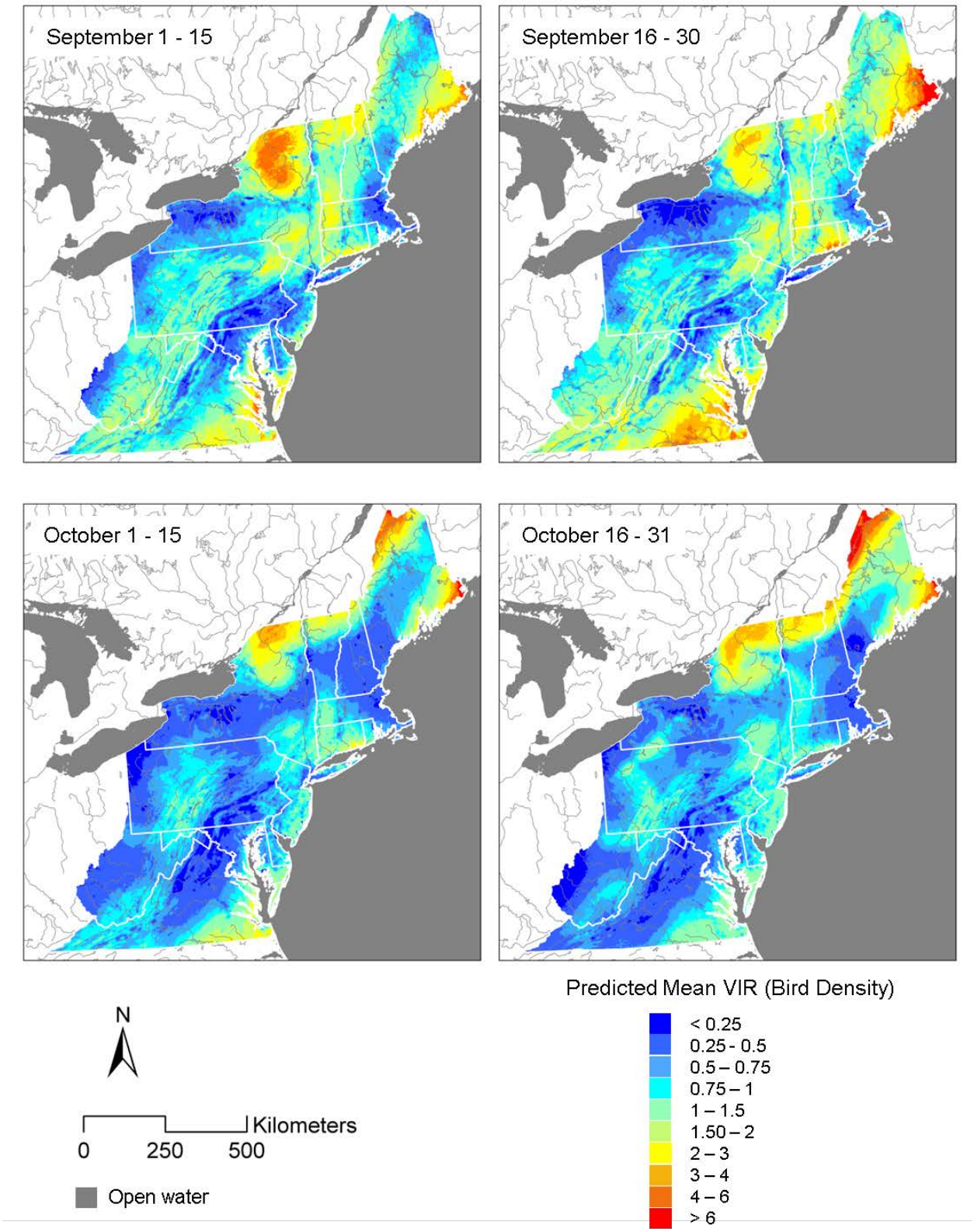

Figure 32. Map of predicted mean VIR during four bimonthly periods averaged across autumn 2008 - 2014 within USFWS Region 5.

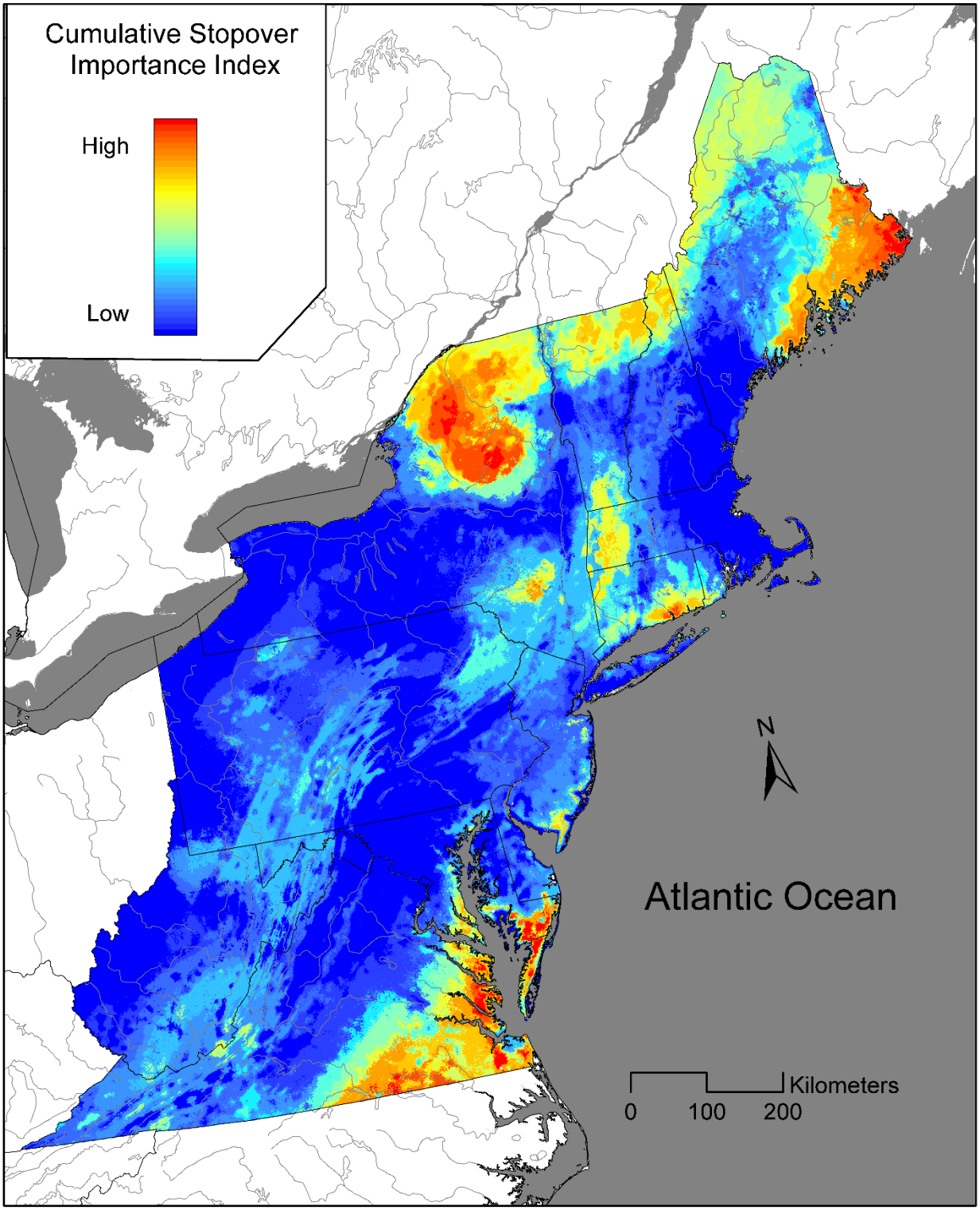

Figure 33. Map of the Cumulative Stopover Importance Index for autumns 2008 – 2014 within USFWS Region 5.

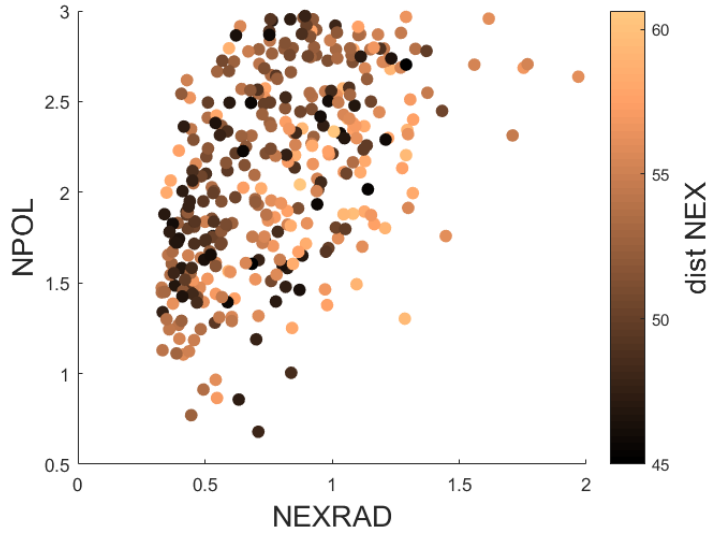

Figure 34. Mean VIR of observed NPOL data versus co-located NEXRAD data as a function of distance to the NEXRAD (dist NEX) radar (see color bar).

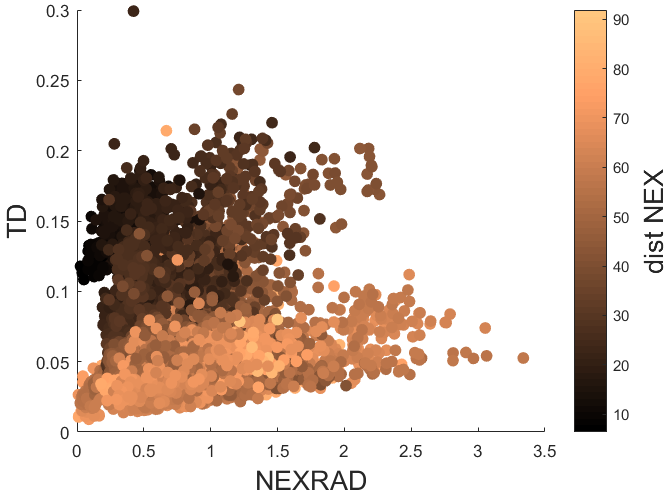

Figure 35. Mean VIR of observed TDWR (TD) data versus NEXRAD data as a function of distance to the NEXRAD (dist NEX) radar (see color bar).

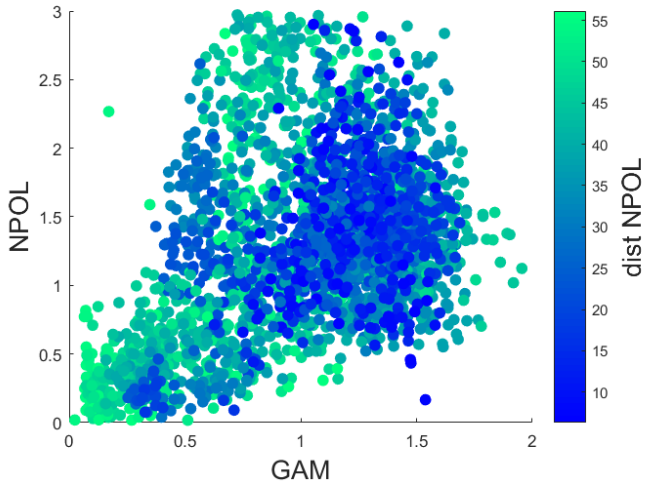

Figure 36. Mean VIR of observed NPOL data versus GAM-predicted data as a function of distance to the NPOL radar (see color bar).

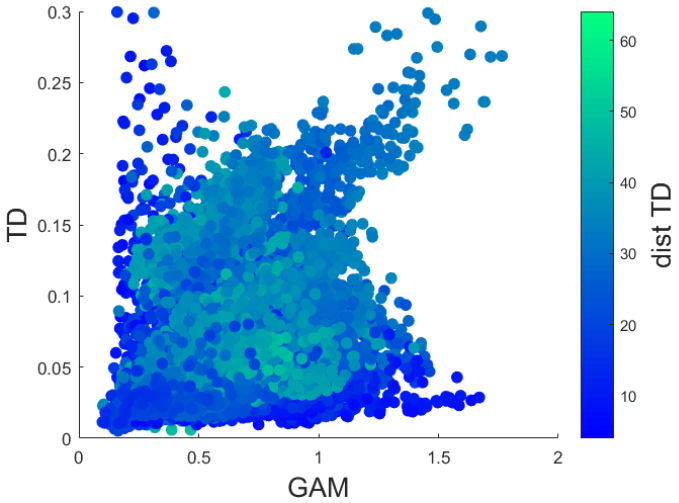

Figure 37. Mean VIR of observed TDWR data versus GAM-predicted data as a function of distance to the TDWR radar (see color bar).

Figure 38. Total number of migrants (Neotropical versus temperate) detected throughout the fall field season for all 48 transects by year. Sampling periods start on August 15 and end on November 7.

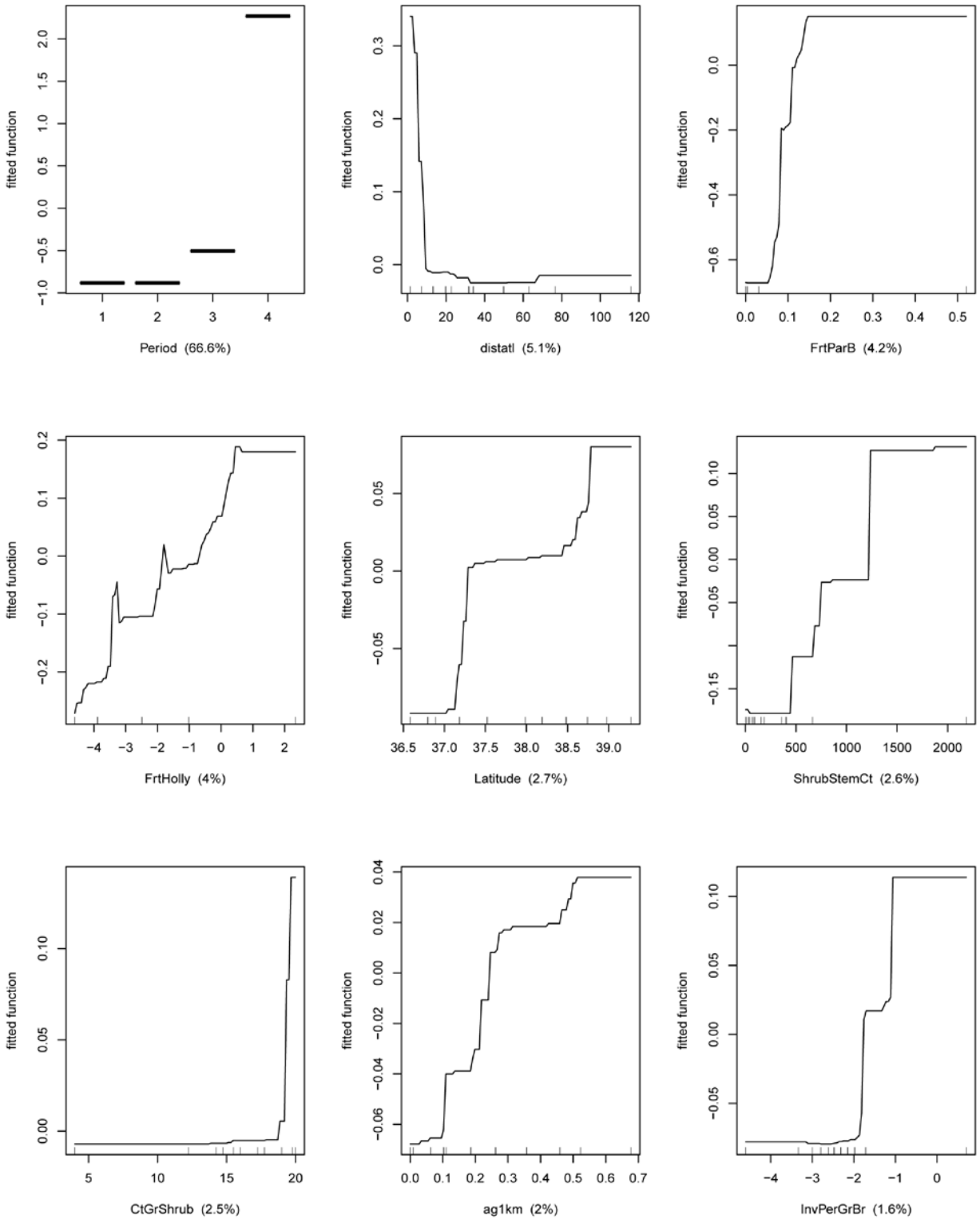

Figure 39. Partial dependence plots for the nine most influential variables that predict migrant density for wintering landbird migrant species included in the analysis. Rug plots show the distribution of data, in deciles, for the X-axis variable. Relative influence in parentheses.

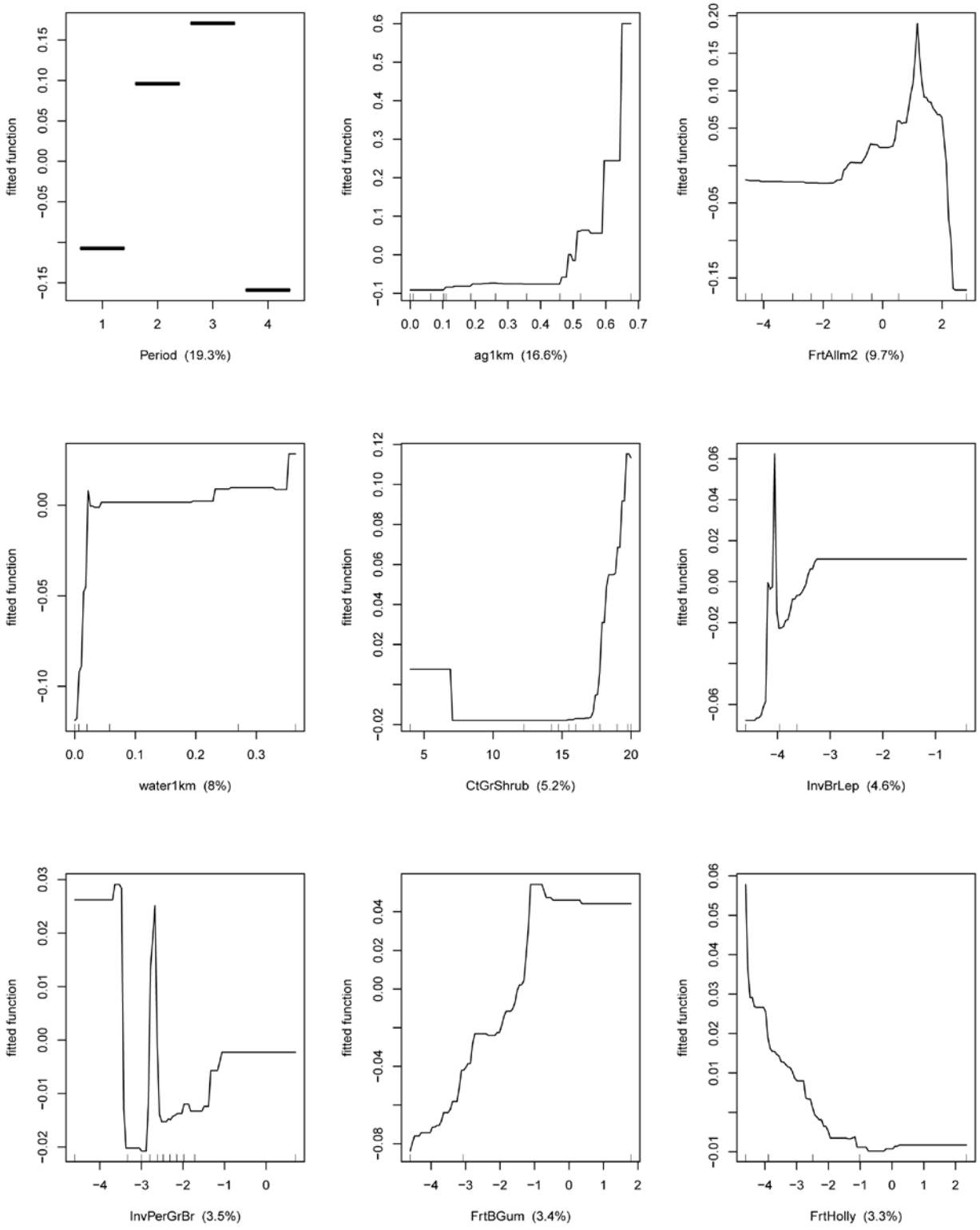

Figure 40. Partial dependence plots for the nine most influential variables that predict migrant density for transient landbird migrant species included in the analysis. Rug plots show the distribution of data, in deciles, for the X-axis variable. Relative influence in parentheses.

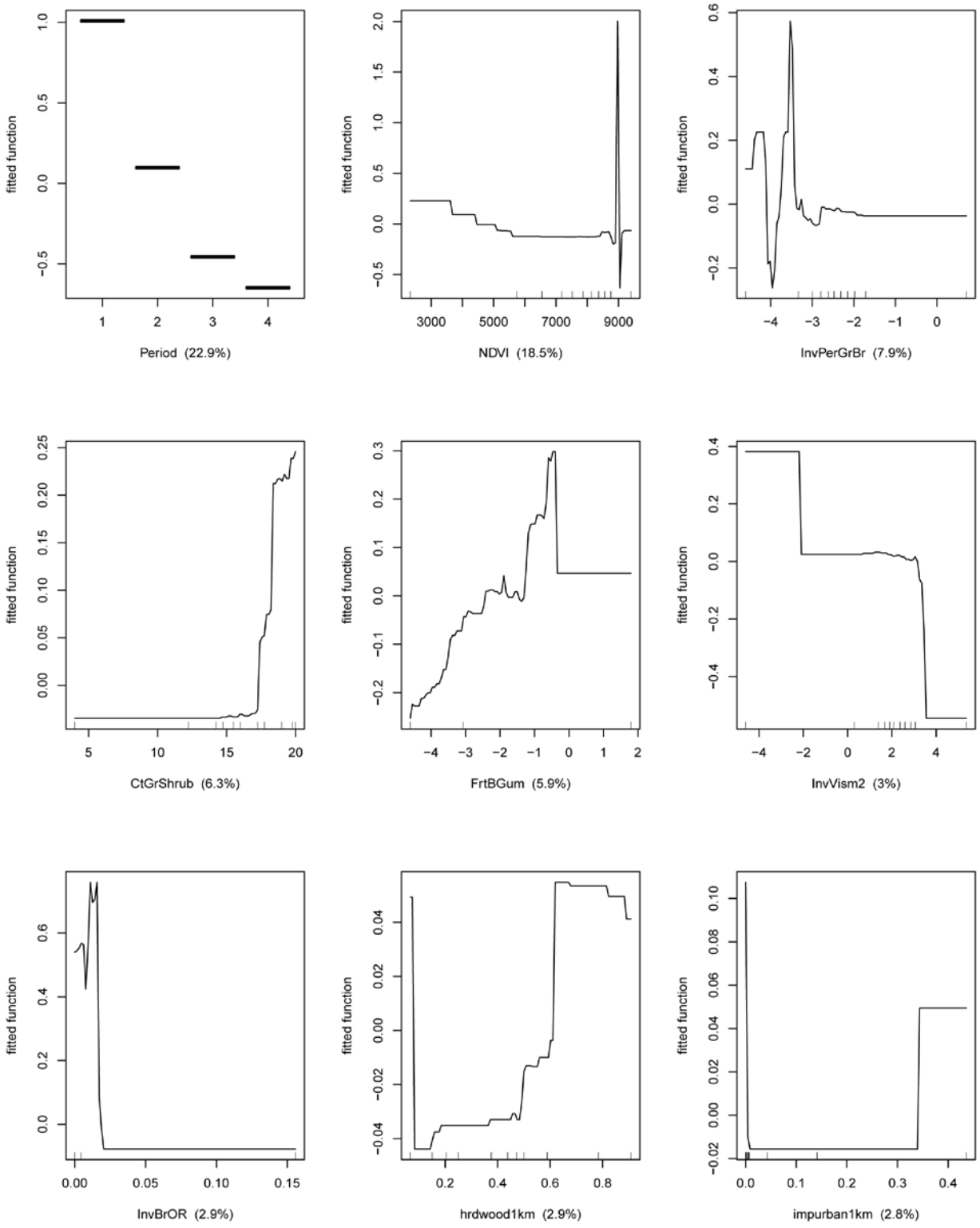

Figure 41. Partial dependence plots for the nine most influential variables that predict migrant density for breeding landbird migrant species included in the analysis. Rug plots show the distribution of data, in deciles, for the X-axis variable. Relative influence in parentheses.

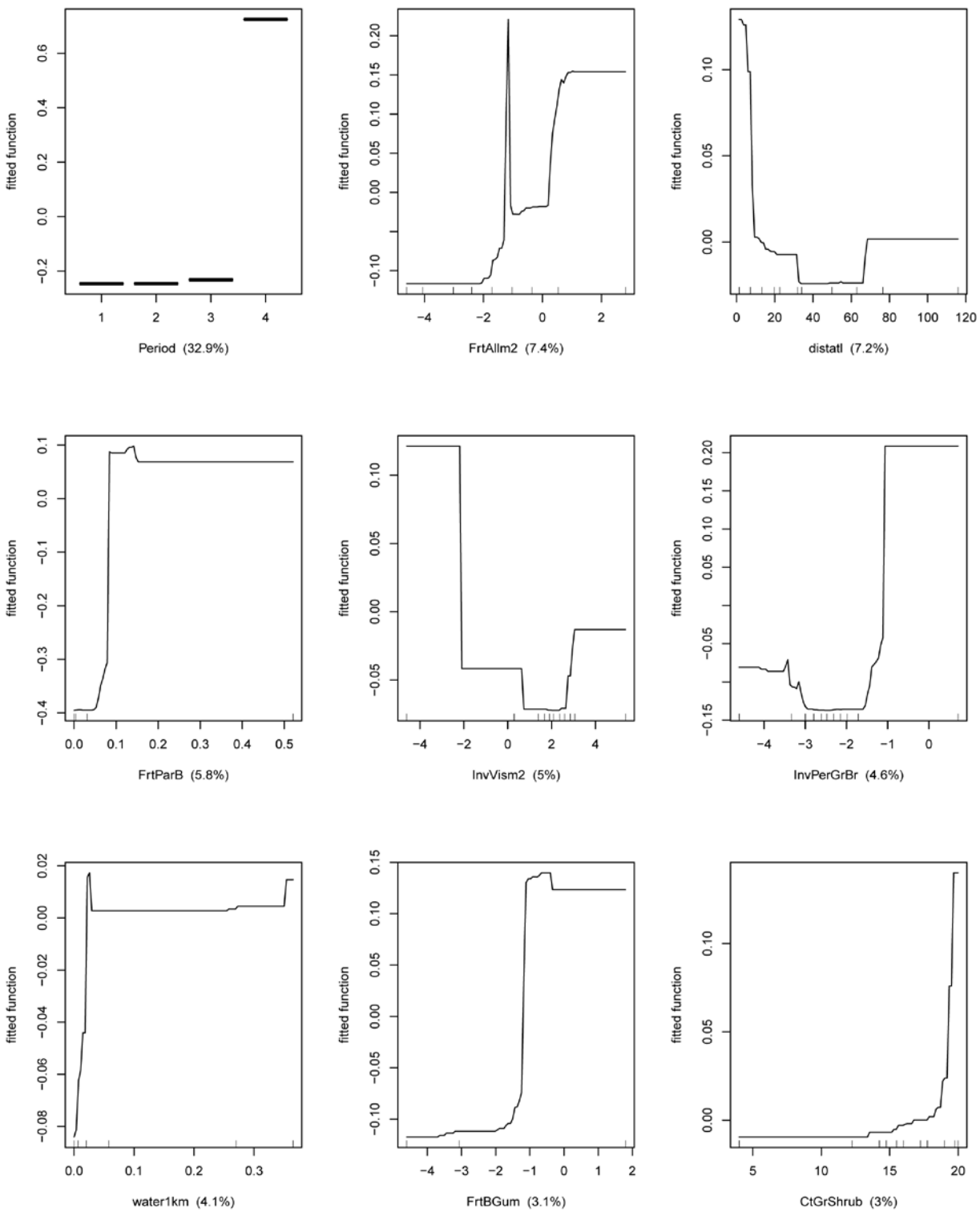

Figure 42. Partial dependence plots for the nine most influential variables that predict migrant density for frugivorous landbird species included in the analysis. Rug plots show the distribution of data, in deciles, for the X-axis variable. Relative influence in parentheses.

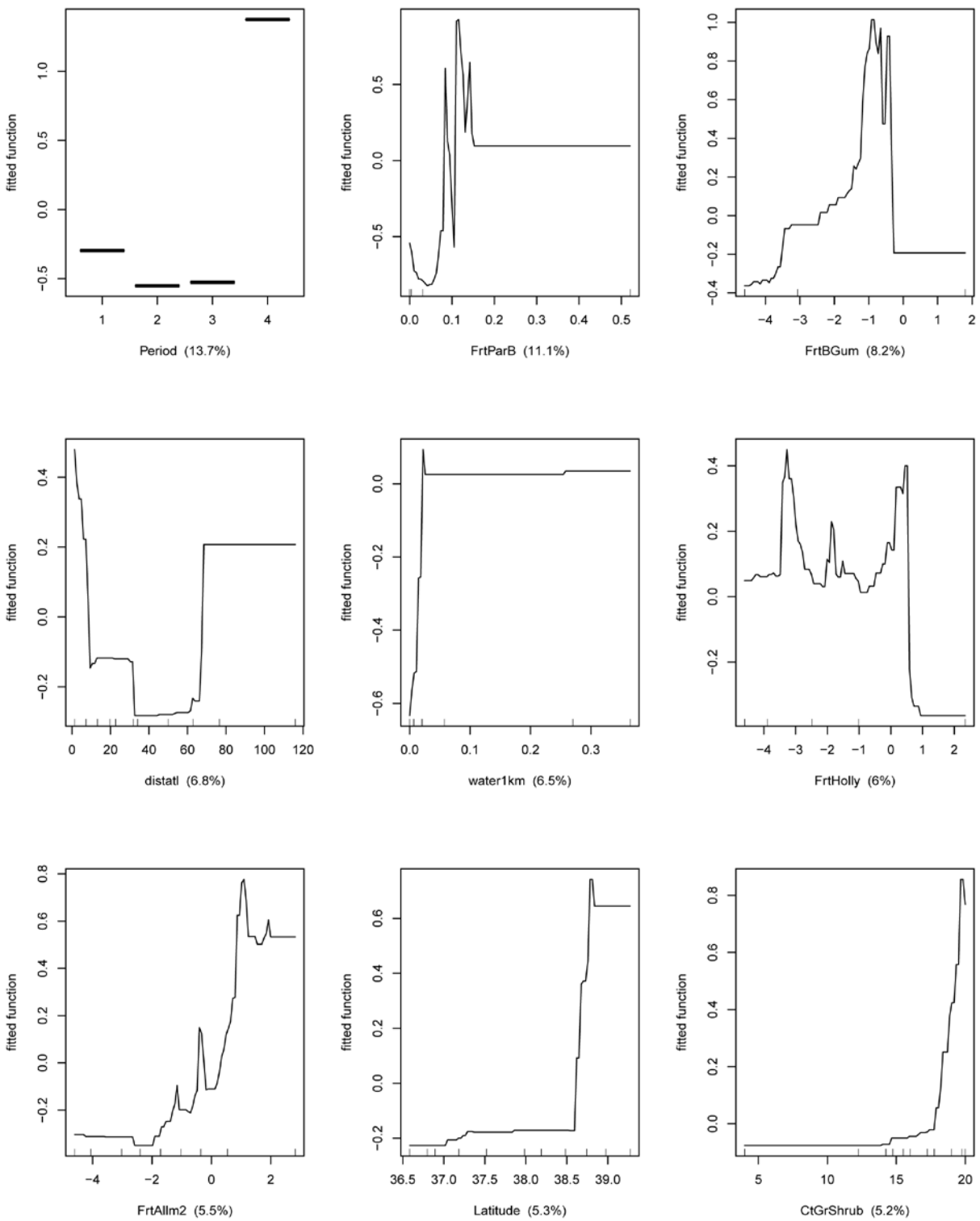

Figure 43. Partial dependence plots for the nine most influential variables that predict migrant density for all nocturnal landbird species included in the analysis. Rug plots show the distribution of data, in deciles, for the X-axis variable. Relative influence in parentheses.

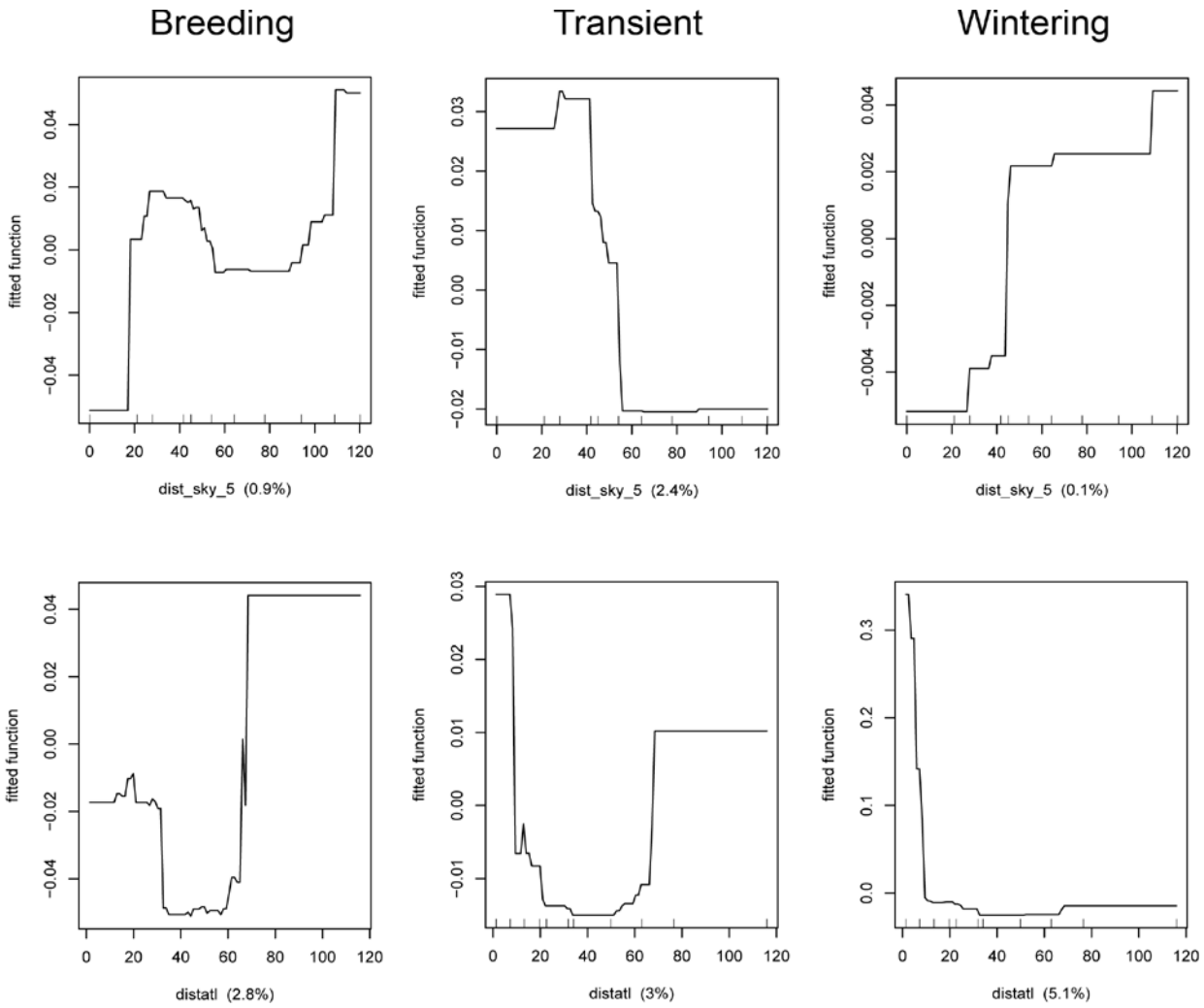

Figure 44. Partial dependence plots for the response of migrant density to distance from bright areas (top row) and distance from the Atlantic coast (bottom row) for breeding, transient, and wintering landbird migrant species included in the analysis. Rug plots show the distribution of data, in deciles, for the X-axis variable. Relative influence in parentheses.

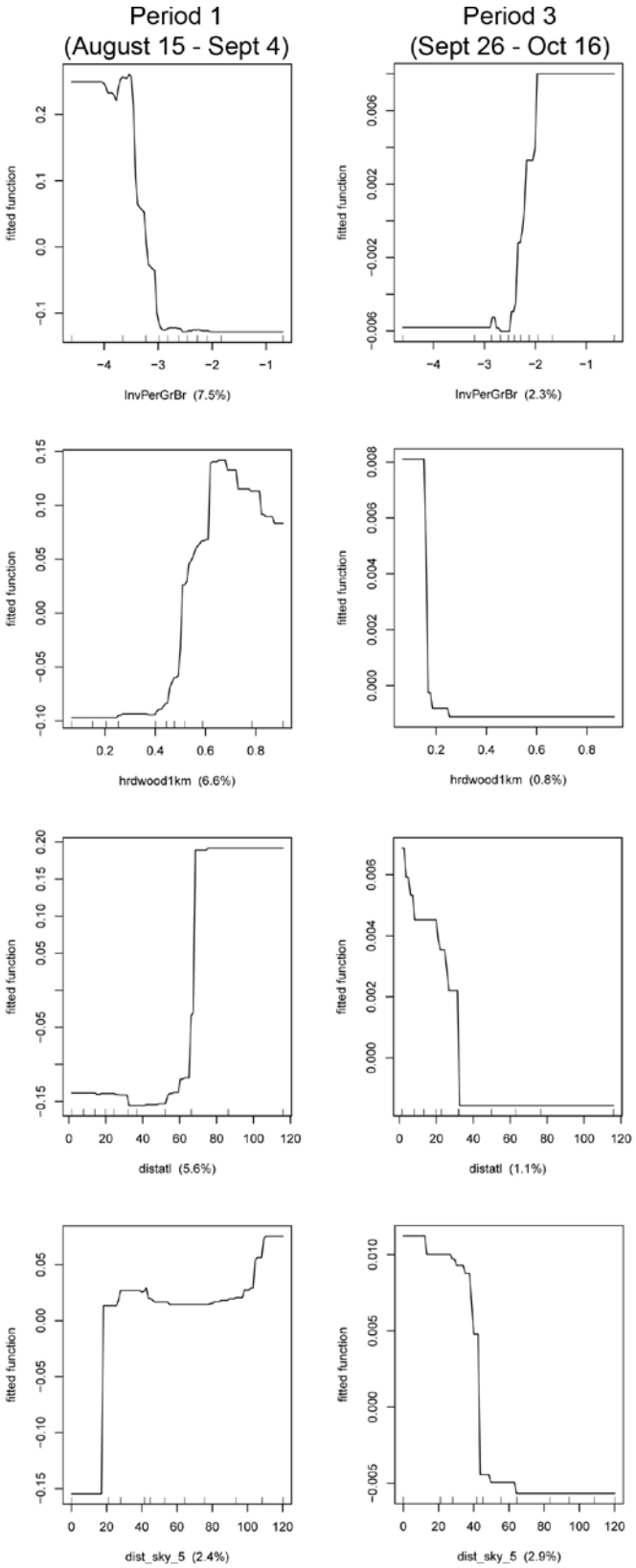

Figure 45. Partial dependence plots for the response of breeding migrant density to 4 select predictors when modeled using data separated by sampling period (Period 1 on the left and Period 3 on the right). Rug plots show the distribution of data, in deciles, for the X-axis variable. Relative influence in parentheses.

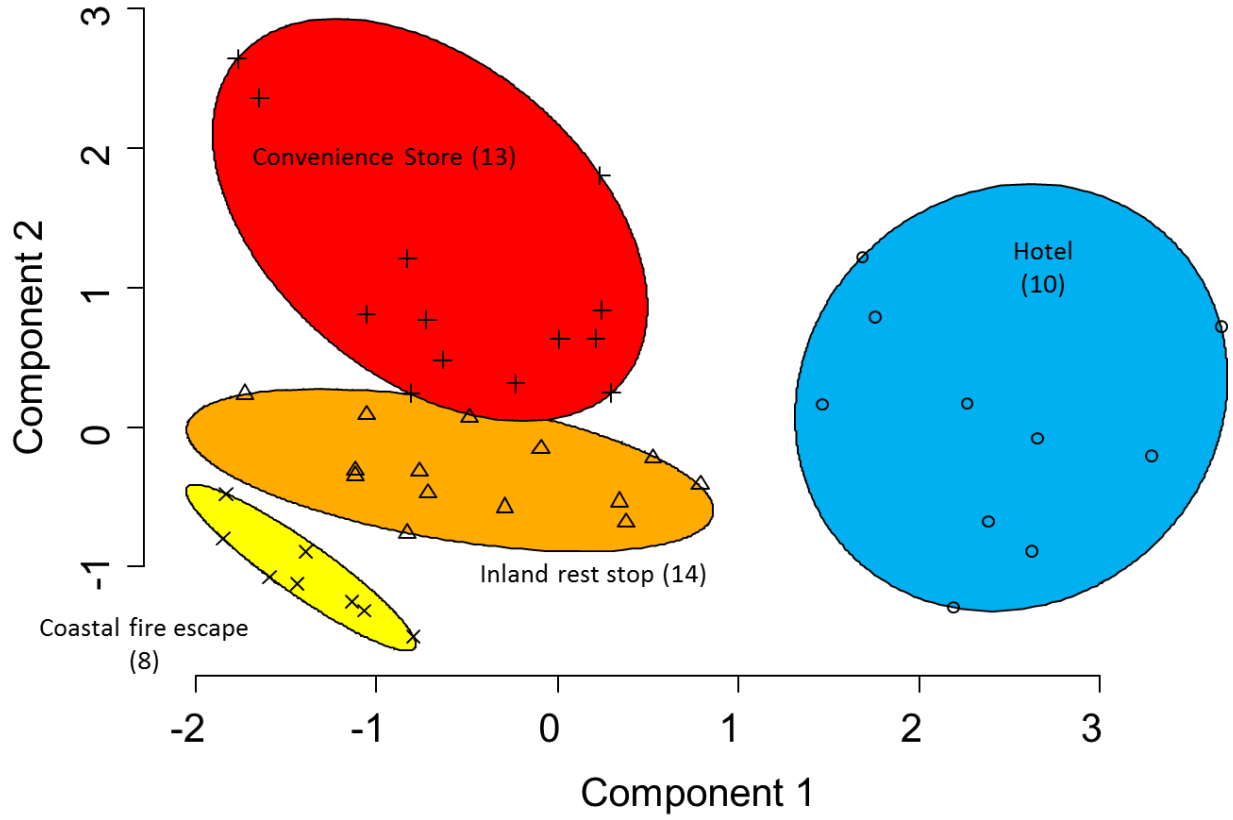

Figure 46. Cluster plots of 45 transect sites along two component axes and designated as members of four labeled stopover functional types by colored ellipses. The number of sites within each cluster group is presented in parentheses after cluster label name.

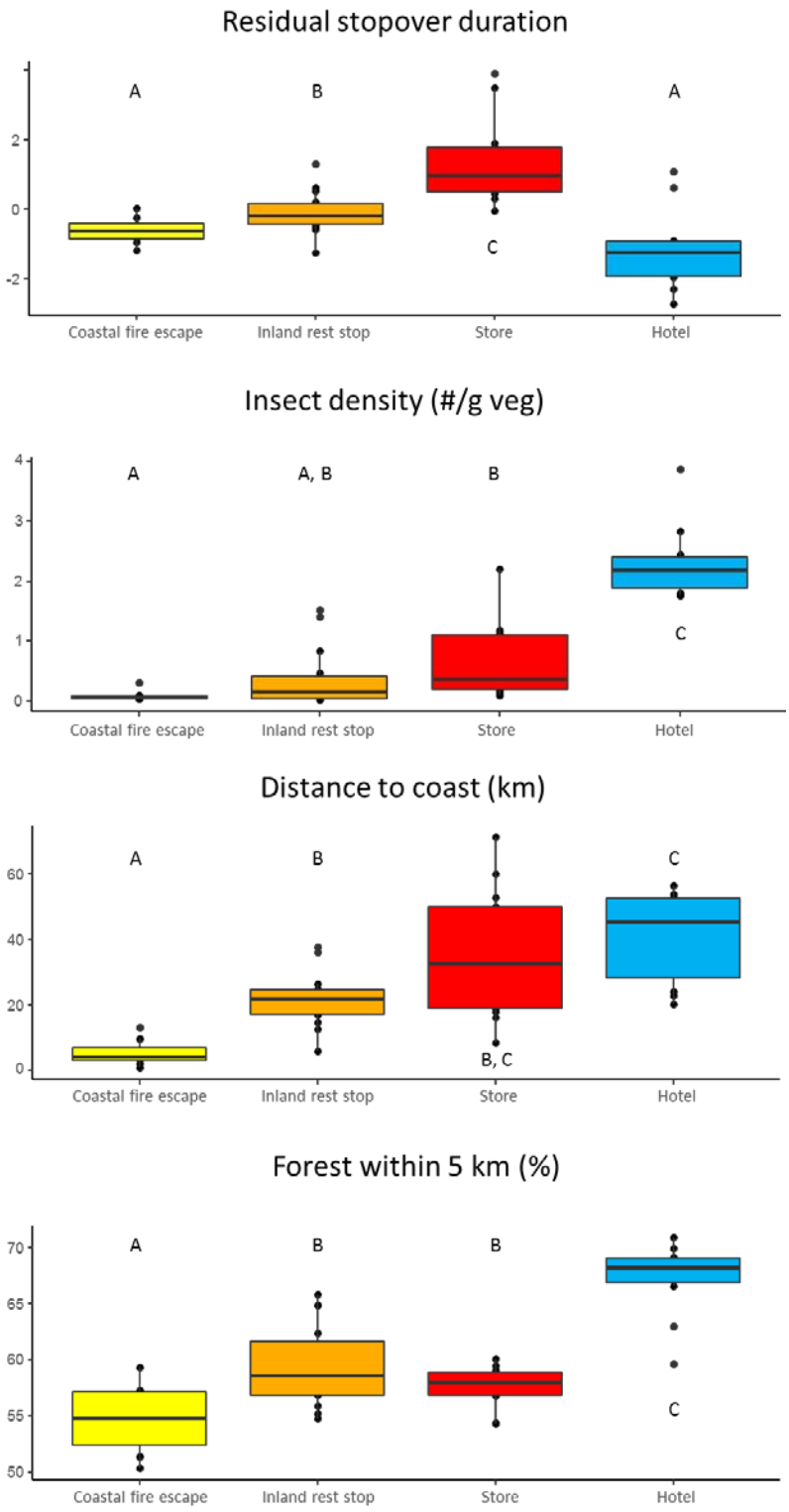

Figure 47. Boxplots of values of residual migrant stopover duration, insect density, distance to coast, and forest cover within 5 km among four stopover site functional type clusters (coastal fire escape, inland rest stop, convenience store, and hotel) comprised of 45 transect sites in the mid-Atlantic and Gulf of Mexico coastal regions during fall migration. Clusters with the same letters above boxes are similar with respect to mean values of each variable.

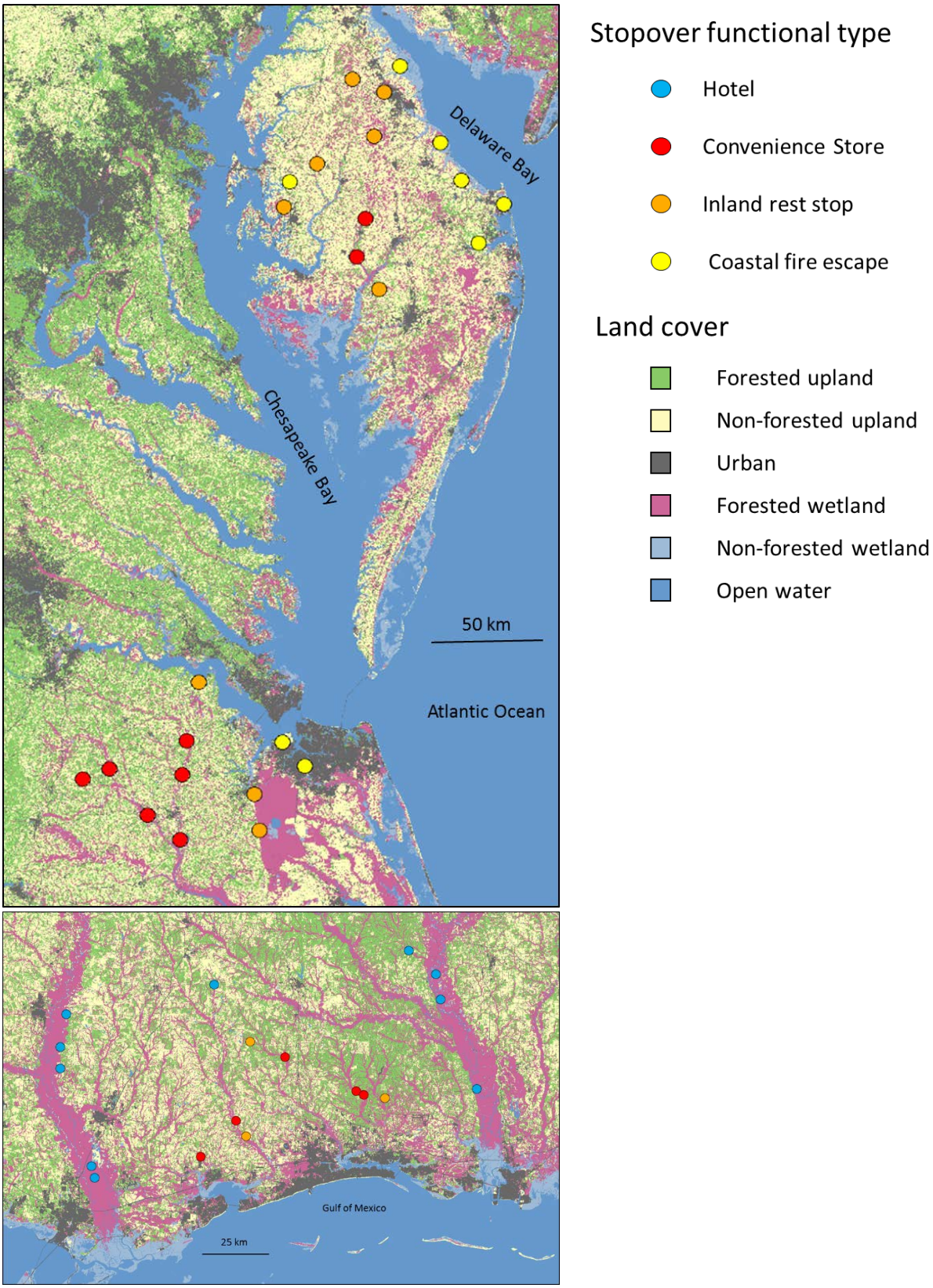

Figure 48. Maps of classified fall migration stopover functional types for 45 transect sites near the Mid-Atlantic (top panel) and Gulf of Mexico (bottom panel) coasts.